UNIVERSITY OF CALIFORNIA SAN DIEGO

Dissolution of Mega-Voids in Resin Transfer Molding

A dissertation submitted in partial satisfaction of the

requirements for the degree of Doctor of Philosophy

in

Structural Engineering

by

Paul Nordstrom Clark

Committee in charge:

Prof. Vistasp M. Karbhari, Chair
Prof. Prab Bandaru
Prof. Gilbert A. Hegemier
Prof. M. Lea Rudee
Prof. Francesco Lanza di Scalea

2007

The dissertation of Paul Nordstrom Clark is approved, and it is accepted in quality and form for publication on microfilm:

_____

_____

_____

_____

_____
Chair

University of California, San Diego

2007

DEDICATION

This work is dedicated to my loving family. To my beautiful wife, Cynthia, thank you for your support and understanding through this protracted effort. To Quinn, your energy and thirst for life are inspiring. To Lillie, your kind heart and loving ways continually warm my heart. I love you all dearly.

I would also like to dedicate this dissertation in memory of Brett Josie. Brett you are a good friend, a kind man and you are missed.

TABLE OF CONTENTS

LIST OF FIGURES

LIST OF TABLES

ACKNOWLEDGEMENTS

This work would not be possible without the help and support of many. I would like to acknowledge and sincerely thank Professor Vistasp Karbhari. Your knowledge and insight into the science of composites are remarkable and you truly helped this effort to be more meaningful.

To Randy Klasen, thank you for your help and guidance on building much of the equipment used for this research.

VITA

1991	B.S., Northern Arizona University
1996	M.S., University of Utah
1999–2000	Ph.D. Candidate, University of Utah
2007	Ph.D., University of California, San Diego
1991–1992	Associate Engineer, Thiokol Corporation
1992-2000	Senior Engineer, Radius Engineering
2000-Present	Program Manager, General Atomics

Licensed Professional Engineer: Utah and Washington

PATENTS

U.S. Patent 5,985,197: Method of Manufacturing Composite Golf Club Head

U.S. Patent 6,319,346: Method for Manufacture of Composite Aircraft Control Surfaces

U.S. Patent 6,248,024: Composite Golf Club Head

U.S. Patent 6,340,509: Composite Bicycle Frame and Method of Construction Thereof

PUBLICATIONS

Clark, P. and R. P. Reed, (2000). Resin Transfer Molding of ITER US CS Model Coil. Society for the Advancement of Material and Process Engineering (SAMPE) Symposium and Exhibition, Long Beach, CA.

Clark, P., Streckert, Desplat, J., and Izhvanov, O., (2003). Solar Thermal Test of Cylindrical Inverted Thermionic Converter. Proceedings of *1st Intersociety Energy Conversion Engineering Conference (IECEC),* AIAA 2003-6102, Reston, VA, (2003).

Clark, P., B.H.C. Chen, Robertson W.H., Streckert H. H., (2004). Stability and Performance of High Emissivity Coatings for Radiation Coupled Thermionic Converters. 8th International Symposium on Ceramics in Energy Storage and Power Conversion Systems, 2004.

Clark, P., B.H.C. Chen, Robertson, W., Streckert, H., King, W., Palisoc, A., (2004). Advances In Design Of 50 kW Solar Power System. Proceedings of 2nd IECEC, AIAA 2004-5777, Providence, RI.

Martinez, M., O. Izhvanov, Robertson, W., Clark, P., Streckert, H., Desplat, J., (2005). Cylindrical Inverted Multi-Cell (CIM) Thermionic Converter for Solar Power and Propulsion Systems. Proceedings of Space Technology and Applications International Forum (STAIF-2005), Albuquerque, NM.

Clark, P.,N. J.L. Desplat, Streckert, H.H., Adams, S.F., Smith, J.W., (2006). Solar Thermionic Test in a Thermal Receiver. Proceedings of STAIF-2006, Albuquerque, NM.

Clark, P. and V. M. Karbhari (2006). Resin Degassing Affects On Air Solubility In Epoxy. SAMPE 2006, Long Beach, CA.

ABSTRACT OF THE DISSERTATION

Dissolution of Mega-Voids in Resin Transfer Molding

by

Paul Nordstrom Clark

Doctor of Philosophy in Structural Engineering

University of California, San Diego, 2007

Professor Vistasp M. Karbhari, Chair

Resin transfer molding (RTM) is a common composite manufacturing process. Voids are a common defect encountered in RTM components. A new type of void, the 'Mega-Void', has been identified and addressed by this research. To produce acceptable RTM components requires that the mega-void be eliminated either through prevention or through dissolution. The latter is the topic of this research.

Three process parameters affecting mega-void dissolution are researched; 1) Preform/mold vacuum , 2) Resin degas, and 3) Resin curing pressure.

To address preform/mold vacuum, analytical and empirical investigations were carried out. Results show that the preform can take-up

and retain water. Additional analytical investigations show that gas flow within the preform is molecular in nature. The consequence of this finding is that the removal of moisture and gases from the preform is difficult. Confirming experiments were carried out showing a significant difference between gas pressures within the mold and the gas pressure external to the mold.

The resin degas and resin curing pressure parameters were studied by researching the solubility of air in epoxy. An experimental apparatus was designed and fabricated wherein a sample of resin could be subjected to a specified level of vacuum for degassing. Subsequently, a measured amount of air was introduced into the resin sample and the combination pressurized to a controlled pressure. The resin and air were then monitored over time to observe the shrinkage of the air pocket as the air was absorbed by the resin. The experimental results show the pressure of residual air and the resin dissolution pressure both significantly affect the absorption of the air pocket. Higher levels of resin degassing are shown to provide a small benefit to gas dissolution.

As a final research effort, composite panels were fabricated using a blind injection setup where a single mold port is used for evacuation and resin injection. In this way, the starting size of the mega-void is fixed and equal to the mold free volume. The three processing parameters were varied in order to show the dissolution of mega-voids when the appropriate parameters are used.

1. INTRODUCTION

Resin transfer molding (RTM) is a common manufacturing process used in the production of composite components. The process involves placing a dry fiber preform into a female cavity mold. A thermoset resin (e.g., epoxy) is then transferred into the mold to infuse the preform. After cure, the mold is opened and the part extracted. The mold typically contains at least one vent port to allow the escape of air as the resin infiltrates the preform. A schematic of the RTM process is shown in Figure 1. Examples of RTM parts are shown in Figure 2.

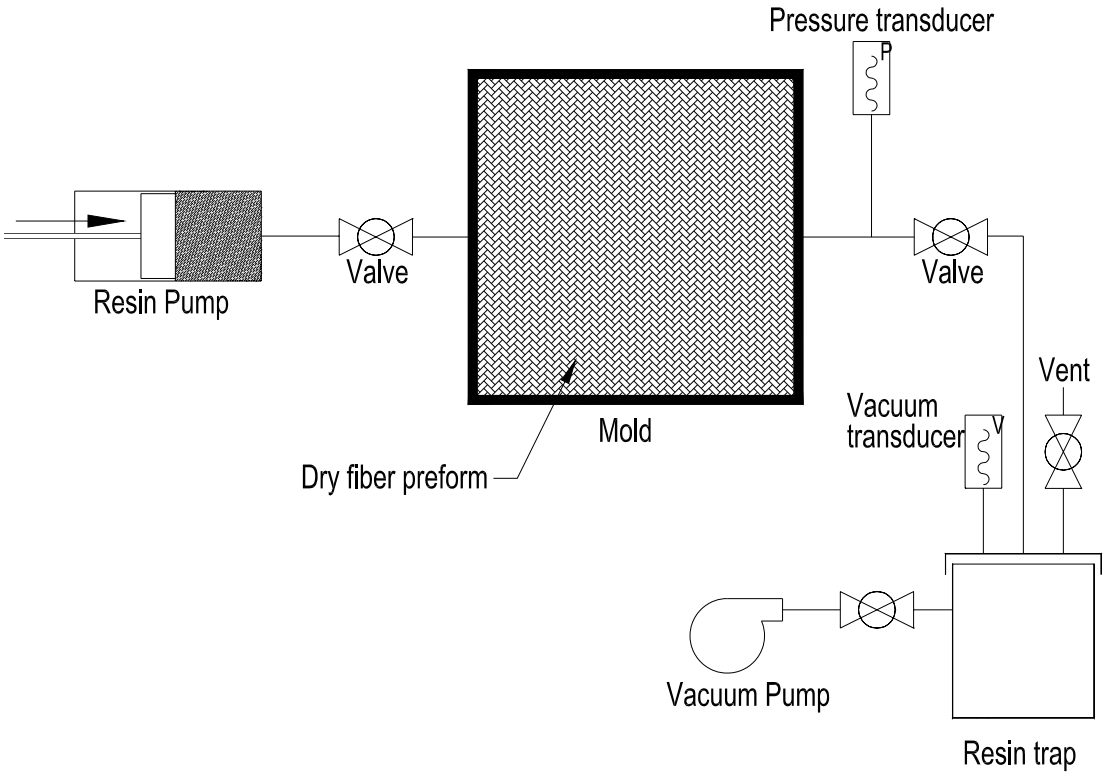

Figure 1. Schematic of a typical Resin Transfer Molding setup

Figure 2. Aircraft control surfaces fabricated using resin transfer molding (source: Radius Engineering, Inc.)

Aside from the selection of resin and preform materials, the parameters that define the RTM process include, resin injection temperature, resin injection flow rate, and resin curing (or hydrostatic) pressure. In addition, vacuum may be used to degas the resin prior to injection and/or to evacuate the mold before and during injection.

The most severe defect encountered in RTM parts are ‘dry spots’ (Ref. 1). These are areas in the finished part that are not impregnated with resin and contain dry fibers. Dry spots are typically the result of gas within the preform that is trapped during injection. The typical solution to dry spots is to

modify the process and/or tooling to allow for the escape of the gas. This might be accomplished for example through purging (or 'burping') resin through the mold which may flush out the dry spot. Another potential solution is the installation of additional vent holes in the mold. On a smaller scale, the finished part may contain voids. Voids are similar to dry spots in that they contain trapped gas. However, they differ as their small size allows heightened mobility during resin flow through the preform. The size of these voids is typically < 1 mm (Ref. 1, 2).

Significant work has been performed to model the flow of resin through the preform and mold (Refs. 3, 4, and 5). The objective of the resin flow modeling efforts is commonly the elimination of dry spots by tailoring the resin flow so as not to trap gas within the mold. These simulation tools are useful for evaluating potential locations for resin inlet and vent ports.

The elimination of dry spots through dissolution of the trapped gas is another possibility. This method has not been previously investigated in depth and is the topic researched and reported on in this dissertation. The elimination of dry spots through gas dissolution potentially has many benefits. Gas dissolution eliminates voids at a fundamental level. This approach could reduce hardware costs by reducing required operating pressures. This in turn can simplify tooling, resin pumping equipment and mold presses (if used).

Chapter 2 of the dissertation contains background information regarding prior research on, voids, the use of mold vacuum, degassing of resin, and gas solubility in the resin.

Chapter 3 lays out the basis of this research and introduces the concept of the Mega-Void and the RTM processing continuum. The Goals and Objectives of this research are presented and lead into the three research Foci; 1) Preform Gas, 2) Resin Degassing and 3) Gas Dissolution in Resin.

Chapter 4 presents the research carried out on Preform Gas. The research comprises preform moisture sorption calculations and experiments, preform molecular gas flow calculations, and preform degassing experiments.

Chapter 5 presents the experimental research conducted on resin degassing and gas dissolution in the resin. Confirmatory scaling experiments were also performed and are presented.

Chapter 6 presents the results of experiments performed to show the validity of the hypothesized processing continuum when applied to the fabrication of composite panels. Experiments were conducted using an unvented mold to validate the hypothesis regarding Dissolution of a Mega-Voids in Resin Transfer Molding.

Chapter 7 presents conclusions resulting from the research performed in all chapters. The implications of the research are discussed along with the potential benefits in both the understanding and implementation of the knowledge.

Finally, Chapter 8 discusses and recommends future research that would further the understanding of mega-voids and how this knowledge could benefit the process of RTM.

2. BACKGROUND

2.1. Voids

Voids are a common defect in composite parts. Voids in RTM fabricated parts have been studied extensively (Refs 6 to 25). Voids are generally categorized to result from one of three mechanisms; 1) resin flow, 2) volatile flashing and 3) cure shrinkage.

2.1.1. Flow Induced Voids

A typical fiber preform is made up of tows of fiber that are woven or stitched together to form a mat or cloth. Within the mat, there are generally spaces between the tows that have a higher permeability relative to the individual tows. Flow between the tows has been described as macro-flow and flow within the tows described as micro-flow (Ref. 13). The formation of voids at the flow front will form either within the tows or between the tows.

Models for macro-flow of resin through a fibrous preform have been developed based upon Darcy's Law (Refs. 3 to 5). For a finite 1-D flow, it may be stated as

$$Q = A \cdot K \cdot \Delta h / L \qquad [1] \text{ (Ref. 26)}$$

where,

- Q = Volumetric flow rate
- A = Flow area perpendicular to the flow path (L)
- K = Hydraulic conductivity (Permeability)
- L = Flow path length
- Δh = Hydraulic head

Micro-flow occurs within tows of the preform due to capillary action (Ref. 13). A capillary suction pressure can be defined as

$$\Delta P_S = (2 \cdot \gamma / R) \cdot \cos(\theta) \qquad [2] \text{ (Ref. 27)}$$

where,

ΔP_S = Capillary suction pressure
γ = Surface tension
R = Channel radius
θ = resin-fiber contact angle

The formation of voids at the resin flow front has been observed (Refs. 2, 6, 25, 28, 29) and analytical models have been developed (Refs. 2, 13, 15, 25). In the literature, voids that form at the flow front have been categorized as microvoids, macrovoids, or mesovoids (Ref. 2).

Microvoids are voids that form within the fiber tows and between individual fibers. They have been shown to form when the macro-flow velocity is faster than the micro-flow velocity (Ref. 13). When the resin micro-flow lags behind the macro-flow of resin through the perform micro voids will form. If the difference in the micro-flow velocity and the macro-flow velocity is significant enough, ‘meso’ voids can form. Mesovoids are larger microvoids that encompass multiple fibers within a tow (Ref. 2). In the context of this study, the term microvoid is used to describe both micro and mesovoids together. Figure 3 shows the three types of flow induced voids.

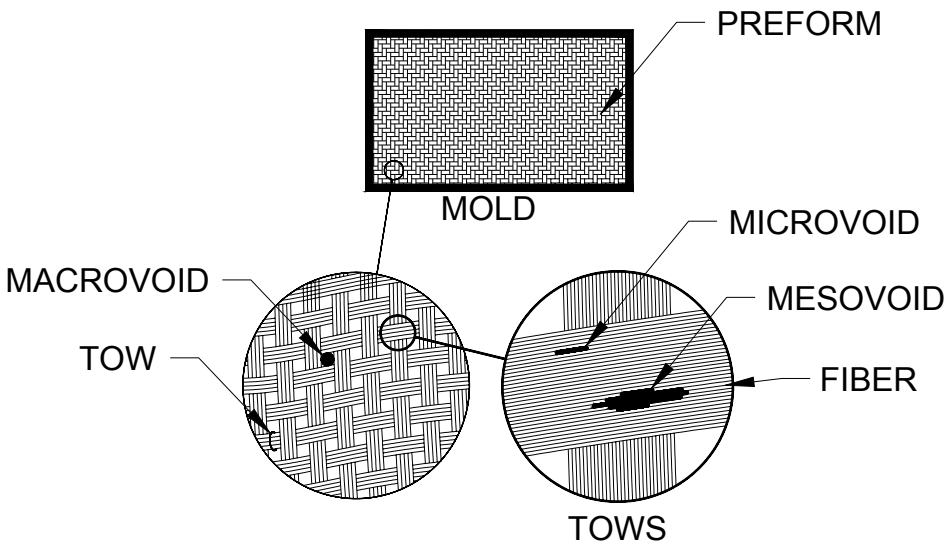

Figure 3. Types of flow induced voids (Ref. 2)

Alternatively, the capillary flow within the tows may lead the flow between tows resulting in entrapment of 'macro voids' in the volumes between tows. Once formed, micro and macro voids have a degree of mobility. Purging or flushing these voids out of the part has been demonstrated with some success but their elimination, once formed has not been demonstrated. The goal of research on these voids is to eliminate them by preventing their formation (Ref. 13).

2.1.2. Volatile Induced Voids

Voids can also form from gas sources within the resin. For example, tiny bubbles may exist in the incoming resin flow that will grow upon heating. Dissolved gases, water and/or other volatiles (e.g., styrene) within the resin may contribute to void growth by diffusing into the void (Ref. 12). Basic

models for heterogeneous and homogeneous nucleation of bubbles from a liquid are presented in (Ref. 30). It has been reported that gases are produced due to the resin chemical reactions during cure leading to the generation of voids (Ref. 2, 23, 31).

2.1.3. Cure Shrinkage Voids

Voids have been shown to form due to resin cure shrinkage. Once gelation has occurred, the resin is constrained in three dimensions by the fiber bed and possibly by the mold. Resin shrinkage due to cure occurs both before and after gelation (Ref. 16, 32). After gelation, as the resin continues to cure and shrink, the resin becomes less able to relieve shrinkage stresses through plastic flow. As the resin cures, there is a contention between the resin shrinkage and its structural ability to sustain the residual stress being induced by the shrinkage. This mechanism has been demonstrated by Eom and Boogh (Refs. 16, 31) where the curing resin ruptured, forming a void into itself.

2.2. Mold Vacuum in RTM

The evacuation of the mold before injection is common practice in RTM and has been shown to decrease the void content (Ref. 2, 33 to 35). The general procedure is to connect a vacuum pump to the resin outlet port. A resin trap is typically used between the mold and the vacuum pump in order to protect the pump against potential resin ingestion. To measure the vacuum level, a vacuum gage or transducer may be installed on the trap or between

the trap and the vacuum pump. A typical RTM setup is shown in Figure 1 (above).

The duration of mold/preform pump-down varies widely. In Ref. 35 there was no delay between the start of mold evacuation and resin injection. In other scenarios, the mold pump down may last for hours (Ref. 36).

2.3. "Vacuum" in the Literature

A problem that is common to the majority of RTM research reviewed is the lack of technical depth when dealing with vacuum. In the literature related to RTM, vacuum is usually described anecdotally. One manufacturer states to "Degas with full vacuum." (Ref. 37). In Ref. 38, another resin manufacturer states that 'full vacuum' should be applied to the tool. Labordus and Hoebergen (Ref. 10) discuss gas concentration in the resin at 'absolute vacuum.' In (Ref. 40), the manufacturer specifies that the resin be degassed under vacuum (<740 mm Hg/29 in Hg). These examples show a lack of understanding of vacuum. Firstly, application of 'full' or 'absolute' vacuum is neither possible nor desired. Secondly, the units used to describe vacuum are not sufficient. The standard units of vacuum are torr (or Pa, mbar), reported in absolute pressure, and expressed in orders of magnitude. A typical rotary vane vacuum pump that might be used in RTM would be capable of ~10^{-3} torr level of vacuum. However, in a poorly maintained condition, the pump might be only capable of 30 torr. However, both of these vacuum levels would constitute 29 in. Hg and thereby satisfy the manufacturers criteria for degas as

stated above. However, these two different vacuum levels may result in significantly different levels of degas. Lastly, citing vacuum in inches of mercury or in percent (Refs. 39, 40, 41, 42) implies the use of a dial gage. In general, these devices have poor accuracy and moreover, reach the limit of their measurement range at the point where accuracy in making the measurement is desired thereby exacerbating the inaccuracy. Another common misconception with vacuum in the literature is that it is treated as discrete (i.e., on or off) (Refs. 9, 13).

Accurately measuring the level of vacuum is not trivial. Vacuum dial gages reading in inches of mercury are not sufficient. Other devices such as thermocouple (TC) gages are accurate over a narrow range. Convection gages provide a wider pressure range of operation but, like TC gages, are sensitive to the species of gas they are measuring. They can also become contaminated over time which impairs their operation. Capacitance manometer gages (e.g., MHK Baratron) are preferred as they provide the widest range of operation and a high degree of accuracy. In addition, this type of transducer is gas species independent. However, the cost of these gages may be prohibitive.

2.4. Resin Degassing

Degassing of resin before injection has been shown to reduce the void content of composite components (Refs. 2, 24, 35). Resin degassing pulls out gas bubbles, dissolved gases, and volatiles. During resin preparation and

mixing, gas bubbles are commonly mixed into the resin. During resin manufacture and storage, the resin may absorb atmospheric gases. Resin volatiles include intrinsic volatiles such as styrene, and foreign volatiles such as water. For example, polyester resin contain significant amounts of styrene. Epoxy may contain as much as 2% water by weight (Ref. 43).

A common degassing procedure is to place a container of preheated, mixed resin into a vacuum chamber and pull vacuum for some duration. Foaming of the resin will typically occur and depending on the resin viscosity, it may rise up inside the container similar to a warm soda being poured over ice.

Numerous liquid degassing procedures are reported in (Ref. 44) including boiling under vacuum, pumping on the liquid in a frozen state, and spraying liquid through a fine nozzle into an evacuated flask. Several authors have recently described inert gas purging (sparging) (Ref. 10, 45). However, it should be noted that this procedure was practiced much earlier as described in (Ref. 44). Sparging involves the percolation of a gas (e.g., air or nitrogen) through the resin to allow diffusion of volatiles into the bubbles. The benefit of sparging is that it eliminates the enthalpy associated with homogeneous bubble nucleation (Ref. 6). In Ref. 10, it was found that a piece of Scotch Brite™ placed in the resin during degas would provide heterogeneous nucleation sites. Once formed, the buoyant bubbles would rise to the surface

with additional dissolved gas migrating into the bubble during its journey to the surface.

An important point that is overlooked by all the literature reviewed to date on resin degassing is the pressure head of the resin. The degassing efficacy of simply pulling vacuum on a container of resin is limited. For example, the pressure at a point in a liquid due to the column height of liquid above it is calculated by

$$P = \rho \cdot g \cdot h \qquad [3]$$

where,

- P = Static pressure
- ρ = Density of the resin
- g = gravitational constant
- h = Depth of the resin

For an epoxy, a resin depth of 1 cm equates to a pressure head of ~1 torr. Using equation [3], Figure 4 can be generated to elucidate the degassing pressure experienced by the resin as a function of resin depth and the degassing chamber pressure level.

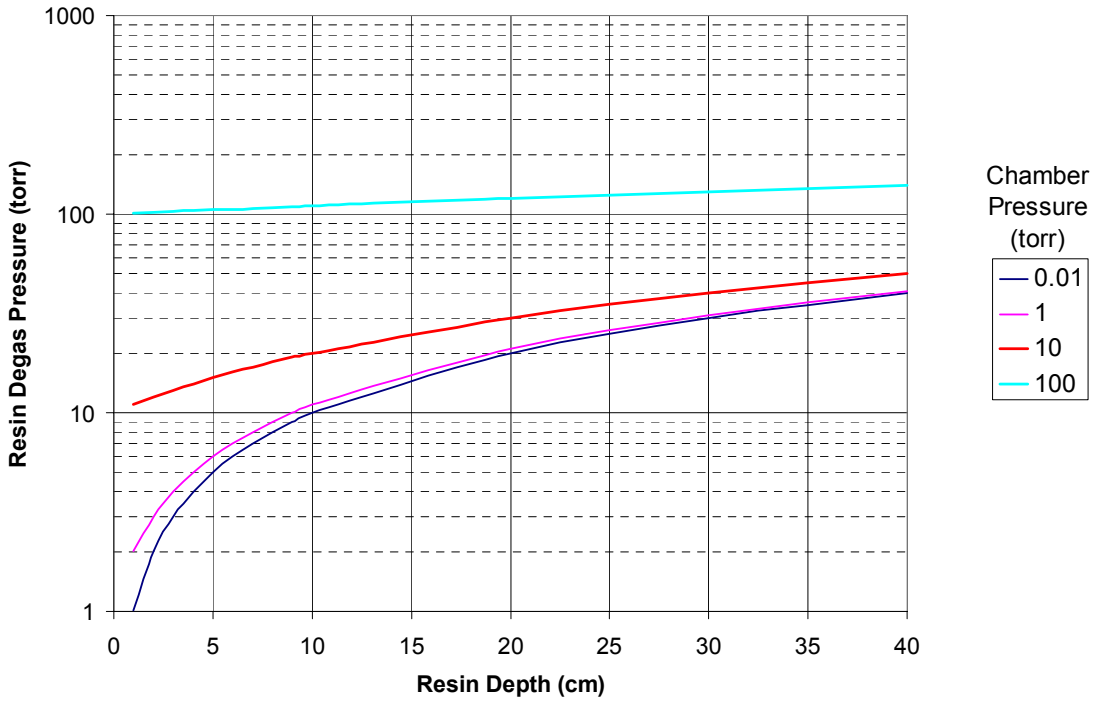

Figure 4. Resin degassing pressure as a function of resin depth and degassing chamber pressure for static (unassisted) degassing

From Figure 4, it is clear that higher levels of resin degassing (lower pressure) require shallower resin depths. The evolution of gas bubbles in the resin imparts a degree of mixing but this is expected to be highly variable and dependant upon the resin viscosity and the level of gas and volatiles present in the resin. The mixing due to resin bubbling also diminishes over time as does the bubbling. The initial flux of gas out of the resin is simply the effervescence of small bubbles within the resin (Ref. 13). The depth of the resin in the container also affects resin degas via sparging.

Resin agitation or shallow resin depths are required to achieve a high level of degas. For example, water and gases that are present in the resin

near the bottom of the container need to be circulated to shallower depths so that they may be exposed to sufficiently low pressures so as to stimulate desorption. Resin agitation that brings about exposure of absorbed gas and water molecules to the liquid/gas interface is expected to result in their release.

Wood (Ref. 46) showed that resin stored in a particular gas environment would come into equilibrium with that environment. This relation was shown to follow Henry's law which can be used to predict the solubility of a gas in a liquid according to the equation

$$S = K_H P \qquad [4] \text{ (Ref. 27)}$$

where,

S = solubility of the gas expressed as mass of solute per volume of solvent

K_H = Henry's law constant for the gas

P = partial pressure of the gas

For example, resin that is exposed to ambient air pressures will absorb nitrogen and oxygen. In order for these 'permanent' gases to be removed requires that the resin be exposed to lower pressures (vacuum). The appropriate level of vacuum will depend on the resin characteristics. For example, polyesters and vinyl esters contain significant amounts of styrene. At room temperature, styrene will boil at approximately 4 torr (Ref. 47). Attempting to degas to vacuum levels below this will result in the volatilization

of the styrene that could possibly affect the resin chemistry resulting in potential acceleration of the Trommsdorff effect. Solvents are commonly employed to lower the viscosity of resins (Ref. 7). In addition, reactive diluents having lower molecular weights and higher vapor pressure are often utilized. These materials are components of the resin but may volatilize during the degas phase and also contribute to the gas load in the mold during injection. The forgoing discussion shows why it has been stated that too high a vacuum will start to remove components of the resin and affect the chemistry. Although possible, no quantitative research has been found on this topic.

Resin can be degassed before or after it is catalyzed. When possible, degas of the components prior to mixing should be performed so as to not consume resin working time (i.e., pot life) once it has been catalyzed. The degas of resin occurs faster with increasing temperature due to the decreased resin viscosity. However, the consequence of increased temperature when working with catalyzed resin is a reduction in the gelation time and the associated time for resin injection.

2.5. Gas Solubility in Resin

The solubility of gases in liquids has been studied extensively (Refs. 41, 42, 44, 46, 47). Raoult's Law (Ref. 27) can be used to describe the pressure in the vapor phase over an ideal solution. It is written as

$$P = P^0 X \qquad [5] \text{ (Ref. 27)}$$

where,

P = vapor pressure of the solution
P^0 = vapor pressure of the pure solvent
X = the mole fraction of the solvent in the solution

Wood (Ref. 46) studied the gas saturation of resin for nitrogen gas. He showed that nitrogen is soluble in resin following Henry's law (Equation 4) and that the solubility of nitrogen in epoxy at standard temperature and pressure (STP) was found to be approximately 20 g/m^3. Air at STP has a density of 1200 g/m^3 so that if the resin is completely devoid of nitrogen gas, it could theoretically be injected into a unvented mold containing residual nitrogen at a level of 20/1200 = 0.0167 atm (12.7 torr) assuming that the final resin pressure was 1 atm absolute (also assuming no dissolution time limitation). Considering that the gas solubility is proportional to pressure, if the final resin pressure were increased to 2 atm absolute, the solubility limit of residual gas pressure increases to 0.033 atm (25.4 torr). In the limit, if the mold contained nitrogen at 1 atm (760 torr), the pressure required to effect complete gas dissolution is approximately 60 atm (900 psi). It is easy to conclude why high hydrostatic resin pressure leads to high quality moldings. Not only is the size of gas pockets reduced by the higher pressure following Boyle's Law, but the gas contained in those pockets is driven into solution in the resin. By holding pressure during gelation, the solubility limit of gasses in solution with the resin remains at a high level. After resin gelation, the pressure is no longer needed to suppress voids.

An increase in the resin temperature will cause an increase in the diffusion coefficient (Ref. 10). This leads to faster void growth or collapse depending on the direction of the diffusion gradient. For example, the void will grow as gas diffuses into it if the surrounding resin is oversaturated with gas (or volatiles) for the particular pressure and temperature conditions (Ref. 48). Conversely, the void will shrink as gas goes into solution in the resin if the surrounding resin is undersaturated. In (Ref. 46) it was found that the gas solubility in resin is independent of temperature and proportional to pressure following Henry's Law (Equation [5]). Therefore, in any injection scenario, a higher hydrostatic pressure will increase the gas solubility in the resin and help minimize voids and bring about their dissolution.

Wood (Ref. 19) showed that the rate of diffusion of nitrogen gas in epoxy is directly related to the resin viscosity. For injection scenarios where one large macrovoid forms, higher temperatures will initially hasten gas dissolution. However, higher temperatures also increase the rate of cure. Even though the diffusion will occur faster initially, it will begin to cease sooner as the resin gels.

The degassing of resin prior to injection removes dissolved gases and volatiles and effectively increases the resin's gas absorptivity. Degas of the resin before injection in effect, prepares the resin for gas dissolution once it is inside the mold. The resin can be thought of as a gas sponge. Having been exposed to atmospheric conditions, the resin absorbs gas from the

atmosphere and is saturated. By degassing, the resin is ‘wrung out’ so that once it is inside the mold, it can absorb gas and swallow up trapped voids, hopefully before gelation. Models for dissolution of the voids are presented in Refs. 9 and 22.

3. MEGA-VOIDS

3.1. Description of a Mega-Void

In the research efforts on flow induced void formation described in Chapter 2.1.1, it is generally assumed (or sought) that the mold is vented such that resin will arrive at the exit port only after the preform is infused and without leaving any large “dry spots” within the mold. Setting up an experiment for this result takes a concerted effort. For example, the elimination of race-tracking by using room temperature vulcanizing (RTV) silicon to sealing the sides of the preform is not uncommon. In Ref. 49, the preforms were carefully cut to minimize the space between the edge of the preform and the side of the mold so as not to leave a lower permeability pathway. Hayward (Ref. 33) described the heighten voidage at the corners of a center injected square panel ostensibly due to the race-tracking of resin that flowed the short distance to the preform edge, and then ran quickly to the corner through the lower permeability pathway at the edge of the preform encapsulating voids in the corner. However, in that study, these voided areas of the test panels were not considered ‘representative’ and so were not tested. Lundstrom (Ref. 6) states that research conducted on voids in simple configurations (i.e., flat panels) is representative for more complex geometries as the formation of voids occurs on a scale much smaller than the mold.

The majority of RTM parts have corners and other non-ideal geometric features. The precise fit-up of preforms near mold cavity edges to eliminate

race-tracking or sealing of preform edges are not practical for part fabrication. In addition, in a complex RTM part, there are a myriad of resin flow paths. In this case, the resin will most certainly arrive at the mold outlet port before resin has stopped flowing into the mold. At this point, there are volumes of trapped gas within the mold. For this study, these volumes have been coined ‘mega-voids.’ Their elimination is sought and so they have been categorized as a type of void. The trapped volumes that persist after cure might be referred to as ‘dry spots’ but based upon the above definition for a mega-void, these volumes are in fact persistent mega-voids. Mega-voids are those voids that encompass a volume containing multiple preform tows. Mega-voids are the result of the inescapable interaction between the mold and preform. The formation of mega-voids is on a scale similar to the mold. A typical RTM setup is shown in Figure 5. Resin flow front lines are shown in the mold along with a hypothetical arrival time. A mega-void is shown inside the mold.

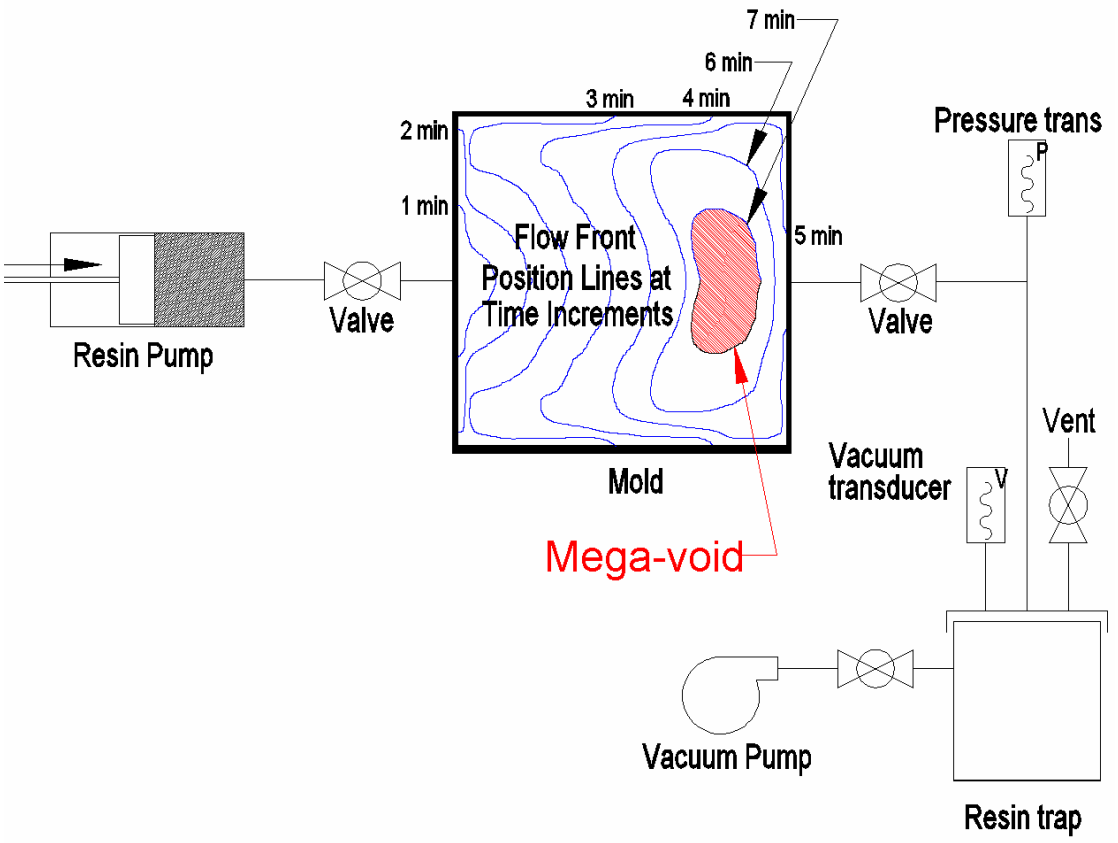

Figure 5. Schematic of RTM configuration showing resin flow lines and the formation of a mega-void

Several possibilities exist for the destiny of the mega-void. It may become small due to resin curing pressure, it might coalesce with other mega-voids. Mold purging (or 'burping') may be performed which could result in the mega-void making it to the vent port. Alternatively, the mega-void might collapse with the residual gas going into solution with the resin.

The ideal fate of the mega-void is for it to shrink and finally collapse. A number of factors influence the potential for the collapse of the mega-void. The factors include:

1. The initial volume of the mega-void
2. The initial residual gas pressure in the mega-void
3. The hydrostatic pressure applied to the resin during cure
4. The solubility of the mega-void gas in the resin

3.2. Processing Continuum

It is hypothesized that there is a continuum of processing conditions that will result in dissolution of the mega-void. For example, a sufficiently high cure pressure (as presented in Chapter 2.5) may eliminate the need for any resin degassing, preform degassing and vacuum use during injection. However, in most situations, a cure pressure sufficiently high to not require the other steps is not possible due to processing aspects such as mold structural limitations, resin injection equipment limitations, press clamping limitations, or pressure limits of core materials within the part. Consequently, a limited injection pressure will dictate resin degas requirements and preform degas requirements. In this way, the goal of this research is to demystify how these three components mutually effect a processing continuum that results in a quality RTM part. A concept for this continuum is shown in Figure 6.

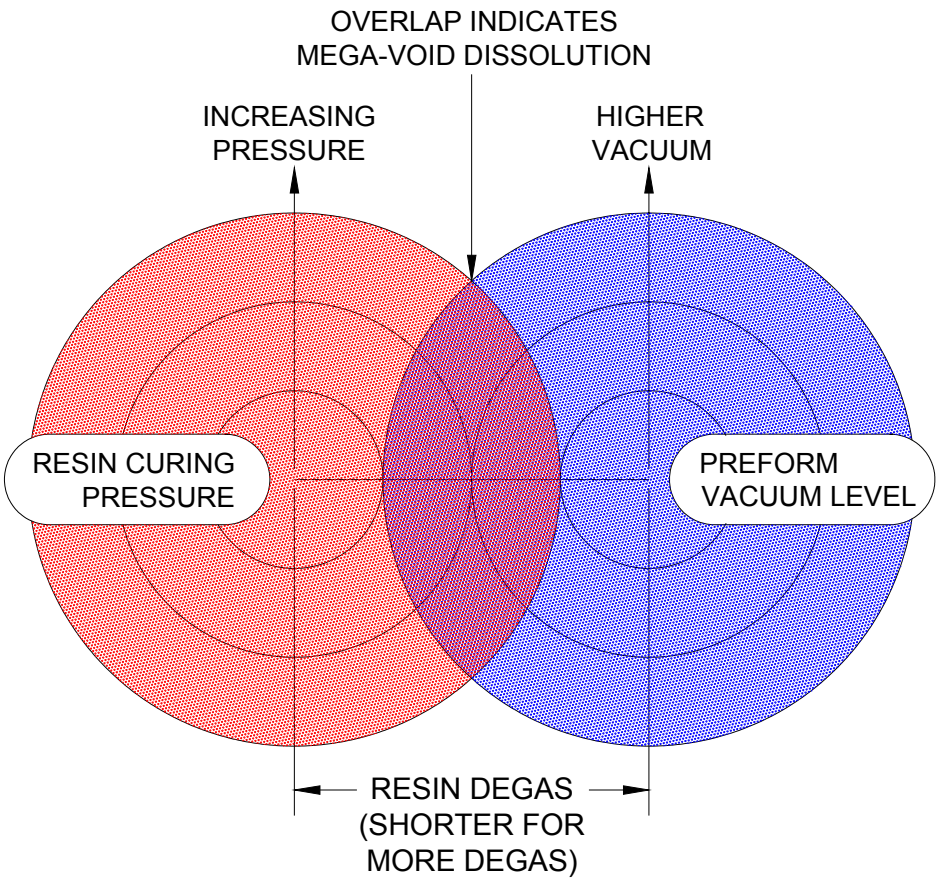

Figure 6. Processing continuum for mega-void dissolution

The continuum shown in Figure 6 consists of two regions, the first representing Resin Curing Pressure and the second representing Preform Vacuum Level. The two regions are separated by an axis representing resin degassing. An overlap area exists that is common to both regions. For process conditions that occur within the overlap area, mega-void dissolution will occur. As the Resin Curing Pressure increases, so does the diameter of its region. Similarly, as the Preform Vacuum Level increases, so does its

diameter. Resin degassing tends to move the two regions closer together, increasing the overlap.

3.3. Mega-Void Initial Volume

The initial volume of a mega-void can vary widely. The volume limits of a mega-void are from zero (nonexistent) to comprising the entire resin volume in the mold. The latter represents the case where the resin inlet and the mold vent are the same (i.e., once the resin injection begins, there is no vent). To maximize part quality, the intent is to minimize the size of mega-voids. Consequently, the design philosophy for RTM molds is to have the resin inlet at one side, or bottom of the mold, and the resin outlet opposite the inlet. In some cases, multiple inlets and outlets might be used. The part, preform, mold design and resin injection approach will all influence the propensity for the resin flow to circumvent the preform and make its way to the outlet before the preform is wet out. The higher the propensity for a mold/preform to race-track, the larger the potential size of mega-void(s).

In order in control and fix the initial volume of the mega-void in this research, an RTM mold with a single entrance/exit port will be used. Any gas evacuation will occur through this port before resin introduction through the same port. This type of injection setup has been coined a ‘blind injection.’ The blind injection setup is shown in Figure 7.

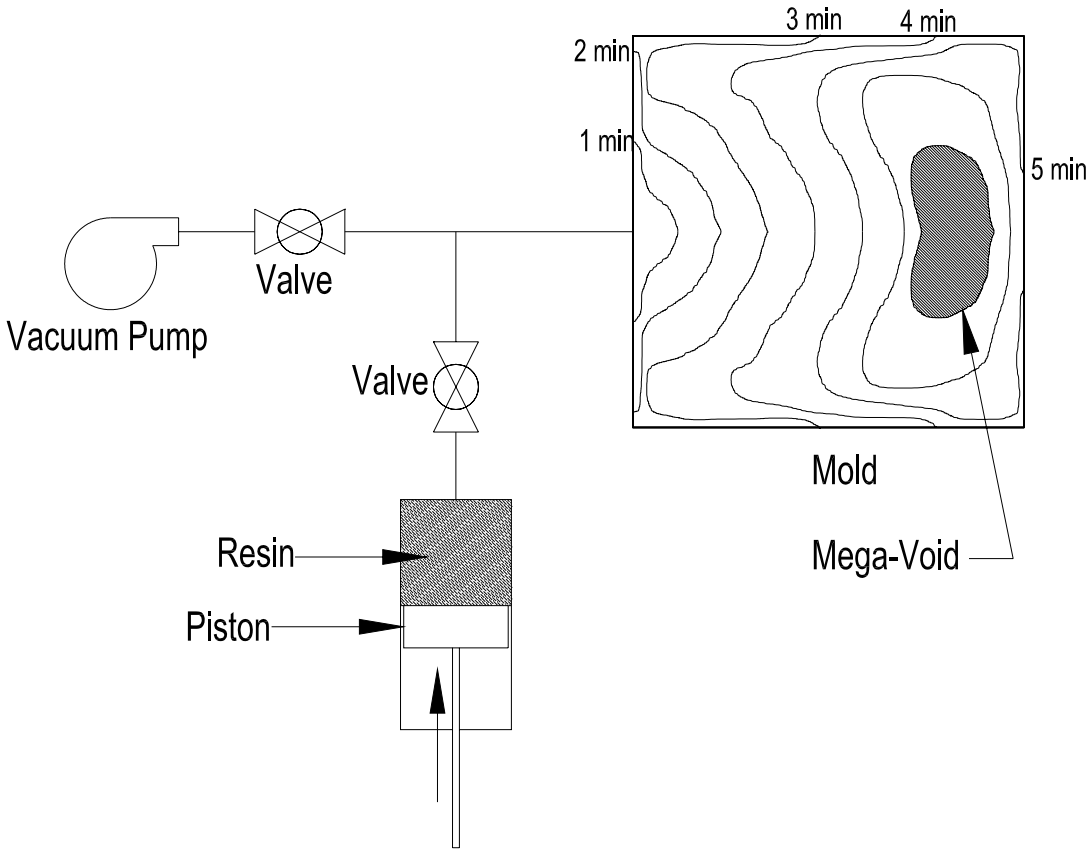

Figure 7. Blind injection setup using a single port for evacuation and resin injection

With this scenario, the initial volume of the mega-void will be the maximum possible for the mold/part. It is expected that processing techniques that lead to the dissolution of the mega-void will also bring about dissolution of the macro and microvoids. This argument is made based upon the fact that dissolution of the mega-void is more challenging compared to macro/micro voids. For example, the residual gas pressure in micro/macro voids will be similar to the initial residual gas pressure in the mega-void. However, once dissolution begins (i.e., gas going into solution in the resin), the mega-void

contains significantly more volume than the micro/macro voids. Consequently, the resin surrounding the mega-void will have to absorb a larger amount of gas and as the mega-void becomes small, it becomes like a macro/micro void surrounded with resin containing a higher dissolved gas content. If the resin surrounding the void becomes saturated with gas for the resin pressure, then dissolution will stop and the void will persist.

3.4. Goals and Objectives

The goal of this research is to develop a fundamental understanding related to formation and dissolution of mega-voids such that it can aid in the fabrication of void-free RTM parts irrespective of mold flow patterns. This work is targeted at high dollar, potentially one-off parts where injection is a critical step. For an example, see Ref. 36. However, the research also benefits all applications of RTM by broadening the understanding of the parameters that effect part quality and allowing the molder to design a process that is sufficient and commensurate with the application.

The objective of this research is to broaden the scientific understanding of processing conditions that effect the quality of a RTM part. These processing conditions include the level and quality of resin degas, the level and quality of preform degas and mold evacuation, and the resin curing pressure. In many respects, RTM processing is still an art rather than a science due to the lack of understanding of the phenomena that occur within the mold. Understanding of the relative importance of each of the processing

parameters and their interactions is important for developing robust RTM part fabrication specifications.

3.5. Research Foci

There are three factors that are critical for the complete dissolution of a mega-void;

1. Preform gas
2. Resin Degassing
3. Gas solubility in resin

There are additional factors that are also expected to affect mega-void dissolution. For example, the preform fiber architecture. However, these are outside of the context of this study.

Preform Gas

In the literature, there is no consensus on the use of vacuum in the mold and hence no clear understanding of Preform Degas. Roychowdhury, Gillespie and Advani (Ref. 12) state, “Processing under vacuum should be avoided.” Young, Wen-Bin and Tseng, Chaw-Wu (Ref. 50) conclude that “Vacuum assistance has no significant influence on the product.” Lundström (Ref. 6) states, “Void content is strongly reduced by an applied vacuum and can be almost complete eliminated.” Chang and Hourng (Ref. 13) state that the “Void will shrink to nothing if the mold has vacuum assistance.” These examples show a wide range of findings and opinions on the use of vacuum in

RTM. This Preform Gas focus in the executed research is aimed at demystifying the prior results and bringing about an understanding of the breadth of conclusions.

Resin Degassing

Unlike preform gas, there is general consensus in the literature as to the benefits of resin degassing. However, the conditions and vacuum levels that constitute an acceptable amount of degas has not been researched nor it is clearly understood.

Gas Solubility in Resin

The solubility of gas in resin has been well studied and the researched documented in the literature. However, the research conducted has been performed using neat resin unaffected by a fabric preform. The prior research found to date has not purposefully address the dissolution of gas within the RTM mold. In addition, the degas state of the resin was not a consideration for the gas dissolution.

Research has been conducted on each of the three factors in order to broaden the understanding and interaction of these factors. In the context of this study, the RTM process involves the degas of resin prior to injection, injection of resin into an evacuated mold, and the holding of hydrostatic pressure during cure. The resin is limited to epoxy using either glass or carbon fiber reinforcement.

Numerous myths have been promulgated related to RTM processing. An adjunct goal of this research is to validate or invalidate some of these myths in order to benefit the science of RTM. The myths include:

1. Degassing of resin prior to injection
2. The use of vacuum on the mold prior to and during injection
3. Water sorption by the preform prior to placement in the mold
4. The use of vacuum on the mold prior to injection in order to remove the aforementioned preform water
5. The treatment of vacuum as discrete
6. The measurement of vacuum levels outside the mold as representative of the actual vacuum levels within the mold

Following in Chapter 4 is the research carried out on Preform Gas. The research comprises preform moisture sorption calculations and experiments, preform molecular gas flow calculations, and preform degassing experiments. Chapter 5 presents the experimental research conducted on resin degassing and gas dissolution in the resin. Chapter 6 presents the results of experiments performed to show the validity of the hypothesized processing continuum when applied to the fabrication of composite panels.

4. PREFORM GAS

There are several contributors to the gas within the mold. First, the mold contains residual air. Second, there may be water present in the preform.

Residual Air

Even at the highest vacuum levels that might be used with RTM, there is still a significant amount of air present in the mold. For example, for a part that requires 0.5 L of resin, the initial quantity of gas molecules in the mold is approximately 1.3×10^{22} based on the fact that a mol of gas at standard temperature and pressure occupies 22.4 L and contains 6.02×10^{23} molecules. If the mold is evacuated to 0.76 torr ($1/1000^{th}$ of an atmosphere), the number of molecules is reduced to 1.3×10^{18}, arguably still a substantial number. In addition, mold release agents are used and there will likely be residual release that will volatilize during processing and contribute to the gas load in the mold.

Preform Water

Before and during lay-up, the preform is exposed to ambient conditions for extended periods of time. During exposure, the preform can absorb and adsorb moisture from the air. Three mechanisms contribute to moisture uptake by the preform:

1. The adsorption of water monolayers on the surface of the fibers

2. The absorption of water in the fiber sizing (hygroscopic)
3. Capillary condensation within the small features of the fiber preform

Fibrous preform materials have a significant surface area due to small diameters of the reinforcement fibers. Consequently, gases will adsorb onto the surfaces of these fibers and be held there until conditions are such as to stimulate their release. Of the common adsorbed gases, water is the most tenacious. Water is much less volatile than would be expected from its molecular weight (Ref. 40) leading to the fact that it takes significant vacuum levels, temperatures and time to liberate the monolayers of water. In a chamber that has been exposed to ambient conditions, after the initial evacuation of gas to the millitorr level, the remaining gas contains 90% to 95% water vapor (Ref. 40). In addition, fibers commonly have an epoxy-based sizing that is used to protect the fibers and enhance bonding to the matrix (Ref. 51). Epoxy is well known to be hygroscopic and consequently, the sizing will contain absorbed water.

Capillary condensation may also contribute to the amount of water contained in the preform. Capillary condensation is the condensation of liquid bridges in small surface features. More fundamentally, capillary condensation is a gas-liquid phase transition shifted by confinement (Ref. 52). Through this phenomenon, water vapor in air will condense into small features even at

moderate levels of humidity. For example, at a relative humidity (RH) of 50%, water will condense in a capillary of 1.5 nm in size and smaller (Ref. 53).

Hayward (Ref. 35) concluded that the use of vacuum during injection did not bring about the removal of moisture from the preform. However, in that study, the vacuum levels used were above the boiling pressure of water at ambient temperature (i.e., the vacuum was not sufficient to fully volatilize water). In addition, the fiber volumes (glass fiber) were not reported but were likely 30% to 40% as reported elsewhere by the same author in Ref. 34. If water were present in Hayward's preform, it is uncertain if it would have been removed by the applied vacuum.

Prior research in the area of preform moisture adsorption is limited. No references have been found that presents a quantitative analysis of the phenomenon. Lundström (Ref. 6) describes baking out a preform and the associated change in resin flow characteristics. However, the goal of the baking in that research was to bake the preform sufficiently hot enough (565 °C) to remove the sizing from the fiber. It is interesting to note that in addition to removing the fiber sizing, the bake-out would have removed the adsorbed water on the surface, the absorbed water in the sizing and any water residing in the preform due to capillary condensation. Depending on the time duration and the environmental relative humidity, the preform may have had a significantly lower water content than the unbaked preforms.

Research on Preform Gas

Research on preform gas was conducted in four areas. Moisture sorption calculations where performed in order to estimate the amount of water that might be contained in a preform prior to placement in the mold. Subsequently, preform moisture sorption experiments were performed to measure mass gains by a preform sample when aged under humid conditions. Next, molecular flow calculations were performed to evaluate the gas flow conditions within a fibrous preform. Finally, experiments were performed to look at residual gas pressures inside the mold as a function of pressures measured external to the mold.

Preform vacuum level is one region of the processing continuum shown in Figure 6 (page 24). As presented in Chapter 3, several mechanisms are responsible for the residual gas pressure within the preform inside the mold. First, moisture that may be present in the preform would contribute to the residual gas level. Following in 4.1, calculations are performed to estimate the amount of water that might be present in the preform. Subsequently, in 4.2, moisture sorption experiments were conducted to empirically evaluate the residual moisture in the preform. The experimental procedure and results are presented. Section 3 of this Chapter describes calculations performed to investigate the nature of gas flow within the preform. The results provide some insight into the difficulty in achieving low gas pressure levels within the fibrous preform. Section 4 of this Chapter presents experimental research that

was conducted to look at residual gas pressures within the mold (preform) as a function of measurements made external to the mold.

4.1. Moisture Sorption Calculations

Fibrous preform materials have significant surface area due to their small fiber diameters. Fibrous materials can hold water through the adsorption of monolayers, via capillary condensation and resin sizing hygroscopicity. Of the common adsorbed gases, water is the most tenacious.

The objective of the Moisture Sorption Calculations is to estimate the water content for carbon fiber and glass fiber preform materials as a function of relative humidity.

The method for the Moisture Sorption Calculations considers three modes of water sorption: water monolayers on the fiber, capillary condensation between fibers and fiber sizing hygroscopicity. Calculate the mass of water for water monolayers using the fiber surface area. Calculate the mass of water via capillary condensation. Calculate the mass of water taken up due to fiber sizing hygroscopicity by calculating the volume of sizing.

The following assumptions were made in performing the Moisture Sorption Calculations

1. Water will condense in features 1.5 nm and smaller at 50% relative humidity, 36 nm for 98% relative humidity (Ref. 54)
2. Fibers are uniformly distributed and fibers contact one another at 25% of available sites

3. Fiber sizing hygroscopicity maximum at 5% by weight (Ref. 32)
4. The fibers are assumed to have a surface roughness factor of five resulting in an increase in the actual surface area by this factor (Ref. 40)
5. Fiber sizing is 0.2 μm thick (Ref. 51)

The following inputs were used in the Moisture Sorption Calculations:

1. Fiber diameter carbon = 7 μm (Ref. 56)
2. Fiber diameter glass = 15 μm (Ref. 56)

Example calculations for water monolayer adsorption are shown in Figure 8 for carbon fiber and Figure 9 for glass fiber.

Givens:

$Carbon\_Fiber_{diameter} := 2.82 \cdot 10^{-4} in$ $\quad Carbon\_Fiber_{diameter} = 7.163 \times 10^{-6} m$

$Carbon\_Surface\_Roughness = 5$

$Monolayers := 50$

Calculation:

$Gas\_Molecule\_Diameter := 0.3 \cdot 10^{-9} m$

$$Surface\_Area\_cubic\_meter\_Carbon := \frac{1m^3 \cdot Carbon\_Surface\_Roughness}{Carbon\_Fiber_{diameter}^2} \cdot Carbon\_Fiber_{diameter} \cdot \pi$$

$$Surface\_Area\_cubic\_meter\_Carbon = 2.193 \times 10^6 m^2$$

$$Gas\_Mols\_Per\_Area := \frac{Monolayers}{Gas\_Molecule\_Diameter^2} \qquad Gas\_Mols\_Per\_Area = 5.556 \times 10^{20} \frac{1}{m^2}$$

$$Gas\_Mols\_Water\_Carbon := Surface\_Area\_cubic\_meter\_Carbon \cdot Gas\_Mols\_Per\_Area$$

$$Gas\_Mols\_Water\_Carbon = 1.218 \times 10^{27}$$

$$Mass\_Water\_Carbon := \frac{Gas\_Mols\_Water\_Carbon}{6.02 \cdot 10^{23}} \cdot 18gm$$

$$Mass\_Carbon\_cubic\_meter := 1800kg \cdot .785$$

$$Percent\_water\_Carbon := \frac{Mass\_Water\_Carbon}{Mass\_Carbon\_cubic\_meter}$$

$$Percent\_water\_Carbon = 2.578\%$$

Figure 8. Water monolayer adsorption calculations for carbon fiber

Givens:

$Glass\_Fiber_{diameter} := 15 \cdot 10^{-6} m$

$Glass\_Surface\_Roughness := 5$

$Monolayers := 50$

$Gas\_Molecule\_Diameter := 0.3 \cdot 10^{-9} m$

Calculations:

$$Surface\_Area\_cubic\_meter\_Glass := \frac{1 m^3 \cdot Glass\_Surface\_Roughness}{Glass\_Fiber_{diameter}^2} \cdot Glass\_Fiber_{diameter} \cdot \pi$$

$$Surface\_Area\_cubic\_meter\_Glass = 1.047 \times 10^6 m^2$$

$$Gas\_Mols\_Per\_Area := \frac{Monolayers}{Gas\_Molecule\_Diameter^2} \qquad Gas\_Mols\_Per\_Area = 5.556 \times 10^{20} \frac{1}{m^2}$$

$$Gas\_Mols\_Water\_Glass := Surface\_Area\_cubic\_meter\_Glass \cdot Gas\_Mols\_Per\_Area$$

$$Gas\_Mols\_Water\_Glass = 5.818 \times 10^{26}$$

$$Mass\_Water\_Glass := \frac{Gas\_Mols\_Water\_Glass}{6.02 \cdot 10^{23}} \cdot 18 gm$$

$$Mass\_Water\_Glass = 17.395 kg$$

$$Mass\_Carbon\_cubic\_meter := 2400 kg \cdot .785$$

$$Percent\_water\_Glass := \frac{Mass\_Water\_Glass}{Mass\_Carbon\_cubic\_meter}$$

$$Percent\_water\_Glass = 0.923\%$$

Figure 9. Water monolayer adsorption calculations for glass fiber

The capillary condensation calculations are based on the formation of a meniscus between adjacent fibers. The small features between fibers are expected to be conducive to the formation of a water meniscus. The area of consideration is shown in Figure 10.

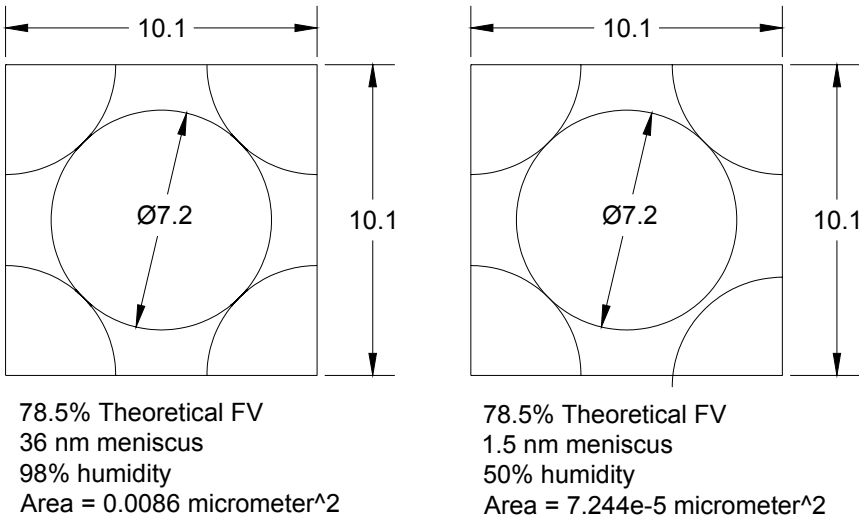

Figure 10. Unit cell for basis of capillary condensation calculation for carbon fibers. Dimensions are in micrometer

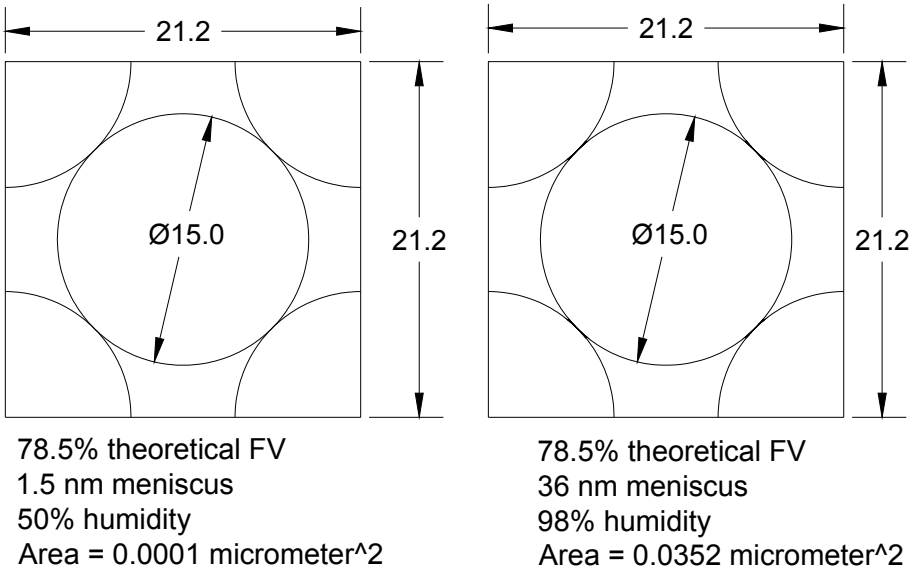

Figure 11. Unit cell for basis of capillary condensation calculation for glass fibers. Dimensions are in micrometer

Example calculations for capillary condensation sorption are shown in Figure 12 for carbon fiber and Figure 13 for glass fiber.

For the water uptake due to hygroscopicity of the fiber sizing, the volume of the sizing is calculated followed by its mass. Water mass is then taken as 5% of this mass. An example of the hygroscopicity calculation is shown in Figure 14 for carbon fiber and Figure 15 for glass fiber.

50% relative humidity

Cell volume	102.8196	
Fiber volume	0.785	
Water volume	0.00028976	
% water by volume	0.00036912	0.037%
Fiber mass	1.413	
Water mass	0.00028976	
% water by mass	0.00020507	0.02%
Fraction of fibers actually touching	25%	
Estimated % water by mass	0.005%	

98% relative humidity

Cell volume	102.8196	
Fiber volume	0.785	
Water volume	0.034576	
% water by volume	0.04404586	4.40%
Fiber mass	1.413	
Water mass	0.034576	
% water by mass	0.02446992	2.45%
Fraction of fibers actually touching	25%	
Estimated % water by mass	0.612%	

Relative Humidity	Weight % Water
50%	0.005%
98%	0.61%

Figure 12. Capillary condensation calculations for carbon fiber

50% relative humidity

Cell volume	449.44	
Fiber volume	0.785	
Water volume	0.0004	
% water by volume	0.00051	0.051%
Fiber mass	1.884	
Water mass	0.0004	
% water by mass	0.000212	0.02%
Fraction of fibers actually touching	25%	
Estimated % water by mass	0.005%	

98% relative humidity

Cell volume	449.44	
Fiber volume	0.785	
Water volume	0.1408	
% water by volume	0.179363	17.94%
Fiber mass	1.884	
Water mass	0.1408	
% water by mass	0.074735	7.47%
Fraction of fibers actually touching	25%	
Estimated % water by mass	1.868%	

Relative Humidity	Weight % Water
50%	0.005%
98%	1.87%

Figure 13. Capillary condensation calculations for glass fiber

Givens:

$Carbon\_Fiber_{diameter} := 2.82 \cdot 10^{-4} \cdot in$

$Sizing_{density} := 1200 \frac{kg}{m^3}$

$Carbon\_Surface\_Roughness = 1$

$SizingPercentMassGain = 5\%$

$Sizing_{Thickness} := .00002cm$

Calculation:

$$Surface\_Area\_cubic\_cm\_Carbon = \frac{1cm^3 \cdot Carbon\_Surface\_Roughness}{Carbon\_Fiber_{diameter}^2} \cdot Carbon\_Fiber_{diameter} \cdot \pi$$

$$Surface\_Area\_cubic\_cm\_Carbon = 4.386 \times 10^3 \, cm^2$$

$$Sizing_{volume} := Surface\_Area\_cubic\_cm\_Carbon \cdot Sizing_{Thickness}$$

$$Sizing_{volume} = 0.088 \, cm^3$$

$$Sizing_{mass} := Sizing_{volume} \cdot Sizing_{density}$$

$$Sizing_{mass} = 1.053 \times 10^{-4} \, kg$$

$$MassGain := SizingPercentMassGain \cdot Sizing_{mass}$$

$$MassGain = 5.263 \times 10^{-6} \, kg$$

$$Mass\_Carbon\_cubic\_cm := 1.8gm \cdot .785$$

$$MassGainPercentage := \frac{MassGain}{Mass\_Carbon\_cubic\_cm}$$

$$MassGainPercentage = 0.372\%$$

Figure 14. Fiber sizing hygroscopicity calculations for carbon fiber

Givens:

$Glass\_Fiber_{diameter} := 15 \cdot 10^{-6} m$

$Sizing_{density} := 1200 \frac{kg}{m^3}$

$Glass\_Surface\_Roughness = 1$

$SizingPercentMassGain = 5\%$

$Sizing_{Thickness} := .00002cm$

Calculation:

$$Surface\_Area\_cubic\_cm\_Glass = \frac{1cm^3 \cdot Glass\_Surface\_Roughness}{Glass\_Fiber_{diameter}^2} \cdot Glass\_Fiber_{diameter} \cdot \pi$$

$$Surface\_Area\_cubic\_cm\_Glass = 2.094 \times 10^3 cm^2$$

$Sizing_{volume} := Surface\_Area\_cubic\_cm\_Glass \cdot Sizing_{Thickness}$

$$Sizing_{volume} = 0.042 cm^3$$

$Sizing_{mass} := Sizing_{volume} \cdot Sizing_{density}$

$$Sizing_{mass} = 5.027 \times 10^{-5} kg$$

$MassGain := SizingPercentMassGain \cdot Sizing_{mass}$

$$MassGain = 2.513 \times 10^{-6} kg$$

$Mass\_Glass\_cubic\_cm := 2.4gm \cdot .785$

$$MassGainPercentage := \frac{MassGain}{Mass\_Glass\_cubic\_cm}$$

$$MassGainPercentage = 0.133\%$$

Figure 15. Fiber sizing hygroscopicity calculations for glass fiber

The results of preform water content calculations are shown in Figure 16 to Figure 21 for carbon fiber and glass fiber preforms.

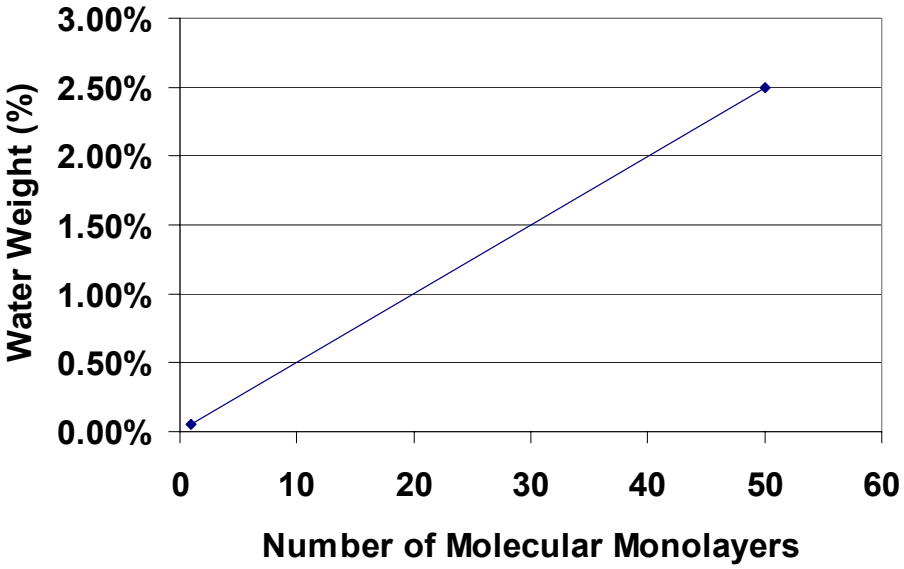

Figure 16. Carbon preform water content due to molecular monolayers

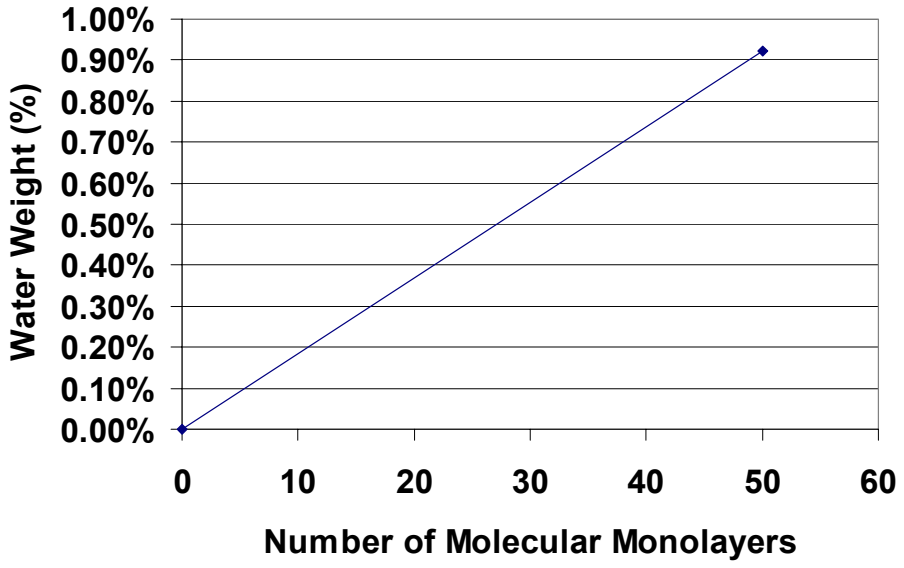

Figure 17. Glass preform water content due to molecular monolayers

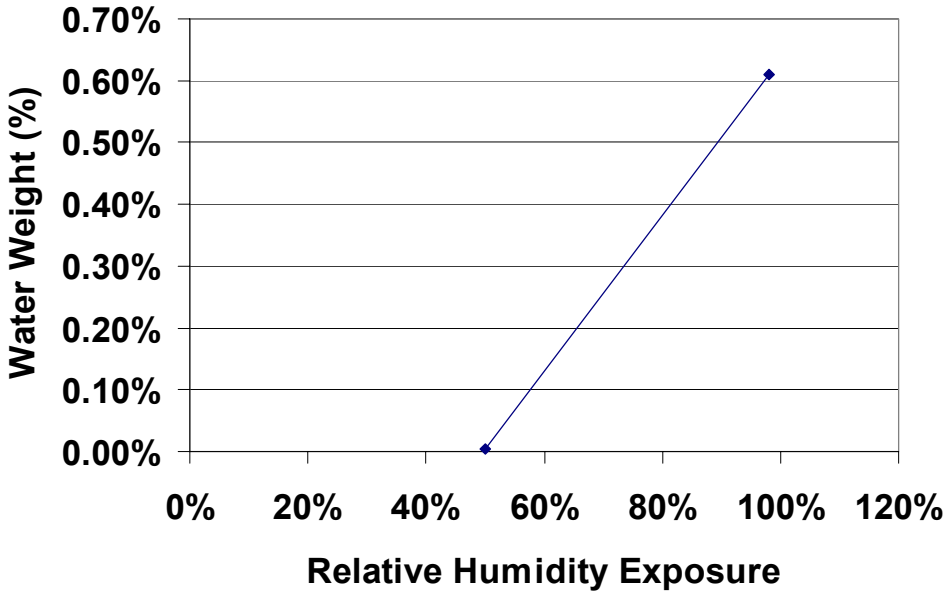

Figure 18. Carbon preform water content due to relative humidity exposure (capillary condensation)

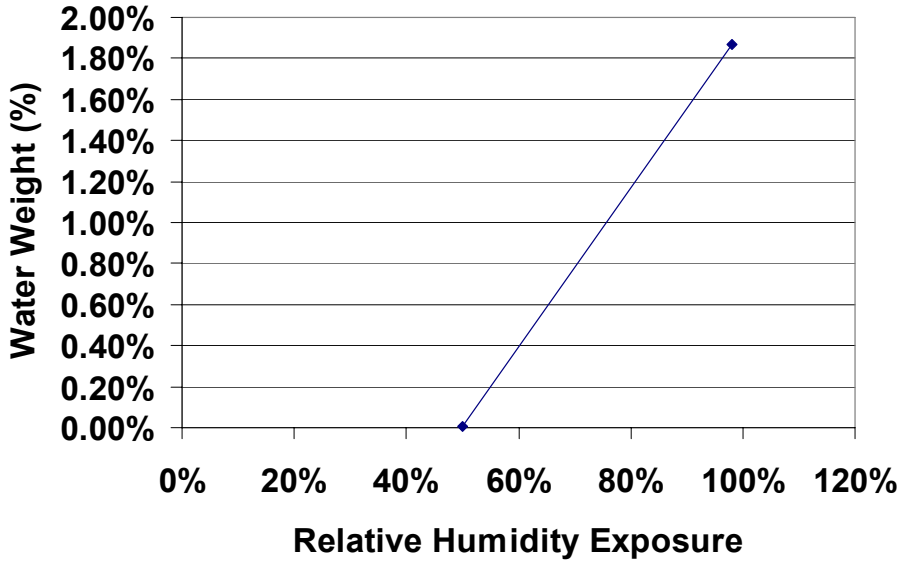

Figure 19. Glass preform water content due to relative humidity exposure (capillary condensation)

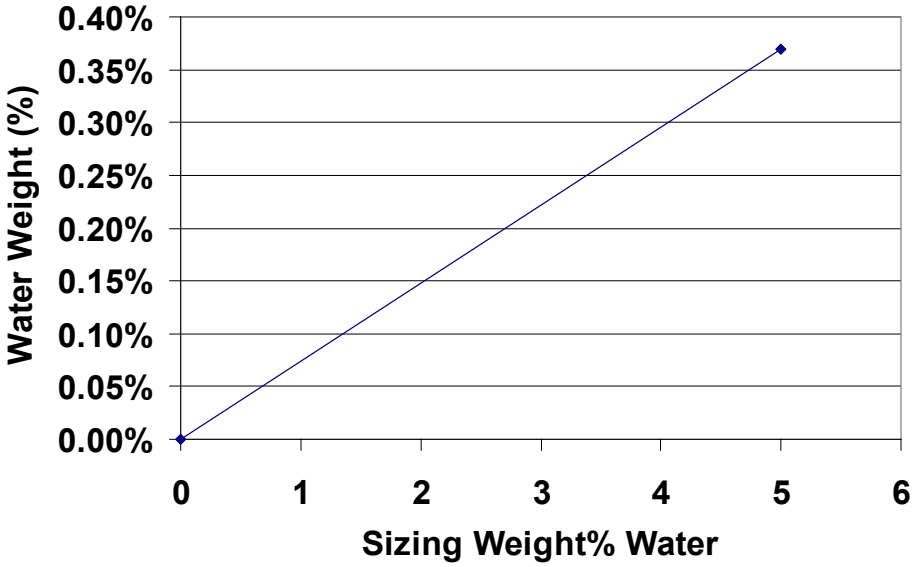

Figure 20. Carbon preform water content due to sizing hygroscopicity

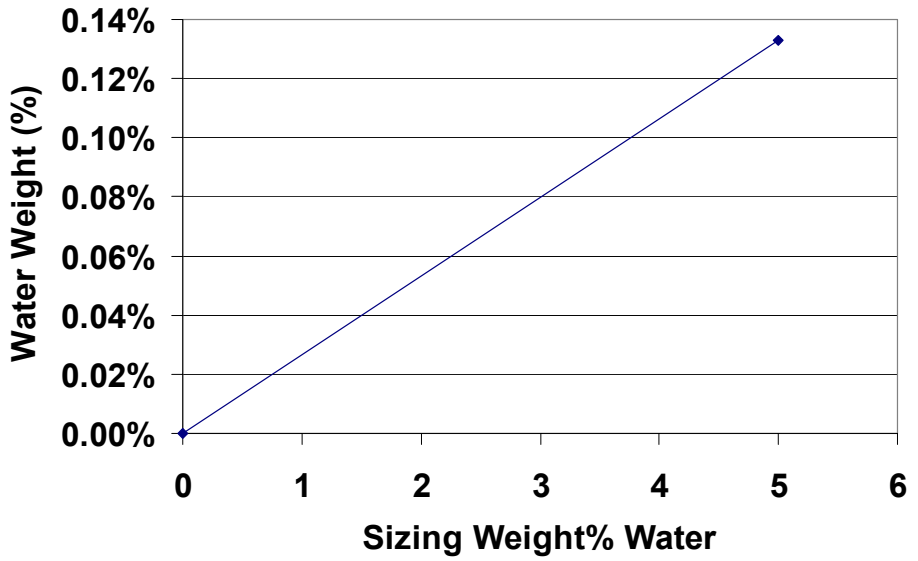

Figure 21. Glass preform water content due to sizing hygroscopicity

Conclusions

The calculations show that carbon fabric has the potential to hold a significant amount of water. Of the three mechanisms proposed for water

uptake by the preform, water monolayers has the largest potential for contribution to water mass in the preform. The calculations show that capillary condensation is the second largest contributor to preform water. Fiber sizing hygroscopicity appears to be the smallest contributor to preform water. Although not performed for glass fiber, these results would apply similarly but the overall magnitude would be reduced due to the larger fiber diameter and high density of glass.

4.2. Moisture Sorption Experiments

Experiments were conducted to measure the residual water content in a sample of glass fiber cloth and carbon fiber cloth as a function of relative humidity.

The objective of these experiments is to measure the mass gain in a sample of glass and carbon fiber as a function of relative humidity storage of the samples.

The experimental setup for the moisture sorption experiments consisted of a heated vacuum chamber for preform drying and an insulated box for sample aging.

The vacuum chamber consisted of a 30 cm (12 inch) long conflat nipple (Appendix 1). One end was sealed with a blind flange while the other end had a conflat to NW15 (ISO KF) vacuum fitting. This was in turn connected to the two stage rotary vane vacuum pump (Appendix 1). For heating, the conflat nipple was wrapped with a silicone pad heater. A thermocouple was secured

to the side of the chamber for feedback to the proportional integral derivative (PID) temperature control system (Appendix 1). A picture of the experimental setup for drying is shown in Figure 22.

For aging fabric samples, an insulated box was constructed from rigid foam insulation. A pan of water was placed in the bottom of the box. A rack was positioned on top of pan. Fabric samples and the hygrometer were placed on the rack. A picture of the box with samples and hygrometer is shown in Figure 23 and Figure 24.

Figure 22. Vacuum chamber used to dry preform samples

(a) (b)

Figure 23. Insulated box for preform water sorption experiments. Box closed (a) and open (b) showing preform samples and hygrometer

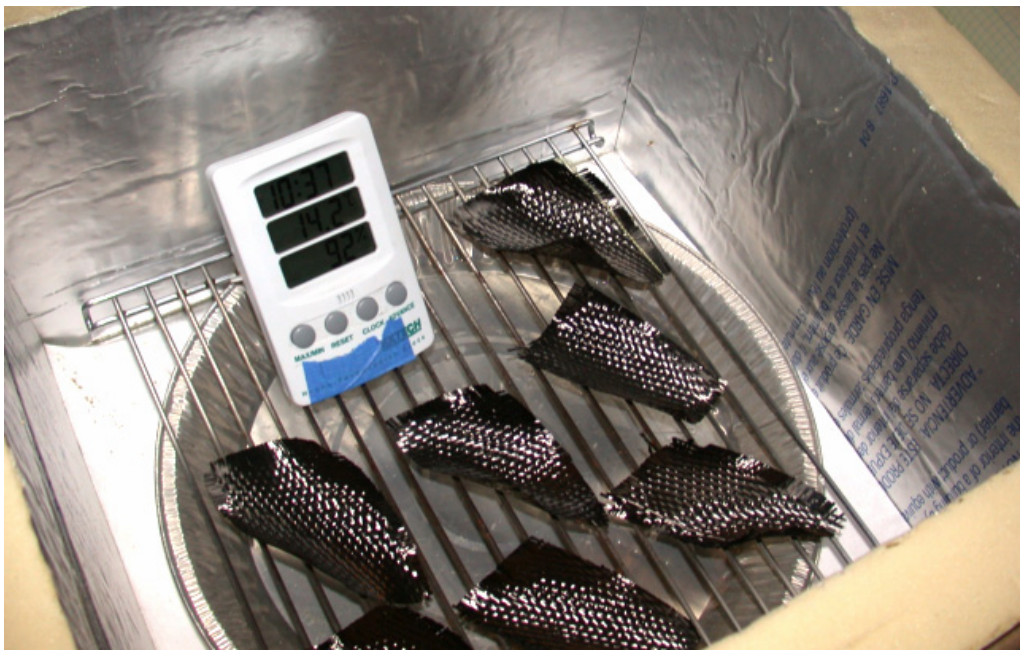

Figure 24. Carbon preform samples during aging in humidifying chamber

Testing

Seven samples of glass and carbon fabric preform materials where cut to approximately 9 cm (3.5 inch) squares. The material used for each are summarized in Table 1.

Table 1. Preform materials for moisture sorption experiments

Fabric Type	Details	Uncompressed Ply Thickness and Fiber Volume (FV)
Glass fiber fabric	Hexcel, 204 grams per square meter (gsm) (6 oz. per square yard) glass cloth, Style 3733	0.28 mm (0.011 inch) 30 % FV
Carbon fiber fabric	Hexcel, 370 gsm, SGP370-4, 8HS, 6k, IM7 GP	0.48 mm (0.019 inch) 40 % FV

(see Appendix 2 for additional information)

Subsequent to bake-out, samples were immediately weighed using a 100 microgram range scale shown in Figure 25 (Appendix 1).

Figure 25. Precision scale used to measure fabric mass changes

With initial mass measurements made, preform samples were aged for approximately 72 h under ambient conditions of approximately 60 % relative humidity and approximately 20 °C. Mass measurements were again taken and the samples were transferred to insulated box. Sample mass measurements were taken periodically.

Results

Results of the preform water sorption test are shown in Figure 26 for fiber glass cloth and Figure 27 for carbon fiber cloth.

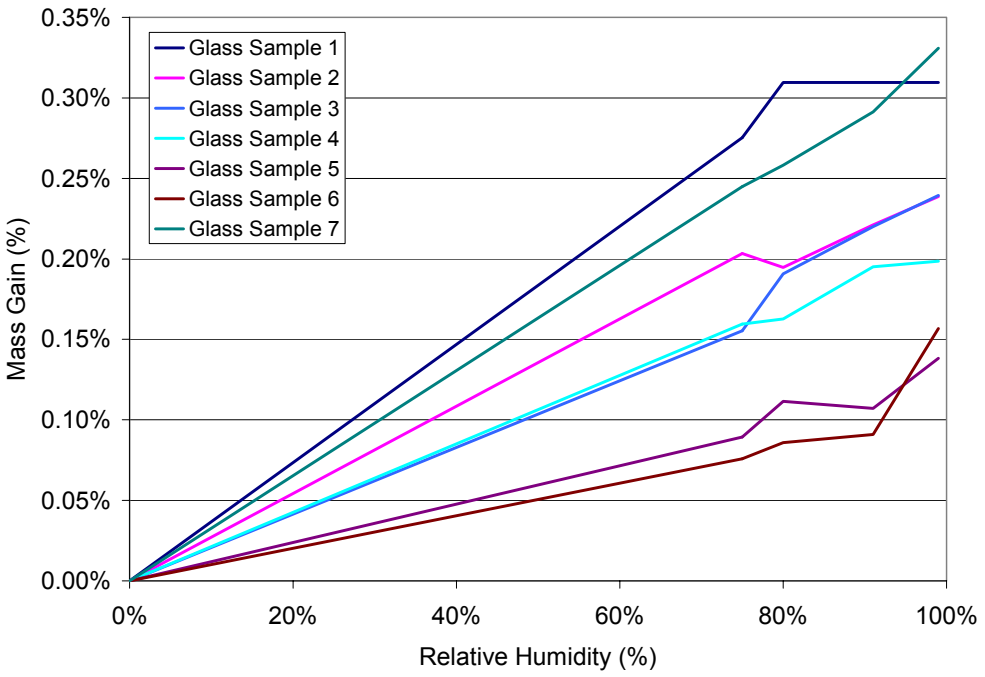

Figure 26. Preform mass gain measurements for fiber glass preform

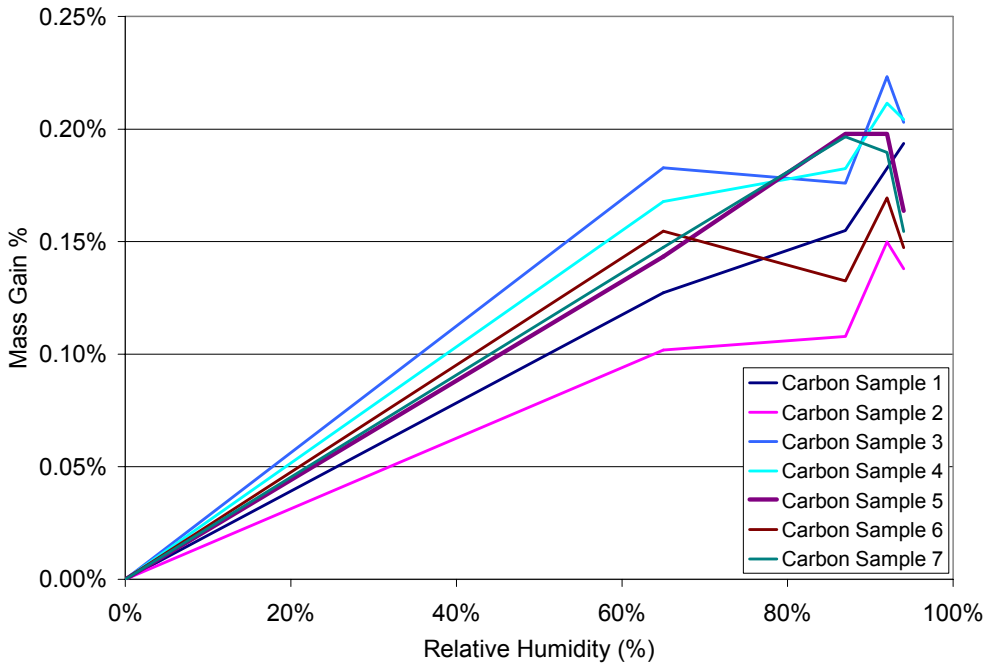

Figure 27. Preform mass gain measurements for carbon fiber preform

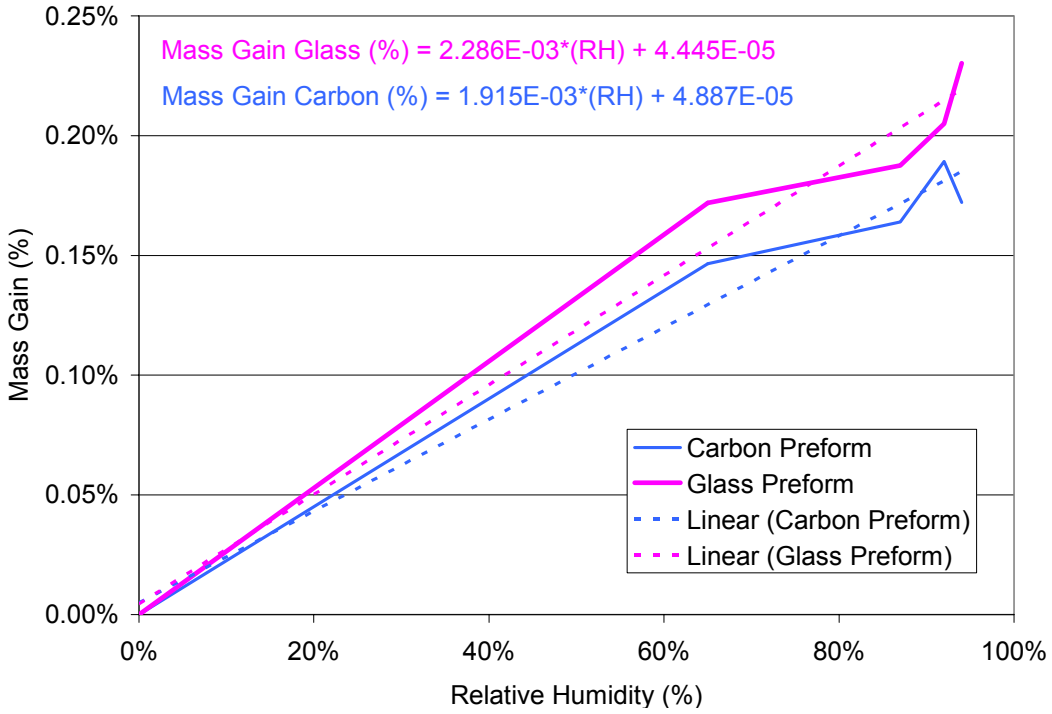

Figure 28. Average mass gains and linear regression analysis for carbon and glass preform water sorption experiment

Conclusions

Glass and carbon fiber preform samples had a measurable weight gain due to aging in a humid environment. The following are concluded.

1. Glass fiber cloth had an average maximum mass gain of 0.22% at an RH of approximately 95%
2. Carbon fiber had an average maximum mass gain of 0.18% at a RH of approximately 95%.

The measured preform water sorption was not as significant as shown possible in calculations presented in Chapter 4.1. The calculations in 4.1

showed that an approximate mass gain of up to 3 % was possible. There are several reasons thought to contribute to the discrepancy:

1. The water monolayer mechanism depends directly on the number of adsorbed monolayers. The actual number of water monolayers is considered to be approximately two.
2. The experimental research here utilized single plies of fabric. The capillary condensation mechanism is predicated on fiber to fiber contact which would increase with increasing number of plies of fabric.
3. The capillary condensation mechanism proposed is not expected to be significant when fiber volumes are low as is the case when a preform is uncompacted (i.e., not under any mechanical consolidation pressure).
4. The hygroscopic component requires longer time durations and/or elevated temperatures during humidity ageing to maximize the moisture sorption.

4.3. Molecular Flow Calculations

The nature of gas flow is determined by examining the Knudsen number. The Knudsen number is a dimensionless ratio of a gas molecule's mean free path (MFP) to the characteristic dimension of the flow path (e.g., diameter). The MFP is the average distance a gas molecule will travel before it sustains a collision with another gas molecule. Obviously, as the density of a gas increases, the mean free path will decrease. For example, a molecule of nitrogen at standard temperature and pressure (STP) has a MFP of ~66 nm

(Ref. 40). However, if the pressure is reduced to 0.1 torr, the MFP increases to 0.5 mm. Now consider the flow of gas through a tube. If the tube diameter is large relative to the MFP, the characteristics of the flow are governed by molecule-to-molecule collisions. This is known as viscous or continuum flow. However, in the situation where the MFP becomes similar in size to the diameter of the tube the nature of the flow is governed by molecule to wall interactions. This is known as molecular flow. In molecular flow, gas molecules will land on a wall briefly before they leave. This dwell time is referred to as the "Sojourn time." An important point is that the arrival and departure trajectory are independent. The stochastic molecule departure is described by a cosine law stated as,

$$P = \tfrac{1}{2} \cdot \cos\theta \qquad [6] \text{ (Ref. 40)}$$

where,

P = Probability of desorption trajectory at angle θ

θ = Desorption trajectory (shown in Figure 29)

It can be shown that the most probable desorption trajectory is normal to the surface ($\theta = 0°$). Consequently, a molecule has an equal probability of going forward as it does going back (Ref. 40, 55).

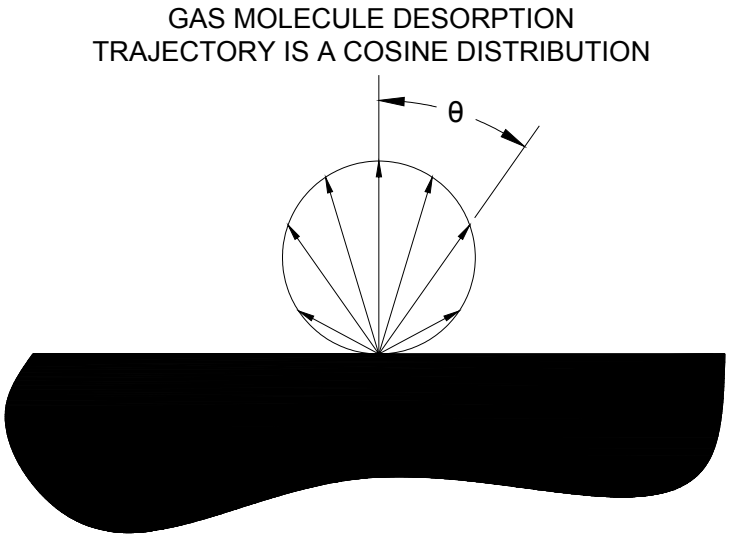

Figure 29. Molecular desorption trajectory follows a cosine distribution

Viscous flow occurs when the Knudsen number is < 0.01 while molecular flow occurs when the Knudsen number is > 1. Gas flow with Knudsen numbers between 0.01 and 1 is referred to as transitional and is neither fully viscous nor molecular.

The objective of this effort is to analytical investigate gas flow conditions within a fibrous preform inside the RTM mold.

The method used to evaluate the nature of gas flow within a fibrous preform required calculating an equivalent characteristic flow dimension. Figure 30 shows a scaled cross section of unidirectional fibers with a 60% fiber volume. The average flow area is shown along with an approximate equivalent flow area. The latter was used in calculations below to evaluate the gas flow through the fiber preform.

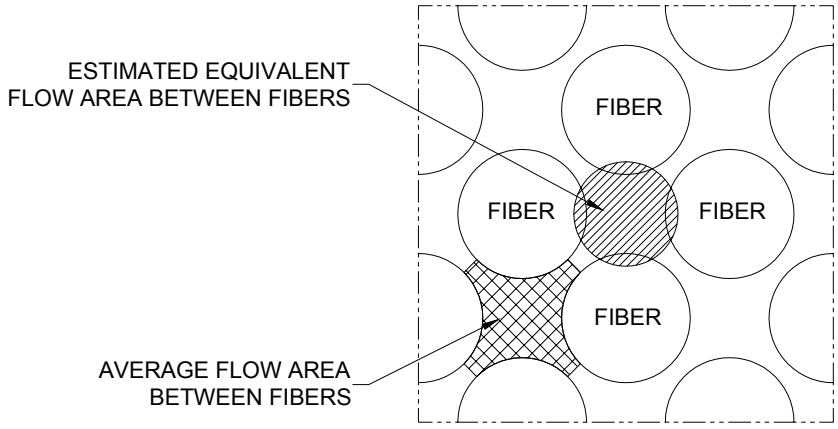

Figure 30. Gas flow areas for rarified gas flow analysis, spacing reflects a 60% fiber volume

Assumptions

The following assumption apply:

1. The fibers are assumed to be uniformly distributed and parallel and continuous. This should be conservative as in reality, the tows are woven and so undulate. In addition, the weave has fibers running in transverse directions making gas flow paths more tortuous. These assumptions are non-conservative with respect to flow between tows where are larger pathway may exist.
2. The flow area cross section between fibers has an irregular shape at best. An equivalent area flow cross section is assumed be circular as shown in Figure 30.

Inputs

The following inputs were used in the calculations:

1. Fiber diameter glass = 15 μm (Ref. 56)

2. Fiber diameter carbon = 7 μm (Ref. 56)

Calculations

A sample molecular flow calculations for carbon fabric is shown in Figure 31.

$FiberDiameter := 15 \cdot 10^{-6} m$

Carbon fiber diameter = 7.17 E-6 m
Glass fiber diameter = 15 E-6 m

$FiberBulkFactor := .14$ $\qquad \frac{.806}{.7071} = 1.14$

$FiberToFiberSpacing = FiberDiameter(1 + FiberBulkFactor)$

$FiberToFiberSpacing = 6.732 \times 10^{-4} in$

$UnitCellArea := \left[\frac{(FiberToFiberSpacing \cdot 2)}{2}^2\right]$

$FiberAreaUnitCell = 2 \cdot \pi \cdot \frac{FiberDiameter^2}{4}$

$FiberAreaUnitCell = 3.534 \times 10^{-10} m^2$

$FiberVolume := \frac{FiberAreaUnitCell}{UnitCellArea}$

$FiberVolume = 0.604$

$FlowAreaBetweenFibers = FiberToFiberSpacing^2 - \frac{\pi FiberDiameter^2}{4}$

$EqvDiameterBetweenFibers = \left(\frac{FlowAreaBetweenFibers}{\pi}\right)^{.5} \cdot 2$ $\qquad EqvDiameterBetweenFibers = 1.214 \times 10^{-5} m$

$AbsPressure := 520 torr$

$d_o := 3 \cdot 10^{-8} cm$

$n := \frac{6.02 \times 10^{23}}{22.4L} \cdot \frac{AbsPressure}{1atm}$

$n = 1.839 \times 10^{25} \frac{1}{m^3}$

$MeanFreePath := \frac{1}{2^{.5} \cdot \pi \cdot d_o^2 \cdot n}$

$MeanFreePath = 1.36 \times 10^{-7} m$

(Ref. O'Hanlon)

$KnudsenNumber := \frac{MeanFreePath}{EqvDiameterBetweenFibers}$

$KnudsenNumber = 0.011$

Knudsen Numbers:

Kn < 0.01	viscous/continuum flow
0.01 < Kn < 1	transitional flow
Kn > 1	molecular flow

Figure 31. Gas flow areas for rarified gas flow analysis, spacing reflects a 60% fiber volume

Results

The calculations show that gas flow through a carbon fiber preform will be transitional at best. Figure 32 shows the three flow regimes for a carbon preform as a function of fiber volume and pressure within the preform. For fiber volume fractions above 40%, the gas flow within the preform will start out in the transition regime and quickly move into the molecular regime.

Fiberglass has a larger fiber diameter relative to carbon fiber. Consequently, the gas flow cross section is larger and the transition to molecular flow occurs at lower pressure levels. Figure 33 shows the three flow regimes for a glass preform as a function of fiber volume and pressure within the preform.

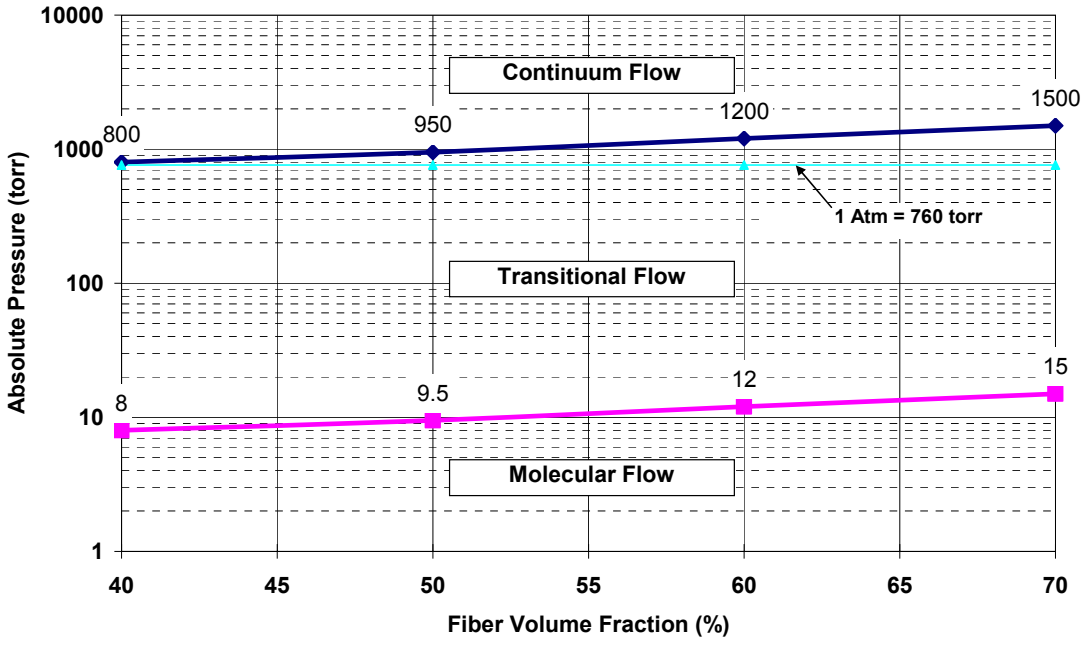

Figure 32. Gas flow regime inside carbon fiber preform

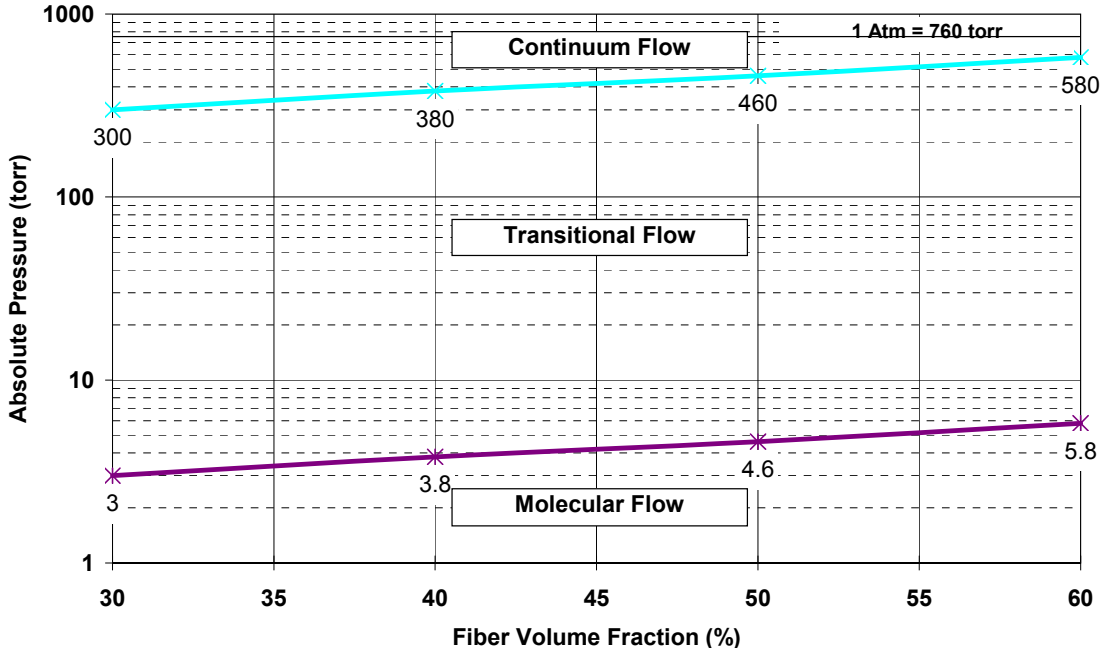

Figure 33. Gas flow regime inside glass fiber preform

Conclusions

The following conclusions are made as a result of the analytical investigation.

1. The nature of gas flow within a carbon fiber preform materials is not viscous in nature. Below mold pressures of approximately 10 torr, the gas flow within the preform is fully molecular.
2. The nature of gas flow in a glass fiber preform is viscous in nature at ambient pressure. At an absolute pressure of ~400 torr the gas flow starts to transitions to, and is fully molecular in nature by ~4 torr.

The consequence of gas flow in the transitional and molecular flow regimes is that the removal of water and other gases from the preform will

occur much slower than if the flow were viscous. The flow of a particular molecule from within the mold to the resin outlet is based on the probability of that molecule making a multitude of surface landings/leavings each with their own statistical distribution which finally results in the molecule entering into the resin outlet (i.e., evacuation port).

Another consequence is that the pressure levels measured outside the mold will deviate significantly from what is present within the preform inside the mold. The location of vacuum measurement is typically near the resin outlet port or on the resin trap as shown in Figure 5. The magnitude of the pressure gradients were experimentally investigated and are reported on in the next Section.

4.4. Preform Degassing Experiments

Experiments were conducted in order to research residual gas pressures within an RTM mold/preform as it relates to measurements made outside the mold. Rarified gas conductance through a compressed fiber bed (i.e., preform) in the context of composite processing has not been previously studied. The effect of initial moisture content in the preform was also studied. Experiments looked at both the flow of gas through a preform and the desorption of any adsorbed water from within the preform.

The objective of these experiments was to measure residual gas pressures within the mold/preform as a function of external pressure

measurements made during mold evacuation. The impact of fiber volume and preform water was also assessed.

Two experimental setups were used for this work. The first setup, the 'Clamped Plate' setup, utilized two 19 mm (0.750 inch) thick aluminum plates between which five plies of 9 cm (3.5 inch) square preform samples were clamped to the specified fiber volume. Four screws fasten the two plates together. The overall thickness of the plates plus preform was measured with calipers and the preload of the four screws adjusted in order to reach the desired thickness for the preform. In this way, the fiber volume fraction for the preform could be controlled by adjusting the preload of the clamping screws. The plates with preform samples are shown in Figure 34 and Figure 35.

Figure 34. Glass preform sample for preform degassing tests

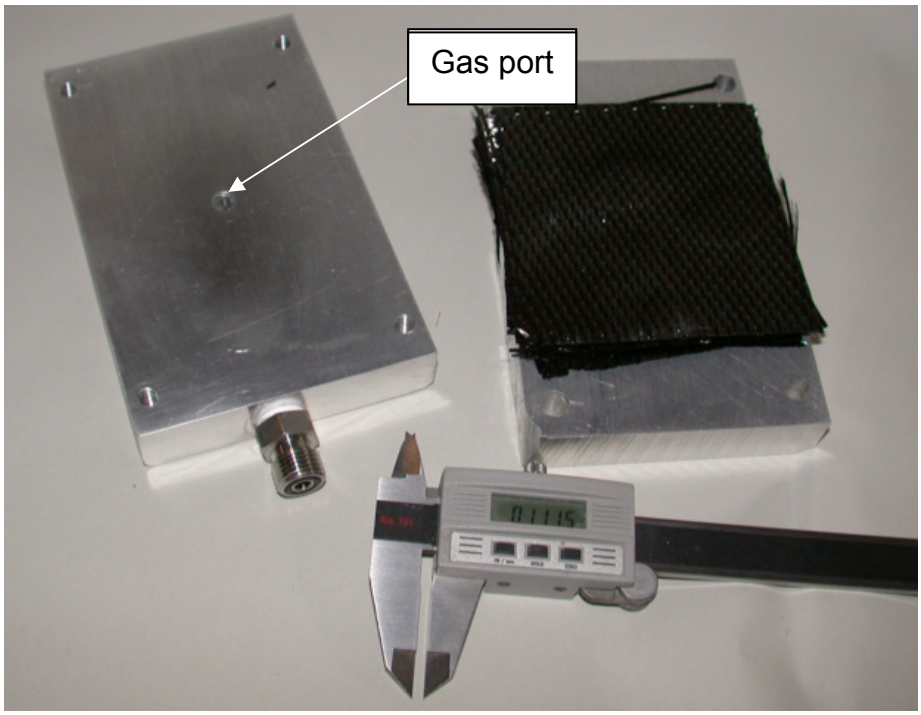

Figure 35. Carbon preform sample for preform degassing tests

For measuring the preform residual gas pressure, one of the plates contains a gas port located at the center of the plate, shown in Figure 34 and Figure 35. This port was connected to the edge of the plate via another port where it connected to a VCO type fitting shown in Figure 34 and Figure 35. For testing, the fitting was connected to a pair of capacitance manometer vacuum transducers that measured the preform residual gas pressure. The plate assembly was then placed inside a vacuum chamber and pumped down. The experimental setup is shown schematically in Figure 36.

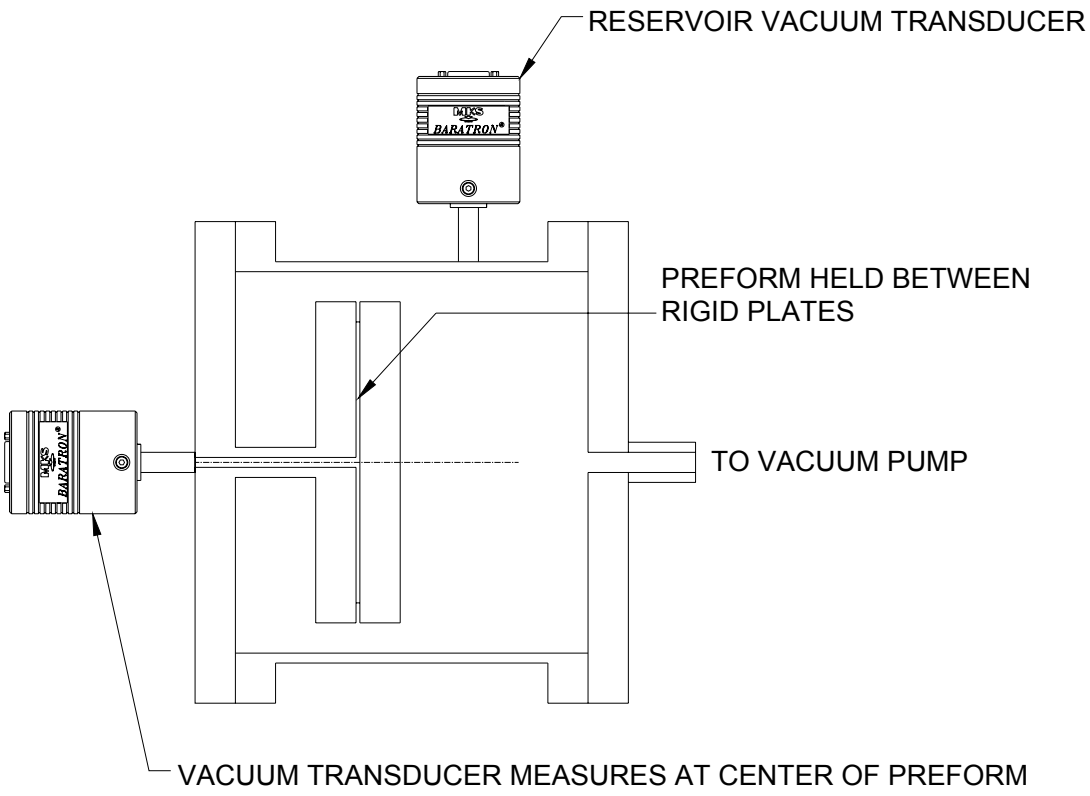

Figure 36. Schematic of preform degassing experimental setup

The vacuum chamber used for these experiments is shown in Figure 37 (also Appendix 1). The preform clamping plates are shown connected to the preform residual gas pressure monitoring line in Figure 38. To facilitate installation and removal of the preform plates, the vacuum chamber was equipped with a gate valve, Figure 39. The vacuum chamber also had a window for observation during testing. The clamping plates can be seen looking through the chamber window in Figure 40.

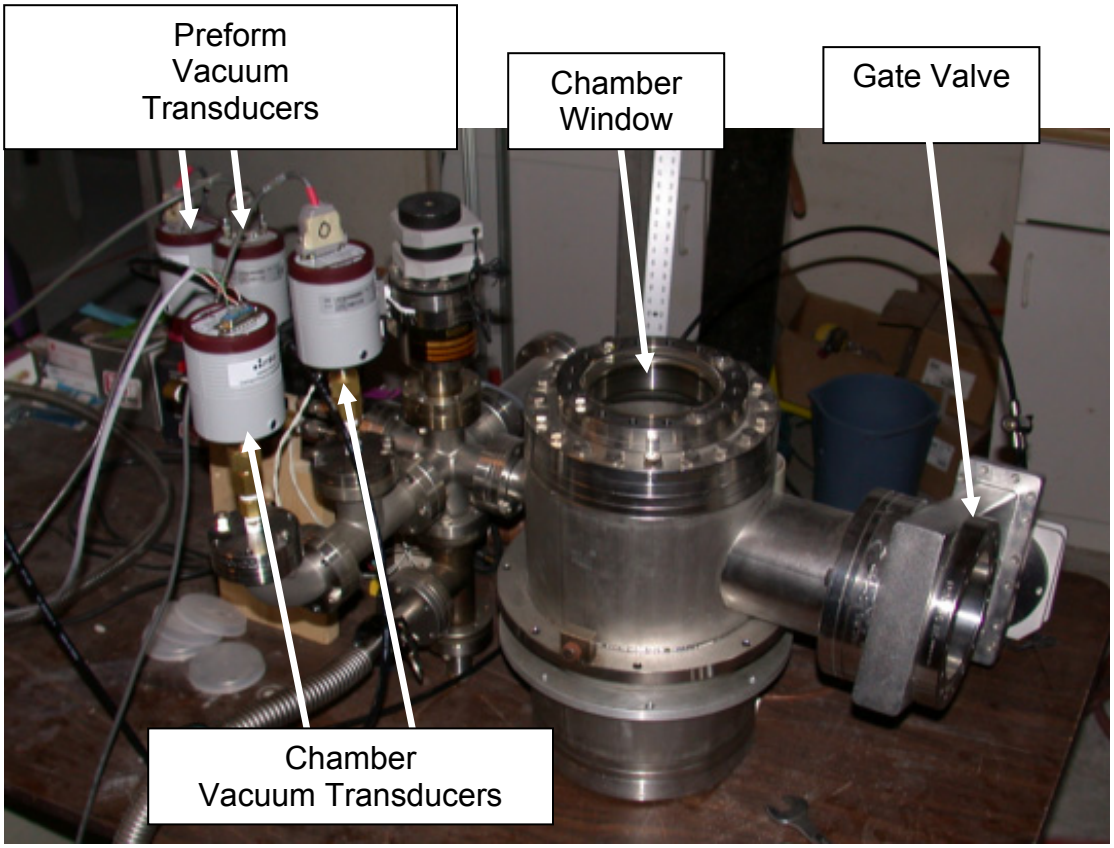

Figure 37. Vacuum chamber used for preform degassing experiments

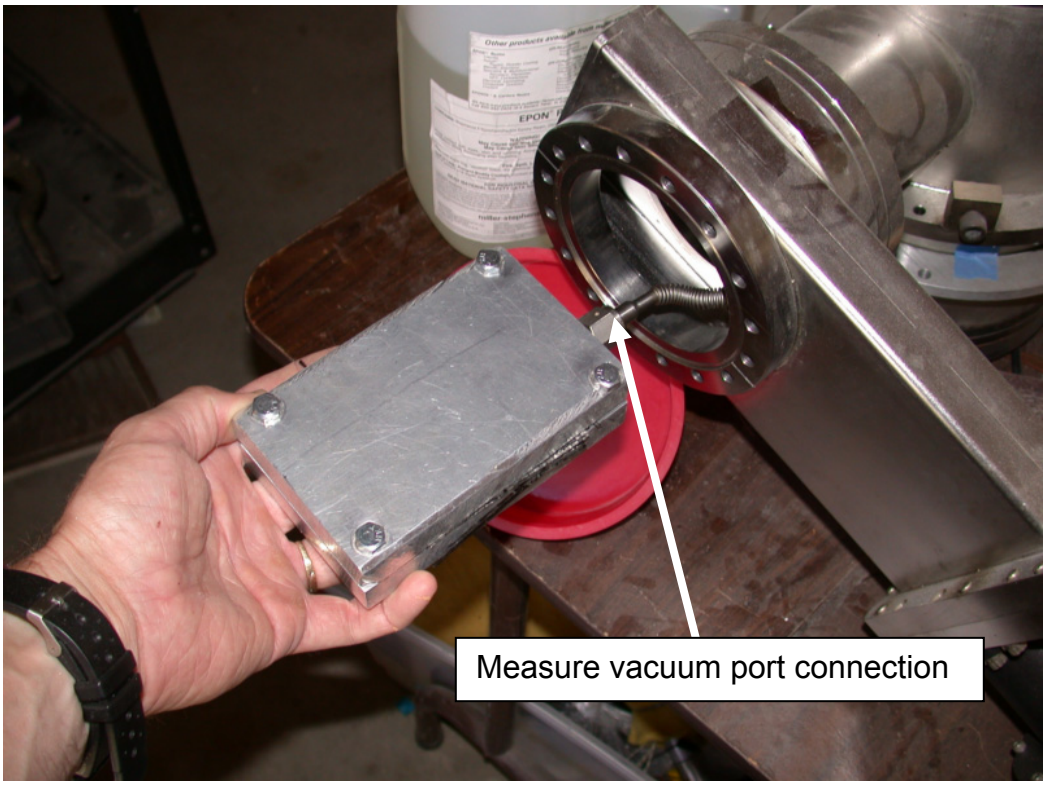

Figure 38. Preform degas tool clamped and connected to vacuum port

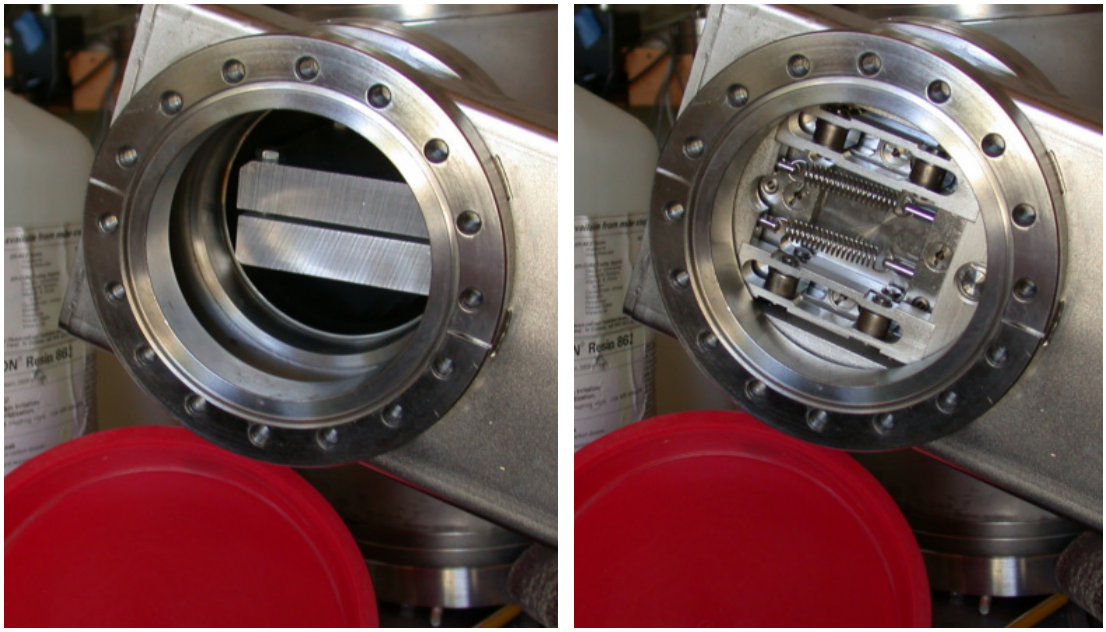

(a) (b)

Figure 39. Gate valve open (a) and closed (b)

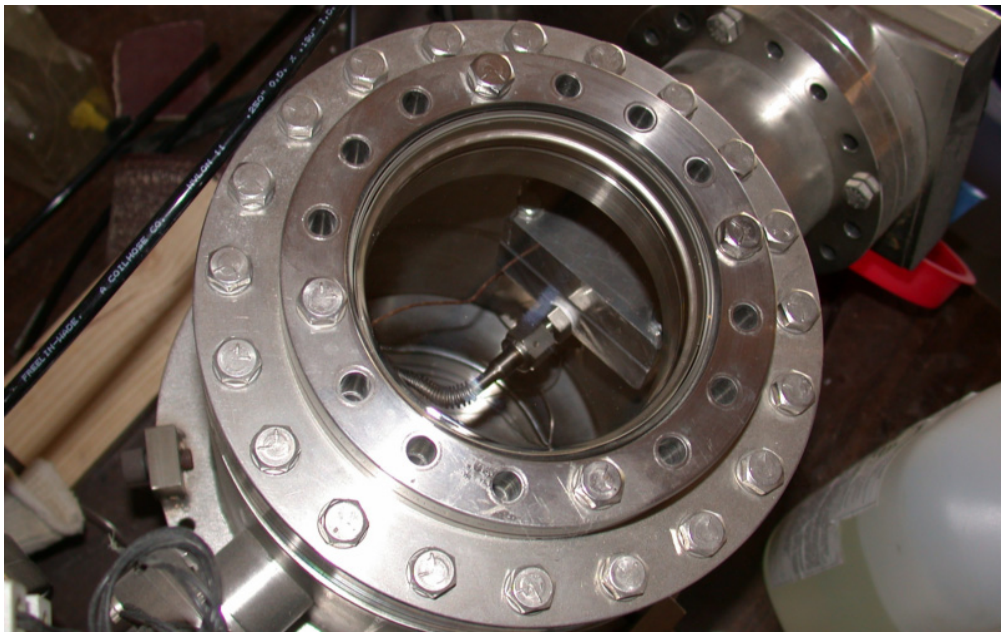

Figure 40. Looking through window at preform clamp fixture inside vacuum chamber

The second experimental setup utilized the panel mold from Chapter 1 with the top mold plate replaced with another modified to have a gas port at the center of the flange. The residual gas pressure in the preform was monitored through this port during mold pump down. The thickness of the cavity in the panel mold is fixed and so adjustment of the preform fiber volume was accomplished by changing the number of plies of material. The panel mold configured for preform pump down studies is shown with a carbon fiber preform in Figure 41. The closed panel mold with vacuum transducers is shown in Figure 42.

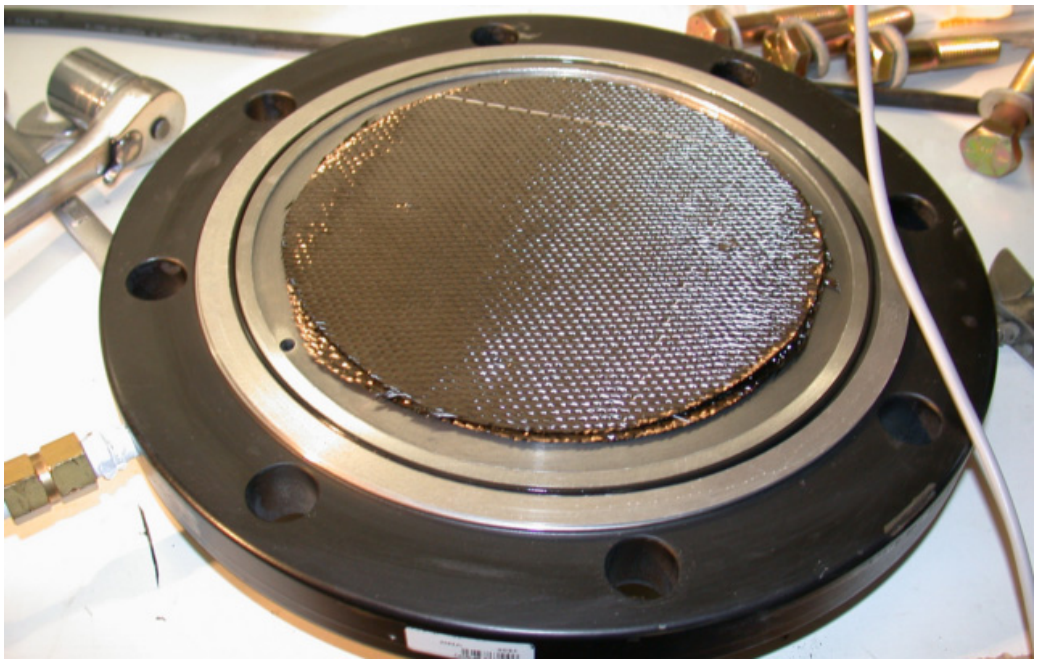

Figure 41. Panel mold with carbon preform stack in place

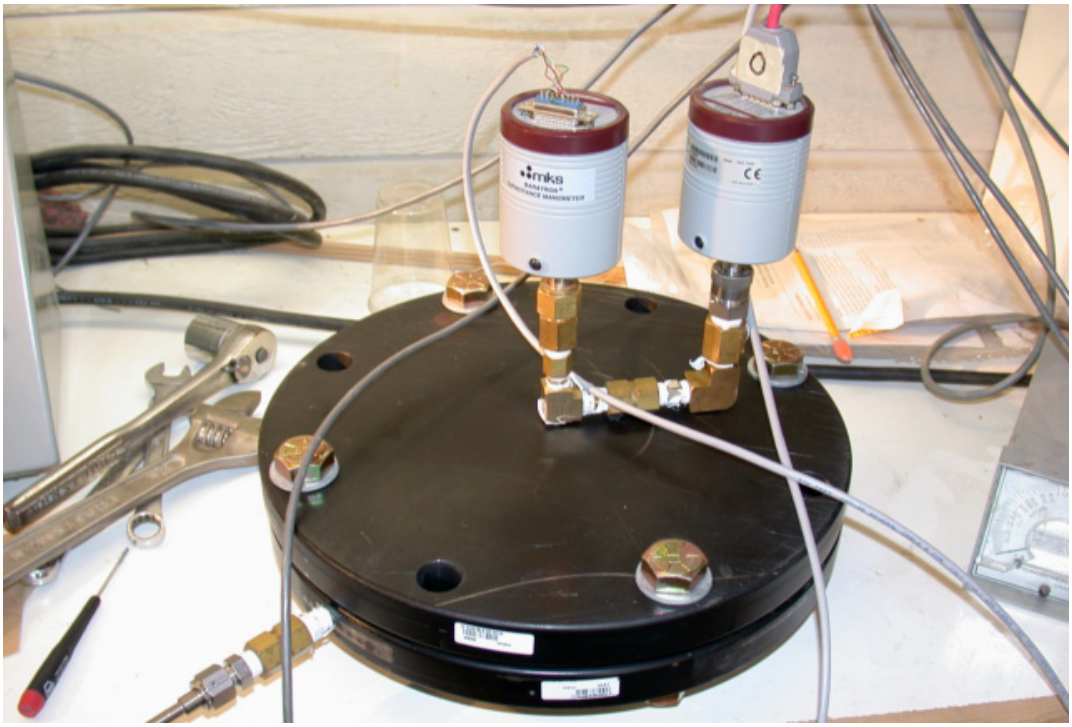

Figure 42. Panel mold closed for preform residual gas studies

Testing

Testing was conducted initially using the clamped plate experimental setup. For this testing, samples of carbon and glass fiber fabric were thoroughly dried at 150 °C for 24 h prior to testing. The moisture content after drying is expected to be minimal. Some samples were tested directly after drying. A second group of samples were aged under conditions of 60 % RH and 20 ºC. In order to investigate the effect of humidity, a set of carbon fiber fabric samples were aged in ~95% RH and 20 ºC for 24 h prior to testing. It is expect that these preform samples gain approximately 0.2 % in mass due to water sorption.

The fabric samples were placed between the clamping plates. The four cap screws holding the plates together where uniformly tightened. The overall thickness of the plates and preform was measured using calipers to assure uniform clamping of the fabric test sample. To test at different fiber volumes, the thickness of the assembly was changed by adjusting the preload in the screws. Experiments with the clamp plate setup were performed at 50 % and 63 % fiber volume for both the glass and carbon preform samples.

Vacuum was drawn on the preform/mold assembly and monitored both within the preform and outside of the mold. All testing was carried out at room temperature of approximately 20 ºC.

Preform degassing experiments with the second test setup involved laying up plies of material in a panel mold and then bolting it closed. To test at

different fiber volume fractions, additional plies of material were added while leaving the thickness of the part cavity unchanged. The carbon fabric used (Appendix 2) has a 370 grams per square meter (gsm) areal weight. Testing was conducted using four, five, and six plies of material to arrive at fiber volume fractions of 40 %, 50 %, and 60 % respectively in the 0.077 inch thick cavity.

The glass fabric used for testing (Appendix 2) was a 204 gsm fabric. Testing was conducted using 9 and 12 plies for fiber volumes of 39 % and 52 % respectively. A summary of preforms tested is provided in Table 2.

Table 2. Preform degassing experiments ply and fiber volume information

Clamped Plate Degassing Experiments

Glass Fabric, 204 gsm	
Plies	Fiber Volume
5	50%
5	63%

Carbon Fabric, 370 gsm	
Plies	Fiber Volume
5	50%
5	63%

Panel Mold Degassing Experiments

Glass Fabric, 204 gsm	
Plies	Fiber Volume
9	39%
12	52%

Carbon Fabric, 370 gsm	
Plies	Fiber Volume
4	40%
5	50%
6	60%

Results

Plots of the pump downs using the clamping plates with glass fabric are shown in Figure 43 for dry preform samples. Carbon fiber fabric pump down

plots are shown in Figure 44 for dry preform samples. Pump down curves for dry and humidified carbon fiber preform samples are shown in Figure 45.

The testing on dry preform samples and samples aged under ambient conditions of ~60 % RH showed no measurable difference in the pump down behavior. Consequently, only one set of curves is provided for these results.

After completion of the clamped plate testing with the humidified carbon fiber preform sample, and the completion of the humidified preform mass gain experiments presented in 4.2, it was concluded that the preform moisture content did not play a significant role in the residual gas pressure within the preform. Consequently, drying the humidification of the preform samples for the panel pump down experiments was not performed. The preform samples for the panel mold pump down experiments were used in an 'as received' condition without drying or humidification.

Plots for preform pump down using the panel mold are provided in Figure 46 to Figure 50. All pump downs in the panel mold were performed on preform samples that were used as received and after aging in the lab for several days before and after preform cutting. Conditions in the lab area were typically 60 % RH and 20 ºC.

Figure 46 show the empty mold pump down baseline. Note that the curves for the manifold and tool are nearly identical as is expected. Figure 47 shows the pump down for carbon preform samples at 4, 5 and 6 plies, 40 %, 50 %, and 60 % fiber volume fractions respectively. Figure 48 shows pump

downs for glass fiber preforms using 9 and 12 plies resulting in 39.1 % and 52.2 % fiber volume fraction respectively. Figure 49 compares the pump downs of carbon fiber and glass fiber preforms both at a fiber volume of approximately 50 %. Quantitative interpretation of the results from Figure 49 is difficult and so Figure 50 was generated showing the relation between manifold pressure and mold pressure.

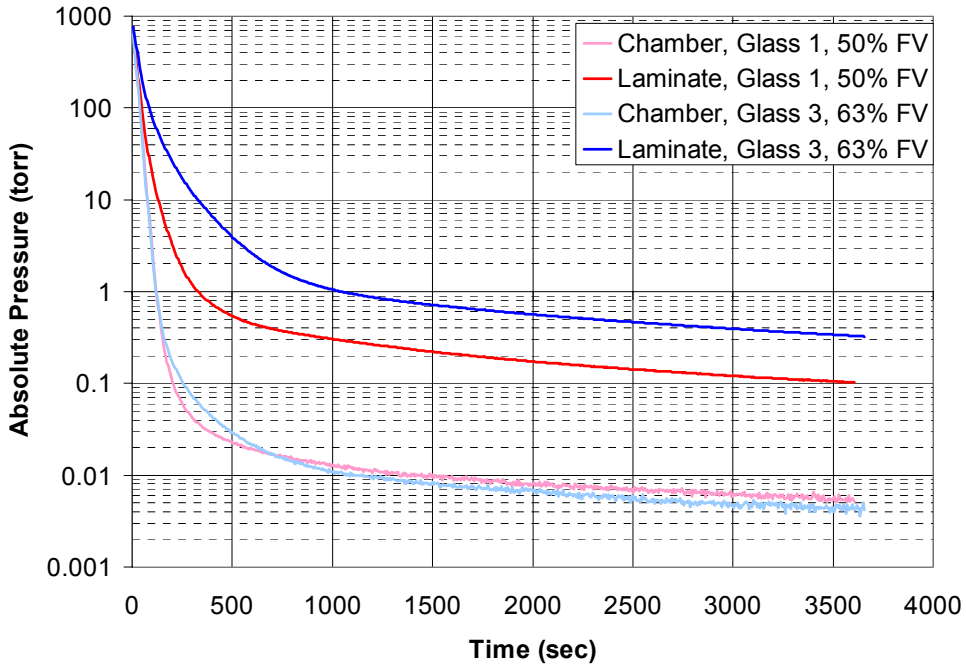

Figure 43. Clamped plate test results for dry glass preform pump down curves.

Figure 43 shows a significant difference in the residual gas pressure measured in the laminate to that measured in the chamber. It can also be seen that the higher fiber volume increases the residual gas pressure at a given time.

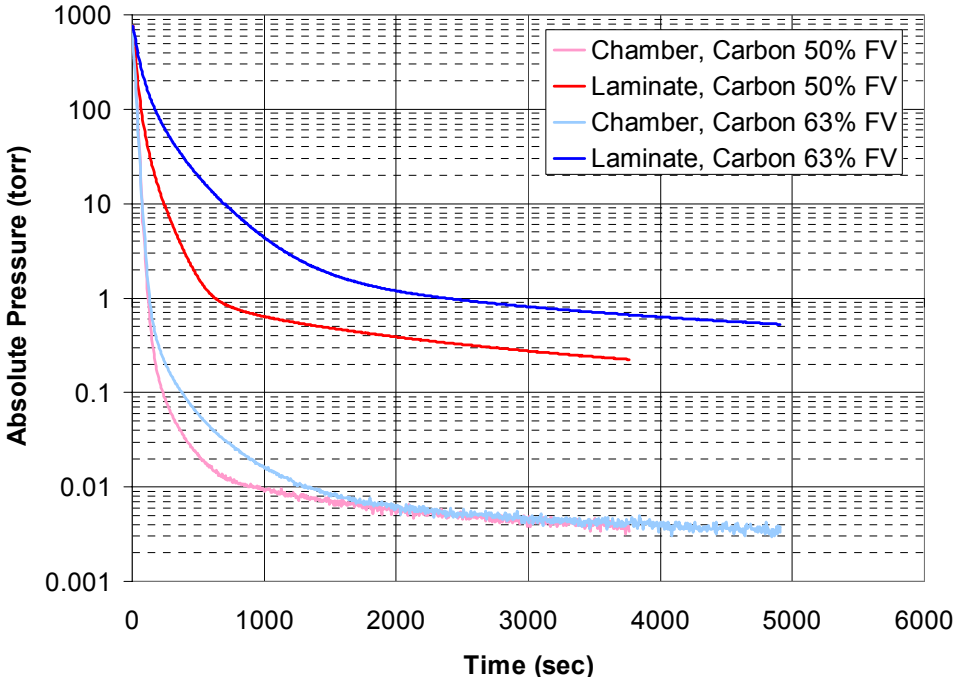

Figure 44. Clamped plate test results for dry carbon fiber fabric

Figure 44 also shows a significant difference in the residual gas pressure measured in the laminate to that measured in the chamber. It can also be seen that the higher fiber volume increases the residual gas pressure at a given time. When compared to Figure 43, at similar fiber volumes, it can be seen that the carbon fiber fabric takes more time to achieve a given vacuum level compared to the glass fiber preform.

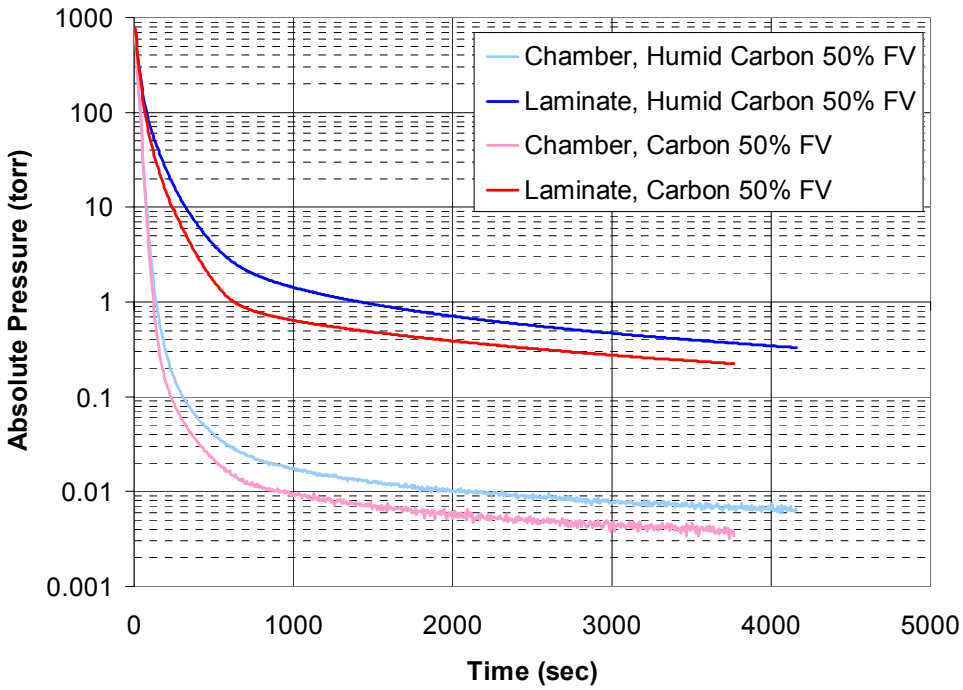

Figure 45. Clamped plate test results for dry and humidified carbon fabric samples

Figure 45 shows a comparison in the pump down behavior between dry carbon fiber fabric and carbon fiber fabric that was aged at 95 % RH for 24 h. Both experiments were performed at 50 % fiber volume fractions. It can be seen that the humidified carbon fiber fabric increases the residual gas pressure in the preform and in the chamber for a given time. When comparing the humidified carbon fiber results at 50 % fiber volume, to the 63 % fiber volume carbon fiber results shown in Figure 44, it is noted that the effect of the moisture on the residual gas pressure within the preform is not as significant as the effect of the higher fiber volume.

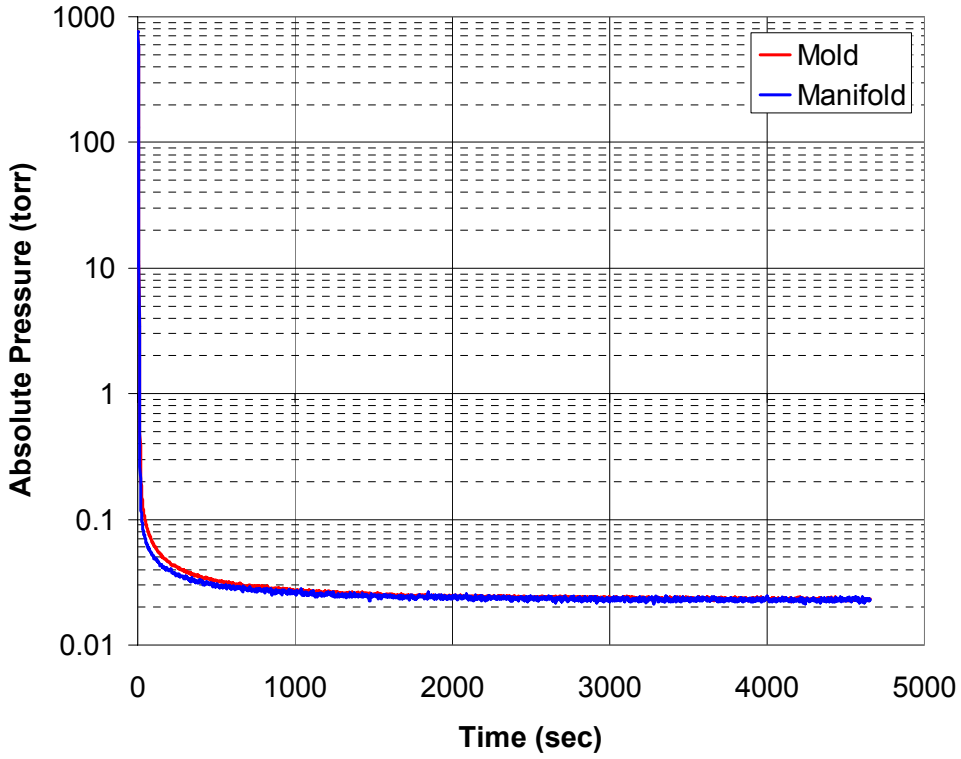

Figure 46. Panel mold test results for the empty mold baseline pump down

Figure 46 shows that pumping down the panel mold without a preform loaded results in nearly identical curves for the measure pressure in the mold and that measured in the vacuum manifold.

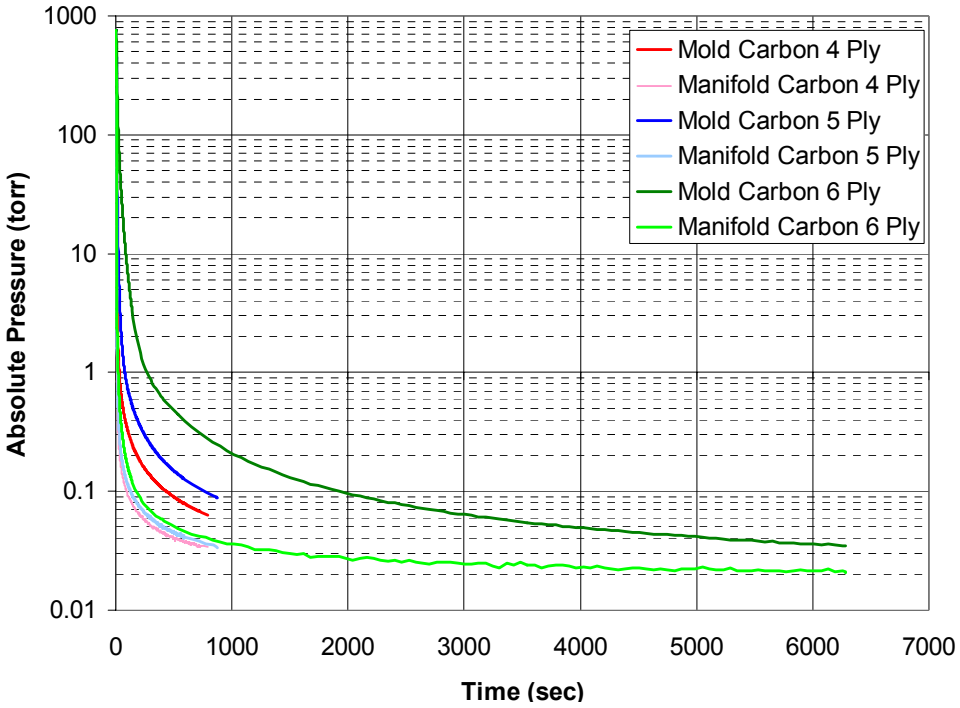

Figure 47. Panel mold test results for the carbon fiber preform

Figure 47 shows the relation between the residual gas pressures measured in the mold to those measured in the vacuum manifold for the carbon fiber fabric experiment. It can be seen that as the fiber volume (i.e., number of plies) increases, so does the residual gas pressure.

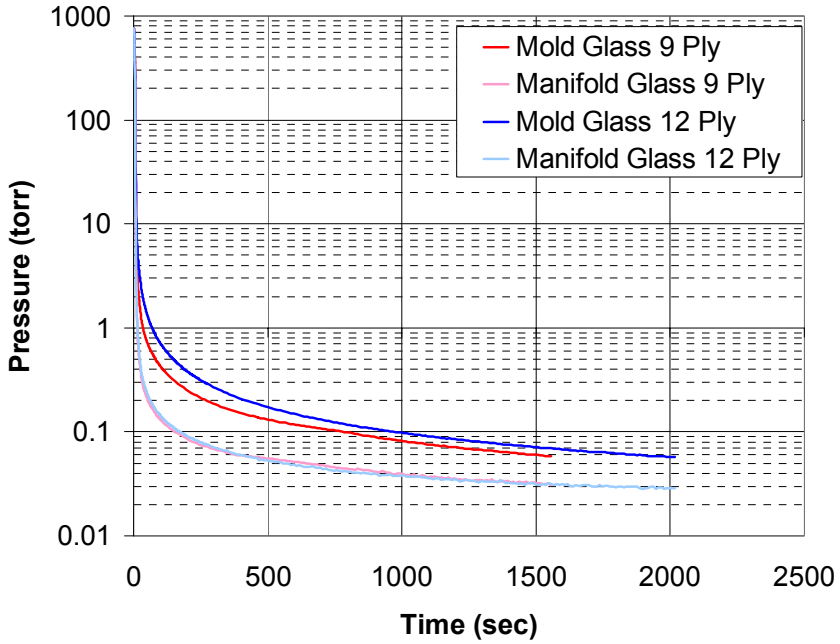

Figure 48. Panel mold test results for the glass fiber preform

Figure 48 shows the relation between the residual gas pressures measured in the mold to those measured in the vacuum manifold for the glass fiber fabric experiment. It can be seen that as the fiber volume (i.e., number of plies) increases, so does the residual gas pressure.

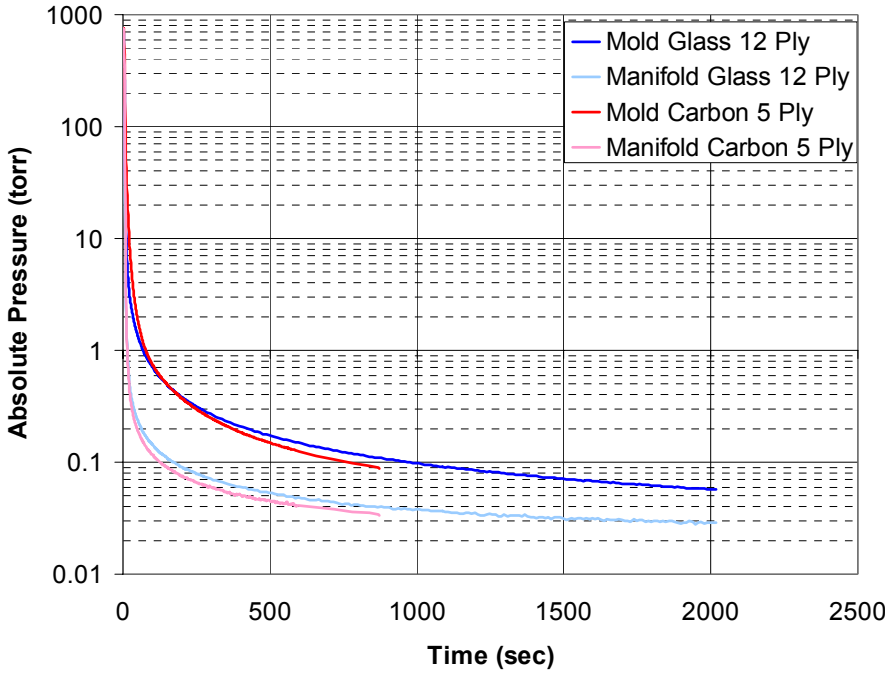

Figure 49. Panel mold test results comparing carbon fiber and glass fiber pump downs

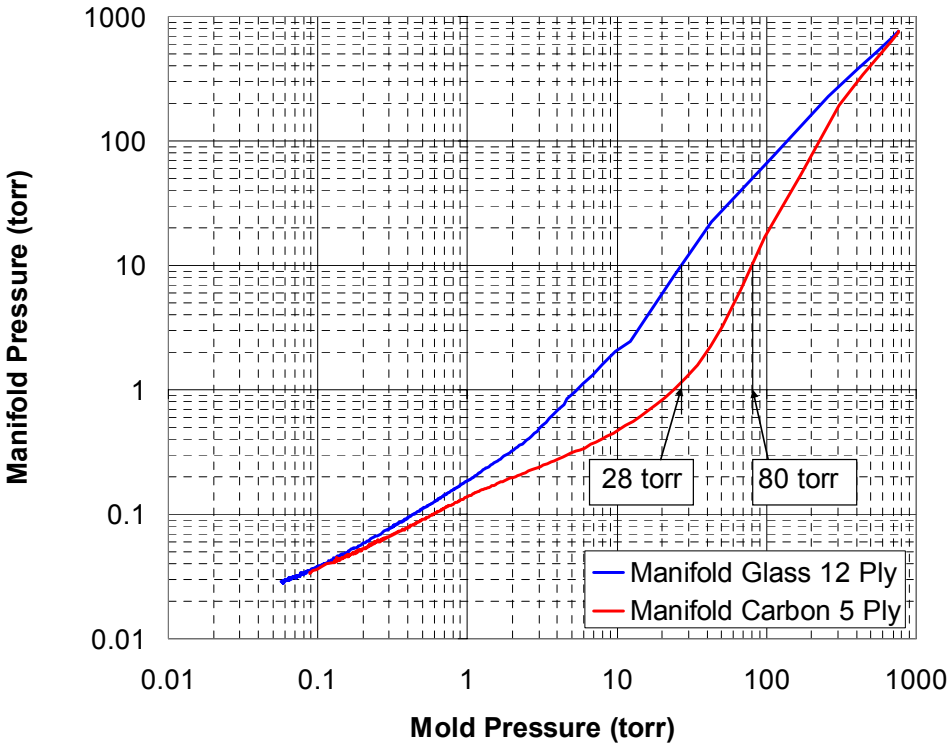

Figure 50. Panel mold test results comparing carbon and glass fiber preform pump downs

Figure 49 and Figure 50 compare the mold residual gas pressures for carbon fiber and glass fiber fabric samples at a similar fiber volume of approximately 50 %. It is difficult to discern a difference directly from Figure 49 and so Figure 50 was developed to better elucidate the difference in mold pressures for the carbon fiber and glass fiber experiments.

Conclusions

The experimental results show a large pressure differential between the pressure measured external to the mold and that measured within the mold. The differential is greater in magnitude as the fiber volume fraction is increased. It is interesting to note that the rate of pressure decay is generally slower in the manifold at high fiber volumes. This indicates that the higher fiber volume sustains a virtual leak for a larger duration compared to lower fiber volumes.

The preform degassing experiments using carbon preform samples that were aged in high humidity conditions showed a higher pressure level within the preform and manifold. The humidified 50% fiber volume sample was similar in response to the dry 63% fiber volume sample and both were significantly slower in pump down compared to the dry 50% sample. However, preform samples that were aged in the lab environment, with reasonable humidity conditions (e.g., 60 % RH), exhibited no measurable difference in pump down relative to dried fabric samples.

Calculations performed in Section 3 of this chapter showed that molecular gas flow in a carbon preform covers a broader pressure range relative to glass fiber preforms. The consequence of this is a larger pressure differential between the mold gas pressure and the external gas pressure. The empirical data of Figure 50 confirms this. For example, at a manifold pressure of 10 torr, the measured preform gas pressure is 28 torr in the glass preform while the carbon preform measures 80 torr.

A consideration for the results of the preform degassing study is the gas volume within the pressure measurement circuit. The volume of gas is small, on the order of 5% of the free volume of the preform. During pump down, this gas must be pumped out through the preform and consequently, the measured preform pressures are expected to be higher than the actual preform pressure. Regardless, trapped volumes of gas are not uncommon within the RTM mold and so the results of the preform gas pressure measurements are considered representative.

Following is a summary list of general conclusion drawn from the research performed on preform degassing:

1. The residual gas pressures within the mold are much higher than those measured external to the mold and can be as much as three orders of magnitude higher.
2. Long periods of time are required to achieve low residual gas pressures within the mold/preform. For the panel mold experiments,

approximately 15 minutes was required to achieve 0.1 torr within the mold at a 50% FV. At 60% FV, approximately 30 minutes was required to achieve 0.1 torr.

3. At similar fiber volumes, carbon fiber preforms have a slightly higher residual gas pressure compared to glass fiber preforms.
4. Higher fiber volume fractions increase the residual gas pressure within the mold.
5. The water content in the preform is concluded to not be a significant contributing factor to the residual gas pressures within the mold.

5. RESIN DEGASSING AND GAS DISSOLUTION

5.1. Resin Study

Degassing of resin before injection is commonly practiced in RTM. In addition, pulling vacuum on the mold prior to and during injection is common. Once injection is complete, holding pressure on the resin during cure maybe performed. Mega-void dissolution is affected by each of these three parameters:

1. Resin degas
2. Preform degas / mold vacuum
3. Resin curing pressure

The objective of the research in this Chapter is to understand how variation in resin degas, variation in preform residual gas pressure and resin curing pressure all affect the solubility of air in an epoxy. The vacuum level that constitutes an acceptable amount of degas has not been researched nor it is clearly understood.

In order to research the solubility of gases in resin, experiments were conducted where a sample of resin was degassed under controlled conditions and subsequently pressurized in a volume containing a known amount of air so that the level of dissolution of the air into the resin could be assessed.

The test apparatus consists of a borosilicate glass test tube that contains the resin. The test tube is sealed at one end. The opposite end is inserted into an aluminum holder that seals against the tube's outside

diameter. A piston inside the holder actuates into the test tube and compress the volume there. The piston is driven by a pneumatic actuator so that the piston force and resin pressure can be controlled. The holder also contains a gas port that is exposed when the piston is fully retracted. Through the gas port, the gas pressure inside the test tube can be controlled for resin degassing and for adjusting the gas pressure inside the test tube for dissolution testing. Once actuated, the piston advances across the gas port and into the test tube trapping the resin and gas present there. To prevent any gas leakage around the piston as it crosses both the gas port and the holder to test tube interface, the piston utilizes a dual O-ring design where vacuum is drawn between the O-rings (guard vacuum) of the piston.

For temperature control, the test tube is housed inside an aluminum chamber that is maintained at 121 °C during testing. The chamber is equipped with a glass window to help retain heat while providing visibility of the test sample. A second window is cut in the chamber in the side opposite the first. An LCD computer monitor is positioned below the apparatus so it can be seen through the first window and in the background of the resin test tube. The monitor is used to display relevant test data (e.g., resin pressure, elapsed time). These data are recorded by time elapsed digital video so that changes in bubble size can be reviewed subsequent to the test.

A cross section of the test apparatus is shown in Figure 51. A picture of the apparatus is shown in Figure 52. The picture of the bench setup is provided in Figure 53.

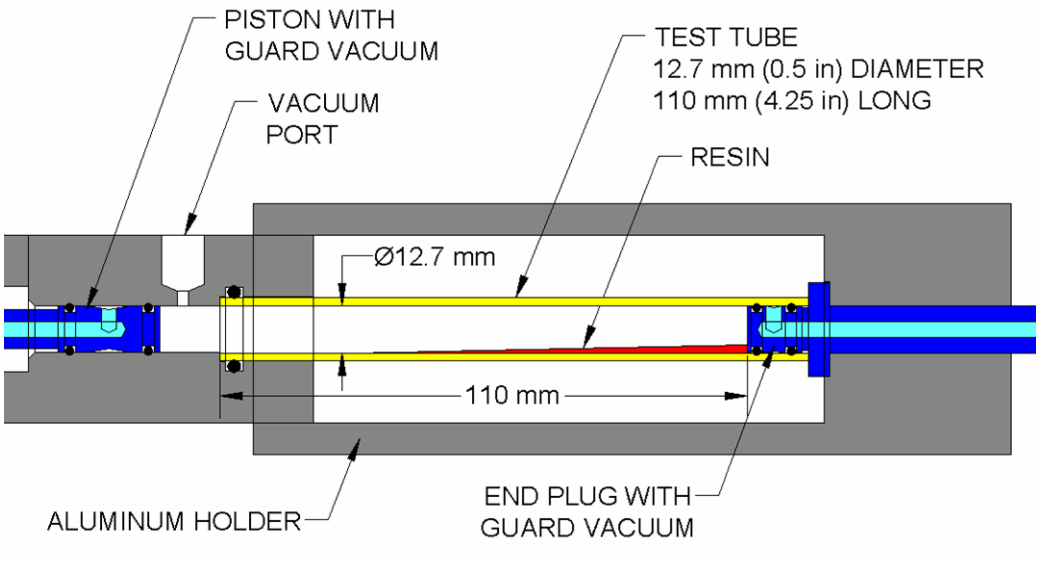

Figure 51. Cross section of resin gas solubility testing apparatus

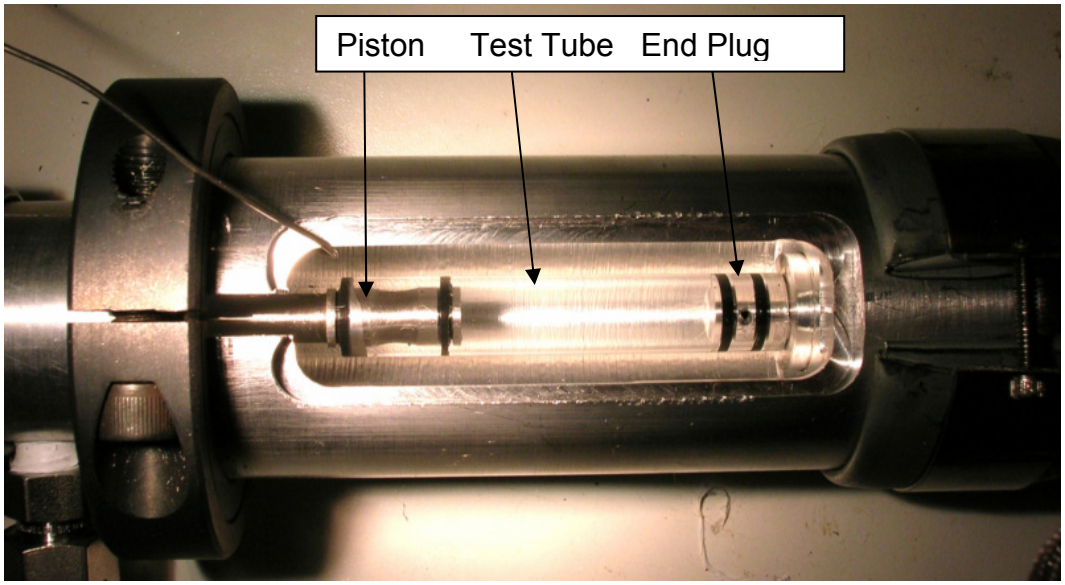

Figure 52. Resin test apparatus: piston, test tube and end plug. Piston and end plug equipped with guard vacuum.

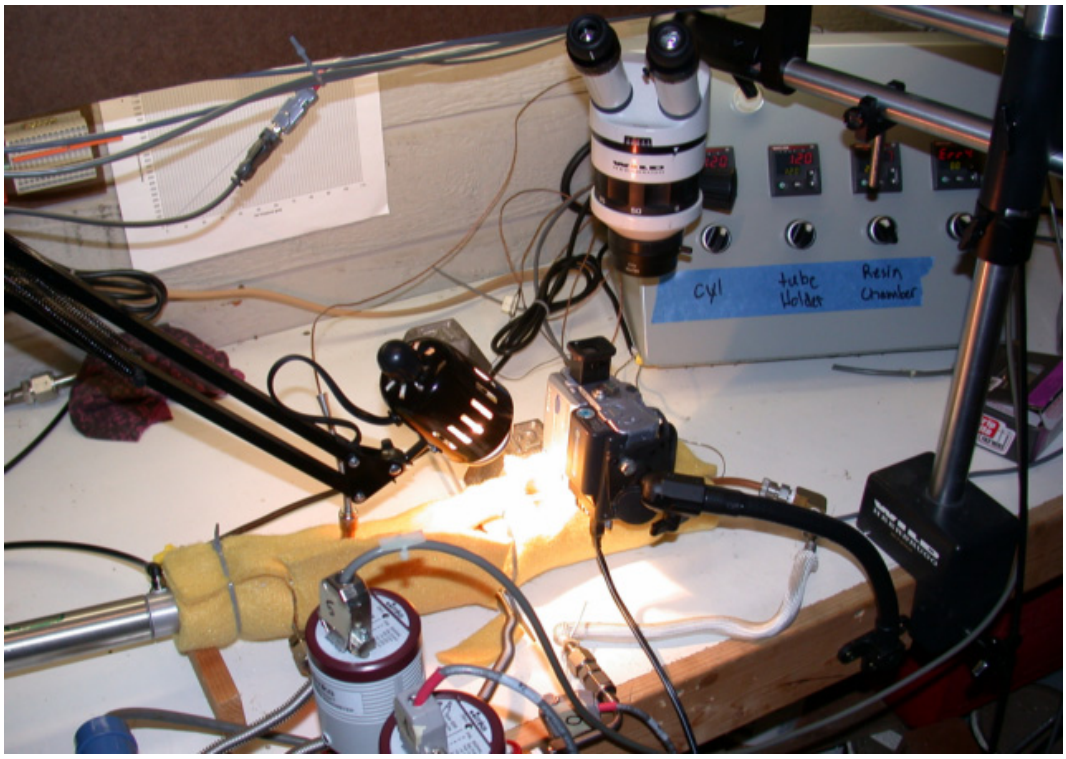

Figure 53. Setup for resin gas dissolution studies, digital camera in position. Microscope swings our of position, camera swings into position

To support the resin test apparatus, a two stage rotary vane vacuum pump is used. The vacuum pump is capable of vacuum levels to 10^{-3} torr. Vacuum measurement is accomplished by a pair of MKS Baratron capacitance manometer transducers. The range of the first is from 0.1 to 1000 torr while the range of the second is 10^{-3} to 10 torr. In addition, a convection gage is utilized as a secondary vacuum level check. A pneumatic pressure transducer is used to monitor the air pressure applied to the pneumatic actuator. This pressure is scaled according to the area proportions

of the pneumatic actuator and the piston of the test apparatus to arrive at the resin pressure.

Control and adjustment of the vacuum level used for resin degas and for the residual gas level is accomplished using a BOC Edwards needle valve. To achieve the desired level of vacuum, the vacuum pump pumps on one end of the vacuum manifold. The needle valve is positioned at the opposite end of the manifold. The valve is then adjusted so that the vacuum level indicated by the transducers, located near the middle of the manifold, indicate the desired vacuum level. The vacuum lines that service the test apparatus are also located in the middle portion of the manifold assuring that they are subjected to the same vacuum level that the transducers indicate. The vacuum manifold is shown in Figure 54.

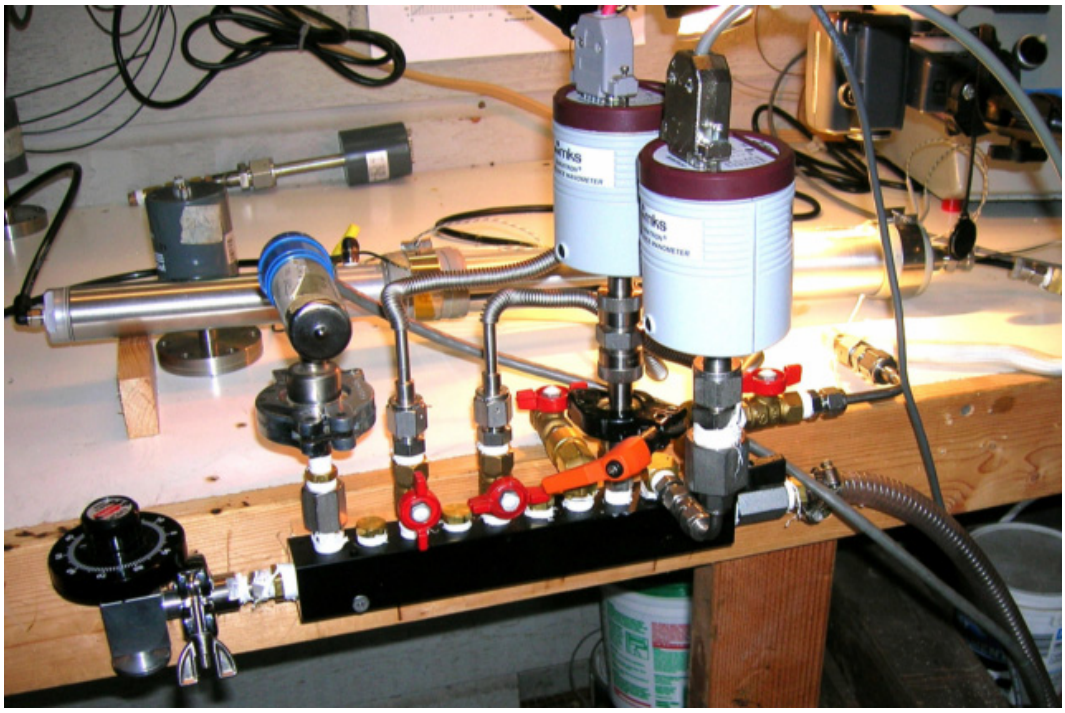

Figure 54. Vacuum manifold for air dissolution testing

A computer data acquisition system is used to monitor and record data from the transducers. Temperature control is provided by a four zone control system using PID controllers (see Appendix 1). The temperature controllers also interface to the data acquisition computer for data logging.

Testing

Test samples of 1 cm^3 of resin were placed into the test tube and preheated to 121 °C. The tube was oriented horizontally to minimize any resin pressure head effects with the resin depth of approximately 1 mm. The pressure head of this depth of resin is ~0.1 torr. Vacuum was then applied to the resin to the prescribed level for degassing for a duration of approximately 10 minutes. Next, air was introduced into the resin chamber increasing the gas pressure to the prescribed level. The test tube piston was then actuated compressing the gas and resin sample. The resin and gas bubble were observed over time to look for bubble shrinkage indicating air dissolution.

The volume for gas within the test tube at the point where the evacuation port is sealed off by the piston is 6 cm^3 making the ratio of gas volume to resin volume 6:1. An equivalent mold residual gas pressure is calculated base on a gas volume to resin volume ratio of 1:1. Consequently, the reported gas dissolution pressure has been increased by a factor of six over the actual pressure applied during the testing to arrive at the pressure of the gas when it occupies a volume equal to the resin.

Figure 55 shows an example picture during a dissolution test.

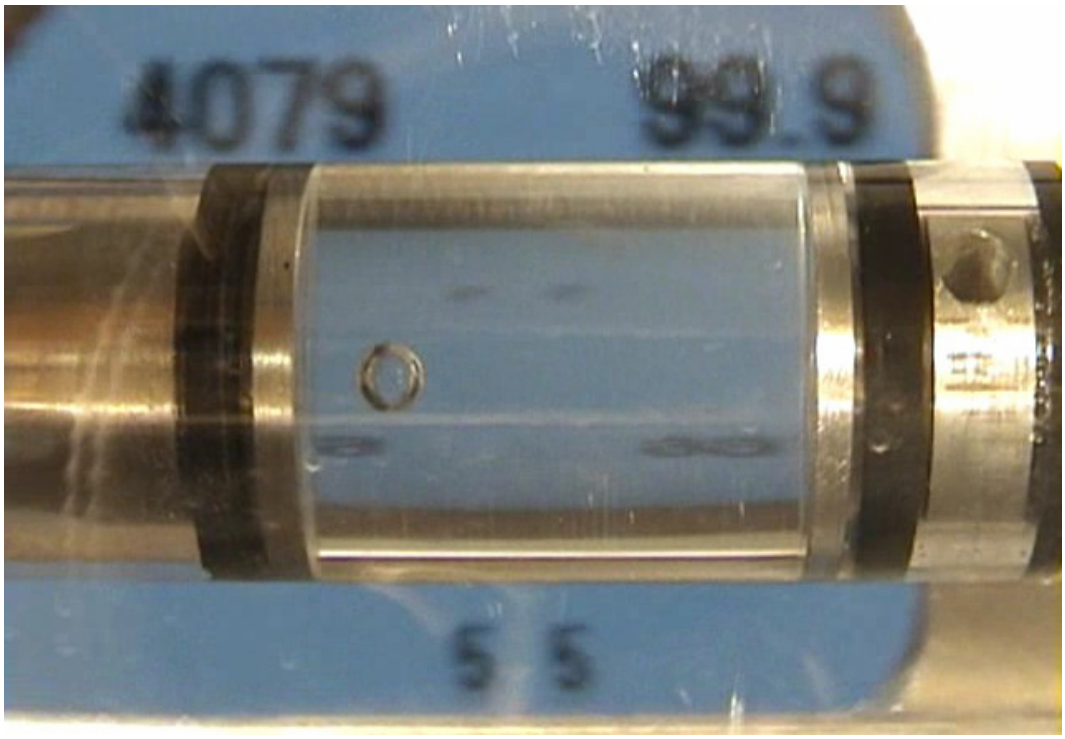

Figure 55. Air bubble during dissolution

An LCD is used to display relevant test data during video capture. In Figure 55, the LCD is showing an elapsed time of 4079 s, the current resin pressure of 690 kPa (99.9 psi) torr resin degas pressure that was used for the test and 5 torr gas dissolution pressure. The 5 torr dissolution pressure shown in the LCD is increased by a factor of six to arrive at an equivalent mold residual gas pressure of 30 torr.

Figure 56 to Figure 58 show a sequence of video frames during example dissolution tests.

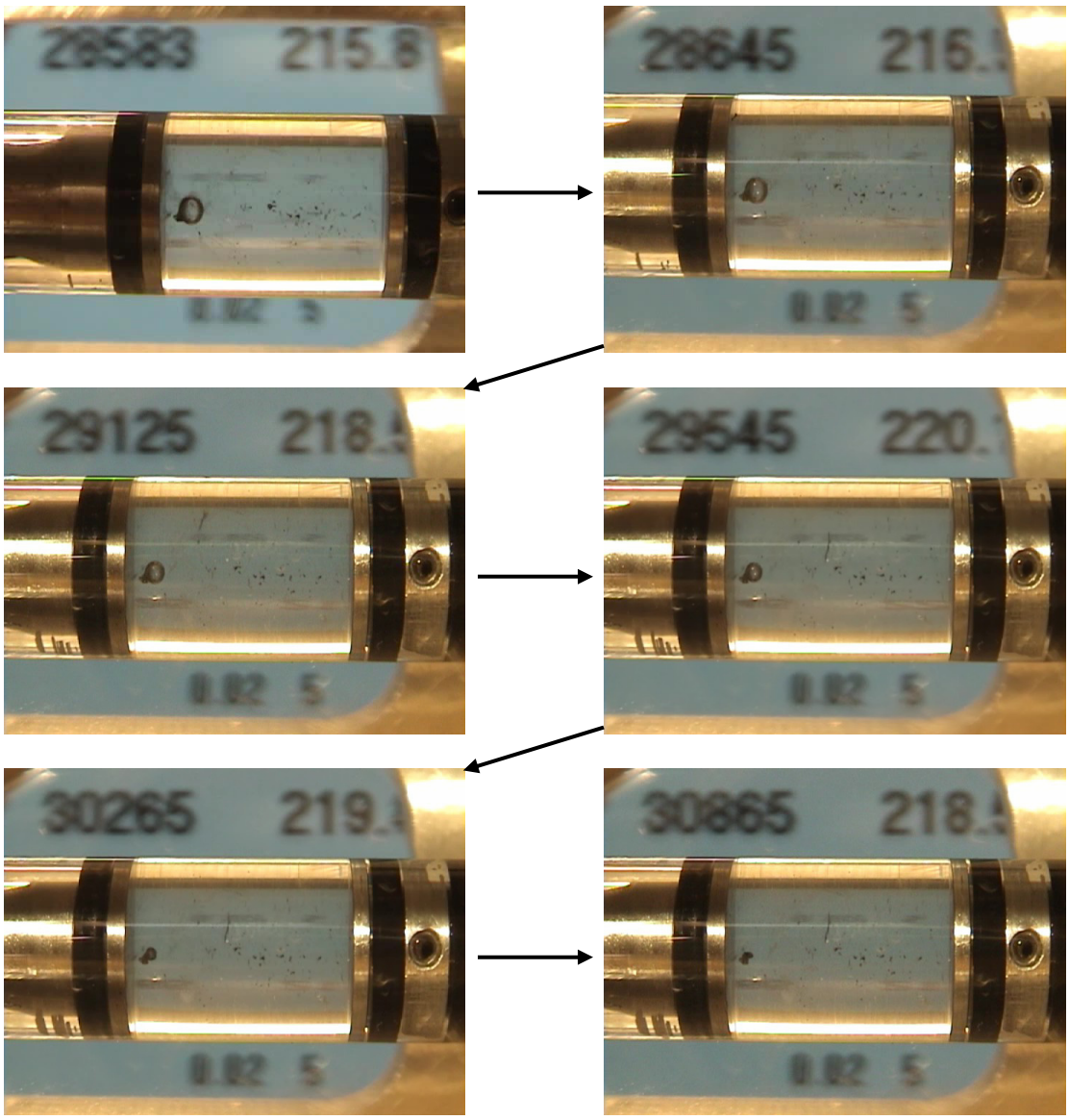

Figure 56. Image sequence of air bubble during dissolution test

Figure 56 shows that a time of 2282 s (38 minutes) was required for dissolution of 30 torr residual gas pressure air in resin that was degassed at 0.02 torr and held under 1500 kPa (220 psi) resin pressure.

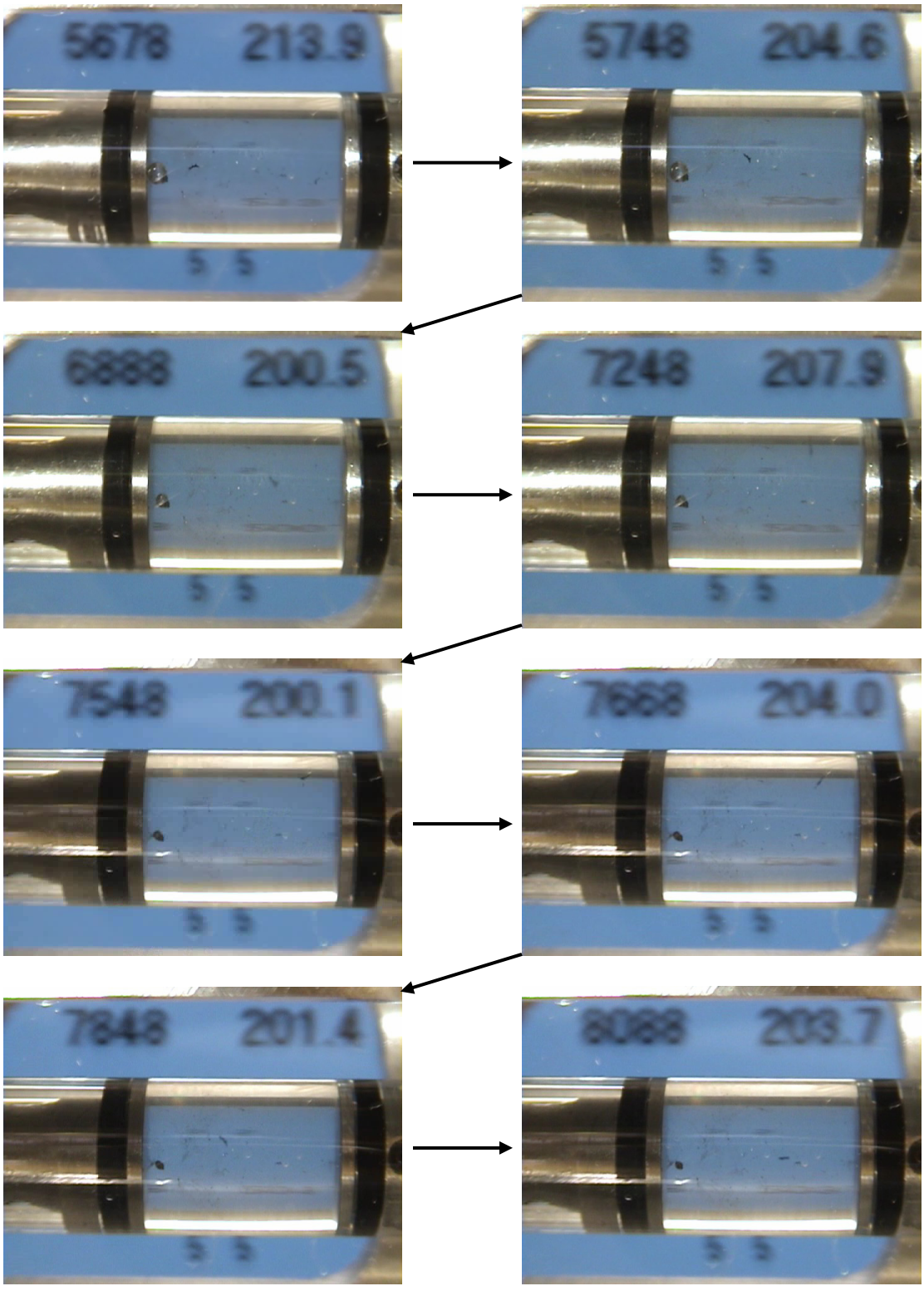

Figure 57. Image sequence of air bubble during dissolution

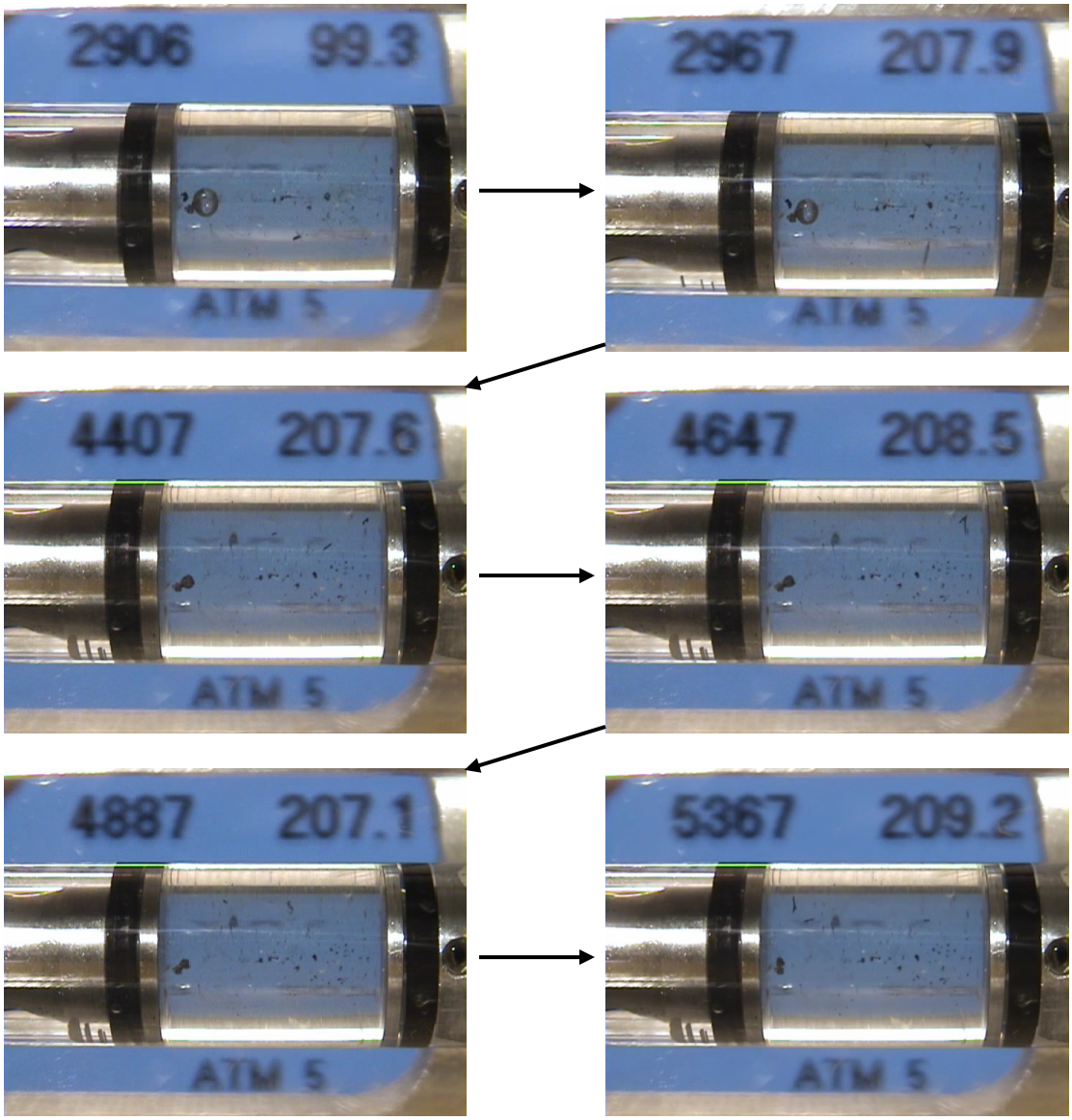

Figure 58. Image sequence of air bubble during dissolution

Results

Twenty tests were performed with degas pressure ranging from atmospheric pressure (i.e., 760 torr) down to $2x10^{-2}$ torr, equivalent residual gas pressure ranging from atmospheric pressure down to 0.12 torr, and resin dissolution pressure ranging from 275 kPa (40 psi) up to 7420 kPa (1080 psi). All testing was performed at 120 °C.

For the first 10 tests, the resin dissolution pressure was increased during the test in order to evaluate the resin pressure required to achieve complete gas dissolution. In the subsequent 10 tests, the resin dissolution pressure was held constant and the duration for dissolution was measured. Test results are presented in Table 3.

Table 3. Resin degassing and air dissolution data

Test	Degassing Pressure		Residual Gas		Dissolution Resin		Dissolution Time	Notes
	kPa	(torr)	kPa	(torr)	kPa	(psi)	(min)	
1	16.88	127	101.3	762	>7420	>1080	NA	No dissolution
2	1.329	10	101.3	762	>7420	>1080	NA	No dissolution
3	1.329	10	7.97	60	3779	550	NA	Complete dissolution
4	0.133	1	101.3	762	>7420	>1080	NA	No dissolution
5	0.133	1	7.97	60	3435	500	NA	Complete dissolution
5a	0.133	1	7.97	60	3435	500	NA	Repeat, Complete dissolution
6	0.133	1	0.80	6	412	60	NA	Complete dissolution
7	0.003	0.02	101.3	762	>7420	>1080	NA	†, No dissolution
8	0.003	0.02	7.97	60	2748	400	NA	†, Complete Dissolution
9	0.003	0.02	0.80	6	412	60	NA	†, Complete dissolution
10	0.003	0.02	0.02	0.12	275	40	NA	†, Complete dissolution
11	0.664	5	3.99	30	2061	300	34	Complete dissolution
12	0.133	1	3.99	30	2061	300	38	Complete dissolution
13	0.003	0.02	3.99	30	2061	300	29	†, Complete dissolution
14	0.664	5	3.99	30	1374	200	40	Complete dissolution
15	0.003	0.02	3.99	30	1374	200	49	†, Complete dissolution
16	0.664	5	3.99	30	1374	200	45	Complete dissolution
17	0.003	0.02	3.99	30	1374	200	38	†, Complete dissolution
18	none	none	3.99	30	1374	200	77	*, Complete dissolution
19	atm	atm	3.99	30	1374	200	40	Complete dissolution

† Resin pressure head ~0.1 torr due to ~1 mm depth of resin in test tube

** Resin held under 200 psi air for ~ 1 h prior to test*

Conclusions

From the testing completed to date, the following trends are observed:

1. Resin degassing at a higher vacuum level results in a modest reduction in dissolution pressure.
2. Resin degas over the range studied does not appear to hasten air dissolution.
3. The residual gas pressure inside the test chamber (mold) significantly affects air dissolution.
4. The resin curing pressure during dissolution significantly affects the rate and magnitude of air dissolution.

Anecdotal evidence has shown that resin degassing is important in order to achieve high quality moldings. The results of this research indicate that resin degas does not have a primary role in abating voids, but rather a secondary role by allowing the minimization of residual gas pressure within the test tube which is primary. The general trend in the data is that degassing at a lower pressure has a small benefit to the dissolution pressure or dissolution time. By comparison, reduction of the residual gas pressure has a significant effect.

For some of these tests, it is possible that the combination of small resin sample (i.e., 1 cm^3) and high resin surface area resulted in rapid resin degas during the few seconds of exposure while the residual gas pressure was reaching equilibrium and prior to the start of dissolution. For example, for

Test #19, the resin was degassed under atmospheric conditions and then the residual gas pressure was adjusted to 5 torr for the dissolution test. During the pressure equalization time of ~5 seconds, the resin may have degassed sufficiently to allow a heightened amount of gas sorption making the results of this test similar to the results of Test #14.

A moderate amount of scatter can be observed in the data gathered to date. It is believed that this demonstrates a low sensitivity to resin degas for this testing and also the stochastic nature of the problem.

5.2. Resin Scaling Study

The resin degassing and gas dissolution experiments described in the first section of this Chapter were conducted on a small 1 cm^3 sample of uncatalyzed resin. In order to evaluate the scaling of those results, experiments were conducted on a catalyzed 20 cm^3 sample of resin. A test matrix was developed based upon the results of the 1 cm^3 experiments. The experimental parameters were designed to probe the hypothesized processing continuum considering resin degas, residual gas pressure and resin curing pressure.

The objective of these experiments is to verify the validity of the results of the experiments presented in Section 1 of this Chapter when applied to a larger sample of catalyzed resin. The scaling test experimental matrix is shown below in Table 4.

Table 4. Resin scaling test matrix

Puck	Resin Degas Pressure	Equivalent Residual Gas Pressure	Resin Curing Pressure	
	(torr)	(torr)	(kPa)	(psi)
1	0.085	1.2	1374	200
2	0.085	28.7	1374	200
3	0.085	28.7	687	100
4	0.085	731	1374	200
5	None	28.7	1374	200
6	None	28.7	137	20

The resin scaling experiments where conducted using a positive displacement resin injection system, designed specifically to support this research. The system comprises a resin cylinder and a pneumatic actuator. A cross section of the resin injector is shown in Figure 59 and a picture of the injector is shown in Figure 60. A piston inside the resin cylinder is driven by the pneumatic actuator to displace the resin out of the cylinder. An O-ring is used to seal the piston to the cylinder. The end of the cylinder is sealed with the 'end plug.' An O-ring is also used to seal between the cylinder and the end plug. Sanitary fittings clamps are used to secure the end plug to the cylinder. The resin cylinder is constructed of aluminum and uses exterior band heaters to heat the system. Thermal insulation surrounds the heaters on the outside of the cylinder.

The pneumatic actuator has a 63.5 mm (2.5 inch) diameter cylinder and can operate up to 962 kPa (140 psi). The resin cylinder has a 44.5 mm (1.75 inch) diameter. The area ratio between the two cylinders results in a two fold increase in resin pressure compared to the inlet pneumatic pressure. For

example, for a resin outlet pressure of 1374 kPa (200 psi), a 687 kPa (100 psi) pneumatic input pressure is required. For control of the resin cylinder (and resin) temperature, a PID temperature controller was used. For control of resin degassing and the residual gas pressure within the cylinder, the vacuum manifold described in Section 1 of this Chapter was used. The lab setup for the Resin Scaling Study is shown in Figure 61.

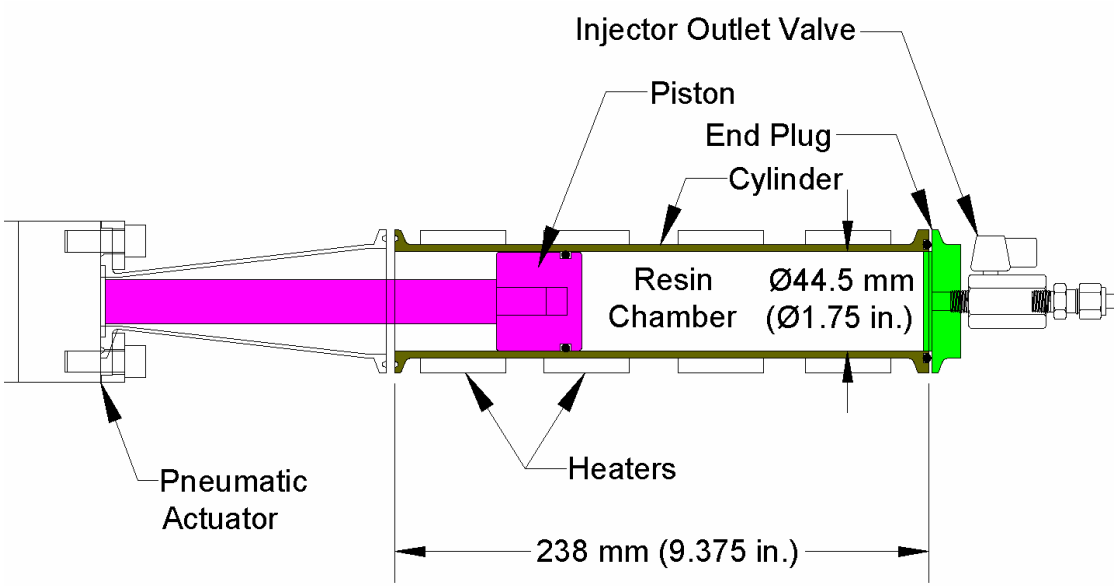

Figure 59. Cross section of resin injector

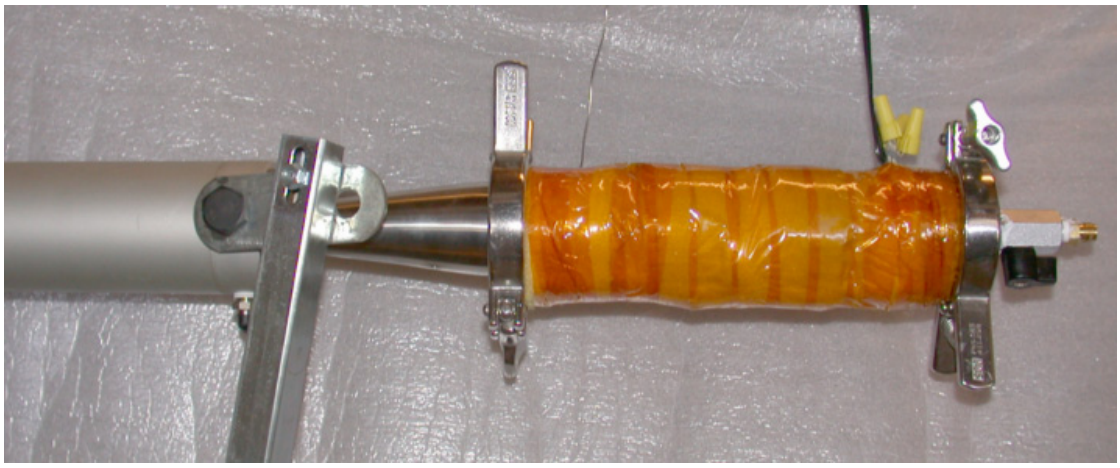

Figure 60. Resin injector

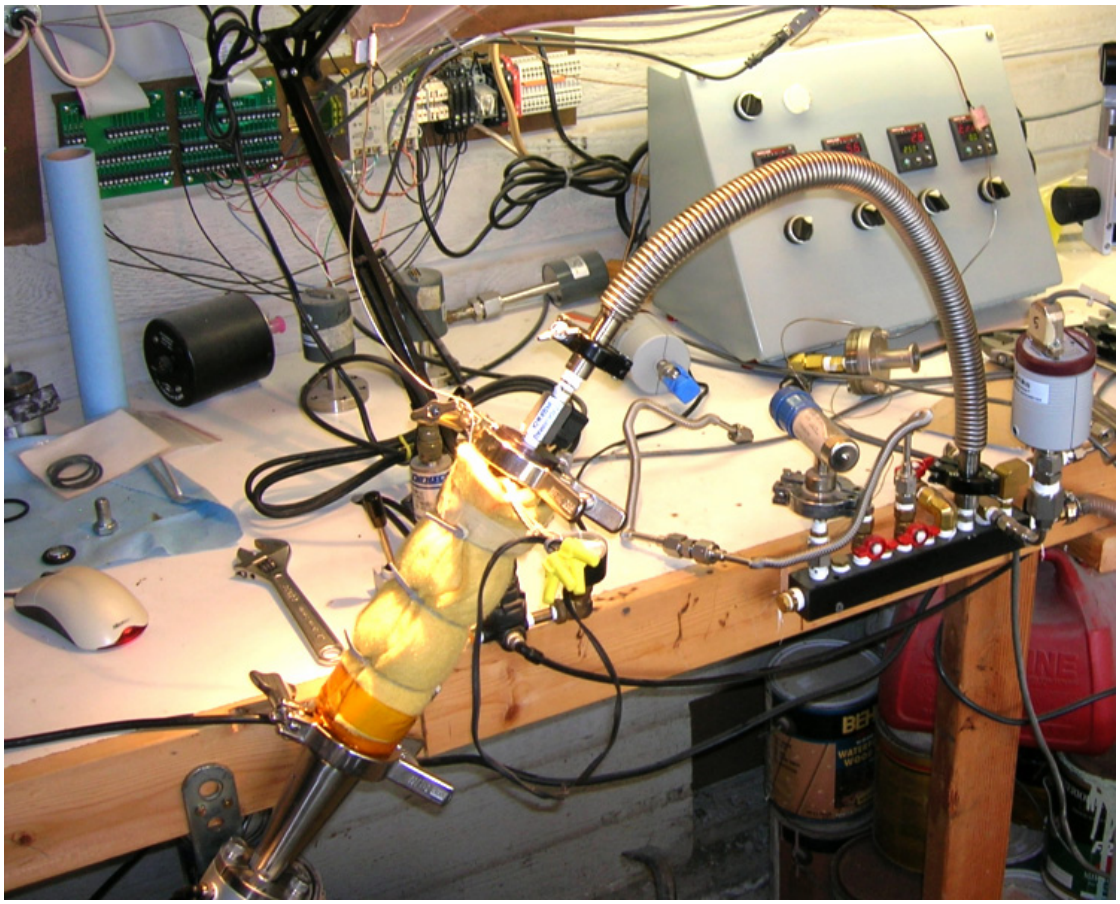

Figure 61. Lab setup for Resin Scaling Study

Testing

The resin cylinder was prepared before each experiment by cleaning followed by the application of mold release. All components were cleaned using Zyvax Surface Clean followed by the recommended seasoning with Zyvax Sealer GP. The mold release used in these experiments was a Zyvax Multishield. After release of the piston, cylinder and end plug, all components were assembled. A ball valve was positioned as the first plumbing component attached to the cylinder end plug in order to minimize the volume between the valve and the resin within the injector (Figure 59 and Figure 60). The system was heated to 121 °C and vacuum applied. Vacuum was typically drawn for a minimum of 10 minutes to achieve vacuum levels below 50 mtorr. With the system preheated and under vacuum, a 20 cm^3 sample of resin was prepared by mixing 15.3 cm^3 of the 862 resin and 4.7 cm^3 of W catalyst (Appendix 5). The resin cylinder was then opened and the resin poured in. The piston was initially fully retracted and the cylinder oriented vertically. After the reinstallation of the end plug, the cylinder was oriented horizontally to minimize resin pressure head effects during degas. The degas vacuum was then applied at the prescribed level for 10 minutes. Once degas was completed, the vacuum level was adjusted to the prescribed level and the ball valve at the end plug closed. The cylinder was then inverted to assure no gas bubbles were trapped between the ball valve and the main body of resin in the cylinder. The piston was then actuated at the prescribed pressure to compress the resin

and residual gas. The resin and gas were maintained under the specified pressure during the four hour cure of the resin at 121 °C.

The volume of gas within the injector when the valve is closed is 287 cm^3 making the ratio of gas volume to resin volume 14.4:1. An equivalent mold residual gas pressure is calculated based on a gas volume to resin volume ratio of 1:1. Consequently, the reported gas dissolution pressure is increased by a factor of 14.4 over the actual pressure applied during the testing to arrive at the pressure of the gas when it occupies a volume equal to that of the resin.

Results

Six resin pucks were fabricated to test processing conditions that would bring about dissolution of gas within the resin test chamber. An example of the puck appearance after piston extension is shown in Figure 62. The results of the testing are shown in Table 5. Several of the pucks fabricated had a void in the O-ring gland. Examples of these voids are shown in Figure 63 to Figure 66. Puck 4 contained largest sized void due to the high residual equivalent gas pressure of 731 torr used for its fabrication.

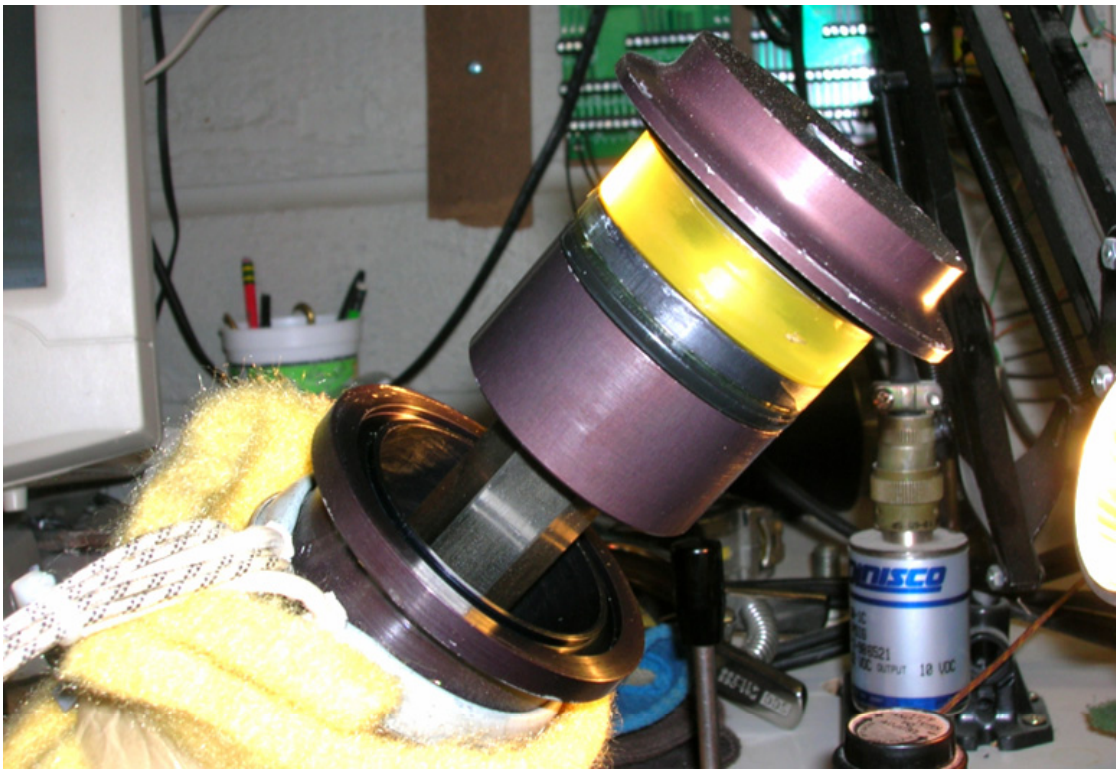

Figure 62. Resin injector with piston extended and resin 'puck' attached to end-plug

Table 5. Results of Resin Scaling Tests

Puck	Resin Degas Pressure	Equivalent Residual Gas Pressure	Resin Curing Pressure		Mass of Gas for Dissolution	O-ring Void Volume	Puck Void Volume
	(torr)	(torr)	(torr)	(psi)	(μg)	(cm^3)	(cm^3)
1	0.085	1.2	1374	200	26.7	0	0
2	0.085	28.7	1374	200	627	0.05	0
3	0.085	28.7	687	100	627	0.1	0
4	0.085	731	1374	200	15,996	0.5	2
5	None	28.7	1374	200	627	0.05	0
6	None	28.7	137	20	627	0.3	0

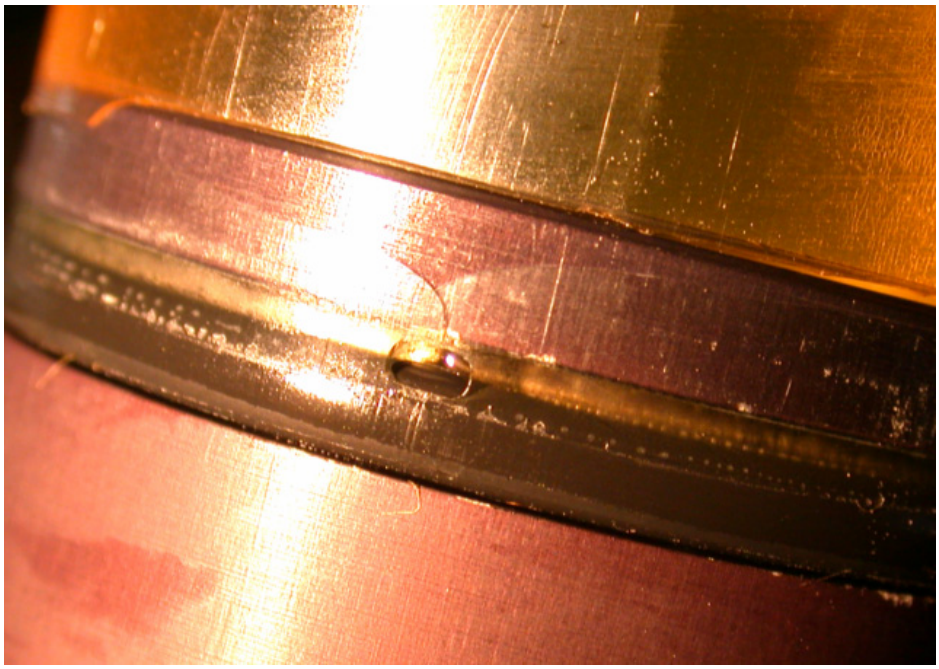

Figure 63. O-ring void in Puck #2

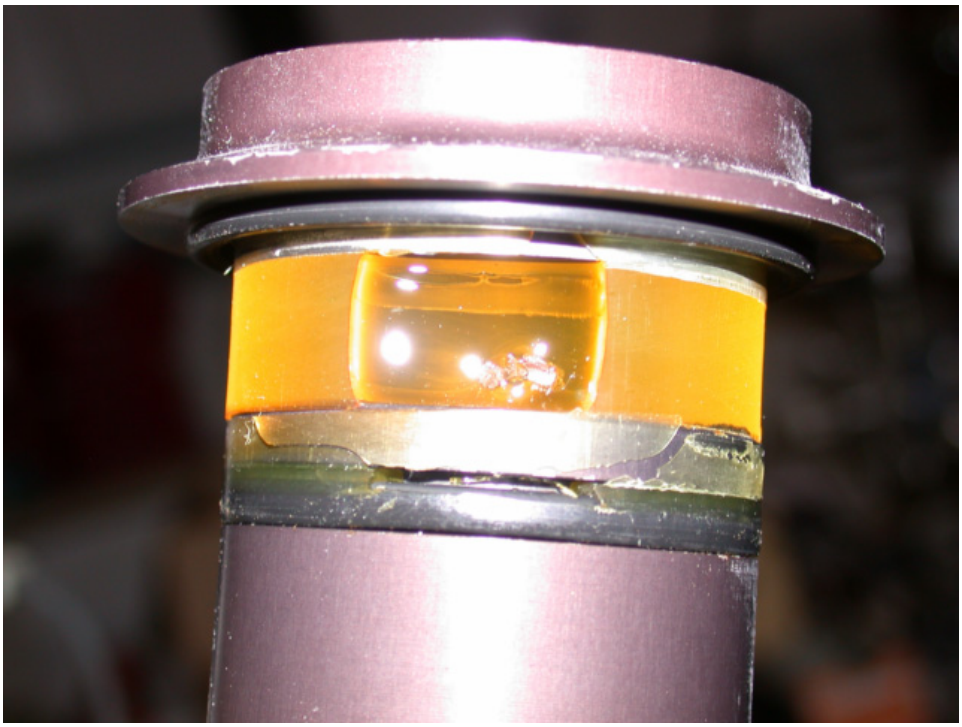

Figure 64. Puck and O-ring void in Puck #4

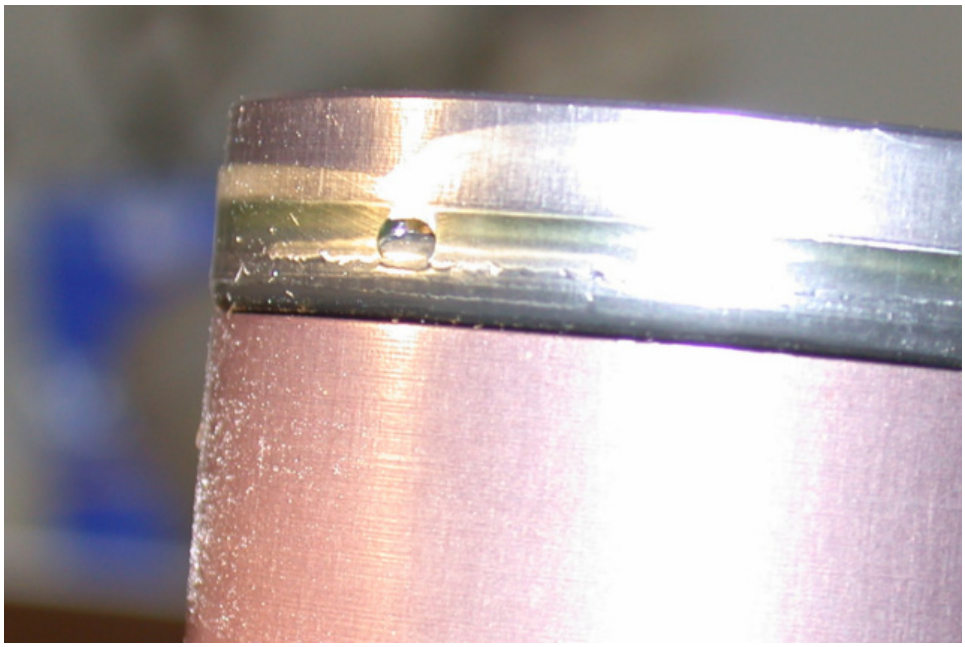

Figure 65. O-ring void in Puck #5

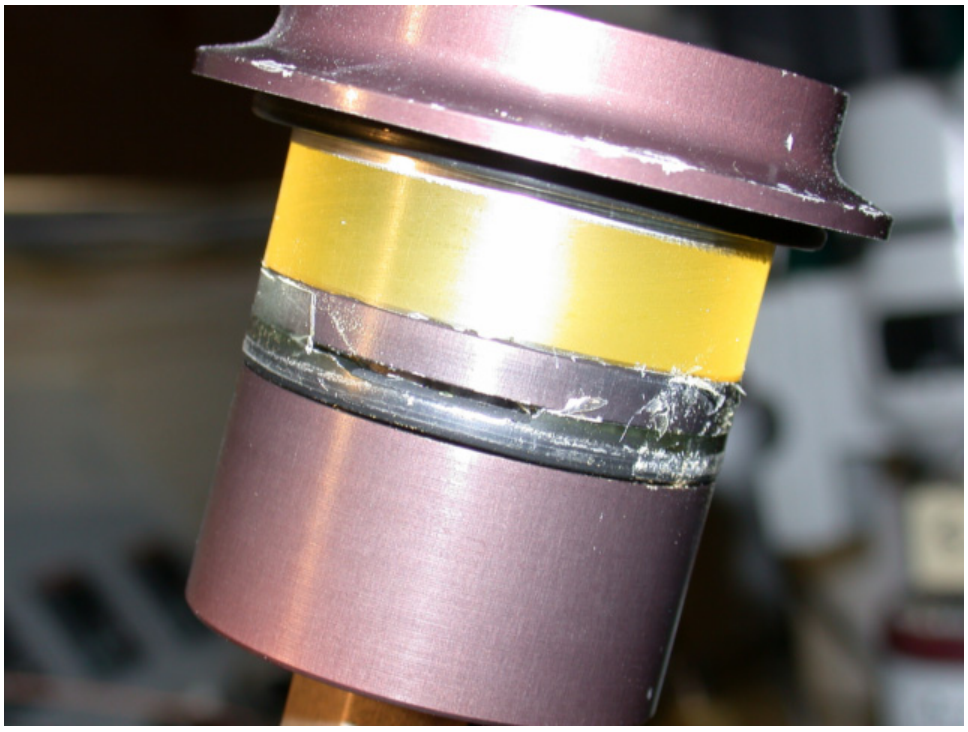

Figure 66. O-ring void in Puck #6

Conclusions

The results of the resin scaling study qualitatively confirm the results of Chapter 5.1. The dissolution of gas seems to be enhanced by the addition of the catalyst. This result is expected as the diffusion coefficient is affected by resin viscosity and the resin viscosity is lowered by approximately 30 % by the addition of the catalyst.

With the exception of Puck #4, all pucks were void free. However, Pucks 2 through 6 contained single voids in the O-ring gland. Pictures of the voids are shown in Figure 63 to Figure 66. The volumetric size of the O-ring voids were estimated and are tabulated in Table 5.

The results of the resin scaling study were not quantitatively satisfying due to the lack of position control of the void. The voids in the O-ring gland had impaired convection around the void making the validity of its persistence questionable relative to a void within the main body of the puck. If these voids are dismissed, the conclusion is that catalyzed resin has even better ability to absorb gas. If the voids are considered as if they were within the puck, then the results show that the presence of the catalyst reduces the gas absorbtivity of the resin. This result is not expected and so these voids have been dismissed as an artifact of the test configuration.

6. PANEL EXPERIMENTS

As a final investigation of mega-voids, experiments were conducted to fabricate composite panels, purposefully introducing a mega-void. Panels were made in order to probe various points within the proposed processing continuum to validate its concept and the dissolution of mega-voids.

229 mm (9 inch) diameter E-glass/epoxy disks were fabricated having a thickness of 1.96 mm (0.077 in). The RTM setup for injection of the panels was configured as a 'blind injection' having a single port through which vacuum is initially drawn and then resin is injected.

The objective of these experiments is to fabricate composite panels that were designed to have a mega-void in order to investigate those process conditions that bring about the dissolution of the mega-void.

A mold was designed and fabricated for molding of panels for these experiments. The mold was constructed from pipe blind flanges as the main mold plates. The eight-inch pipe flanges are steel and have an outside diameter of 343 mm (13.5 in.) and a thickness of 29 mm (1.14 in.). Sandwiched between the plates are a pair of concentric aluminum rings. The inner ring defines the outside diameter of the part cavity. A gap between the rings contains an O-ring that forms the seal between the upper and lower mold plates. Eight ¾-inch bolts are used to secure the flanges together. A cross section of the mold is shown in Figure 67.

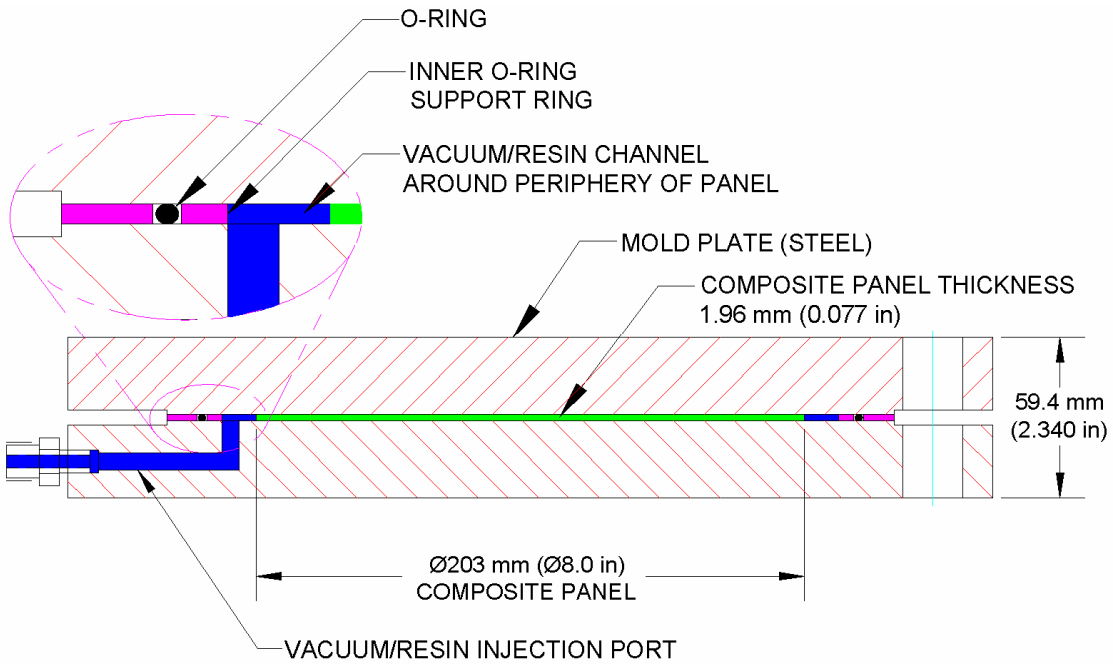

Figure 67. Cross section of panel mold

Three steel mold plates were used and are shown in Figure 68 during preparation. The mold port for vacuum/resin was drilled radially on the outside diameter of the lower mold plate intersecting a hole drilled in the through thickness direction from within the part cavity as shown in Figure 67. The bottom mold plate with aluminum support rings is shown connected to the vacuum manifold in Figure 69. A close up view of the vacuum/resin port is shown in shown in Figure 70. The second mold plate shown in Figure 68 has a port located at the center of the flange through which preform residual gas pressures were measured and reported on in Chapter 4. This second plate was not used for panel fabrication. The third mold plate does not have any ports or modifications and was used as the top plate for panel molding.

Figure 68. Mold plates during cleaning, seasoning and release agent application

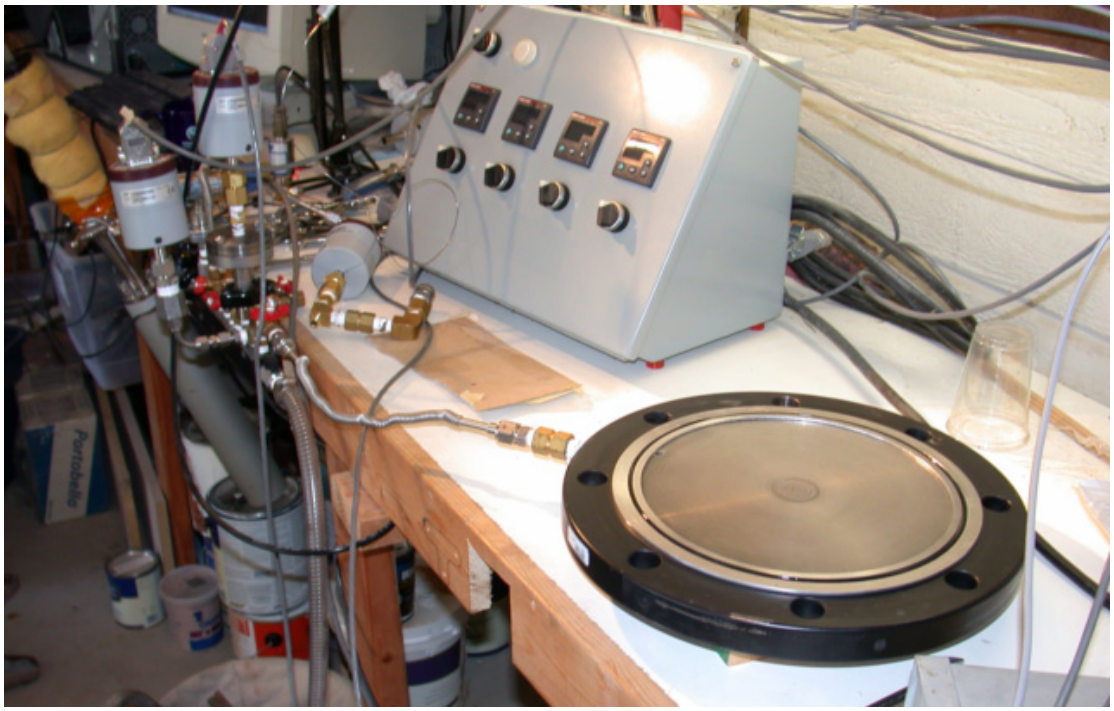

Figure 69. Bottom mold plate with vacuum connection. Vacuum manifold can be seen in background at left.

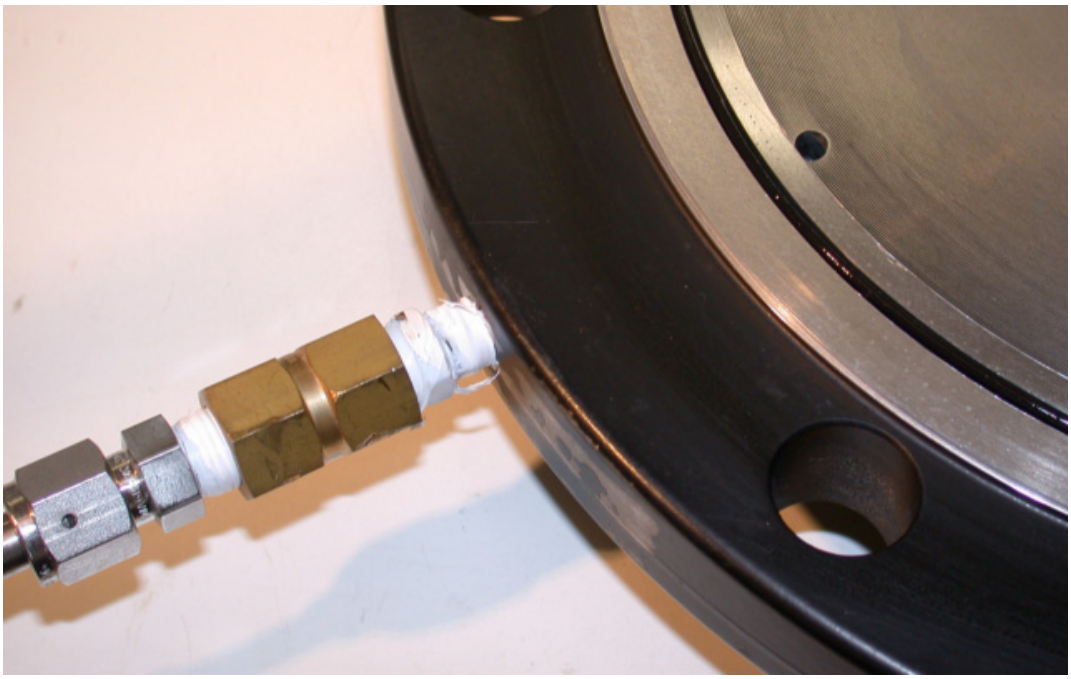

Figure 70. Close up of vacuum/resin port. Penetration into mold cavity is visible at right. Also visible are the O-ring and aluminum support rings.

Heating of the panel mold was accomplished via a pair of 640 W silicone pad heaters. The heaters were bonded to the outside surface of the bottom and top mold plates. Each mold plate was fitted with a thermocouple for feedback to the PID temperature control system.

The resin injector described in Chapter 5, Section 2 was used to inject resin into the panel mold. The injector was positioned next to the mold and connected with a 102 mm (4 inch) length (approximately) of ¼-inch copper tubing. Two-ferrule compression fittings (e.g., Swagelok) were used. A diagram of the experimental setup is shown in Figure 71.

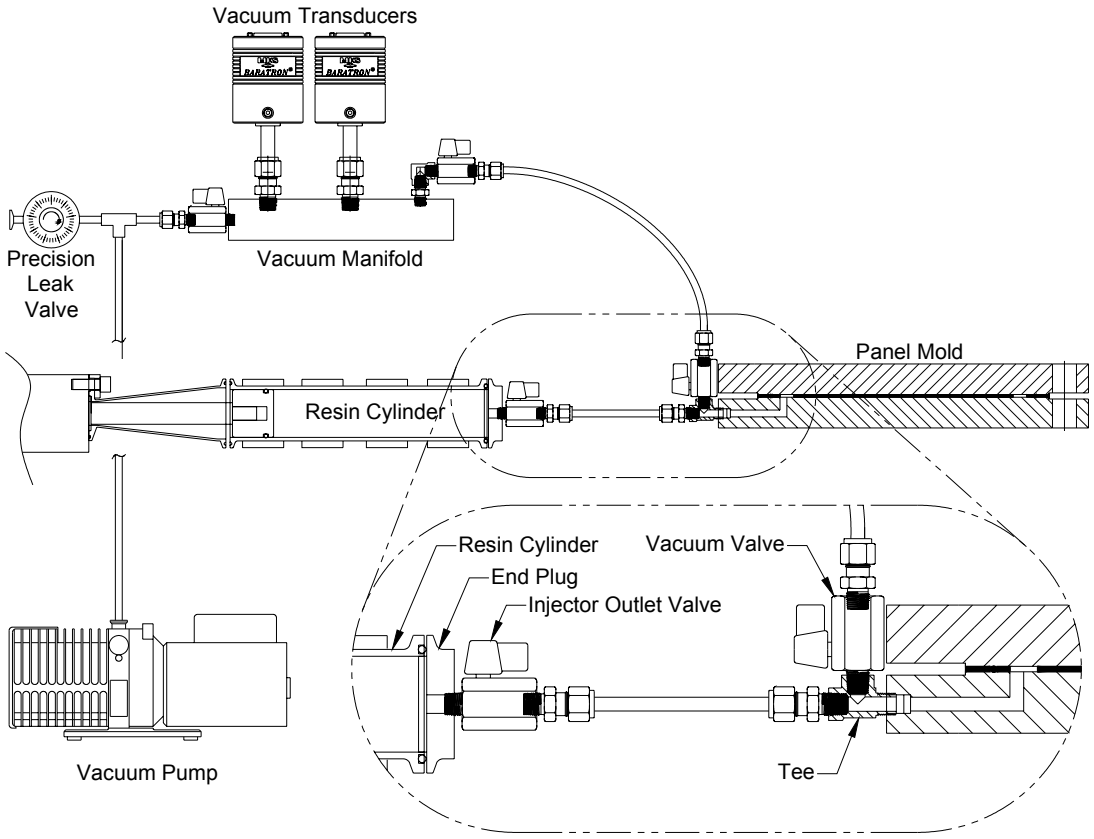

Figure 71. Experimental setup for panel injections

A ball valve was placed at the outlet of the resin injector in the line running to the mold. A tee fitting was positioned at the vacuum/resin port on the mold. A line from the tee connects to the vacuum manifold for mold evacuation and resin degassing. The mold and plumbing setup is shown in Figure 72.

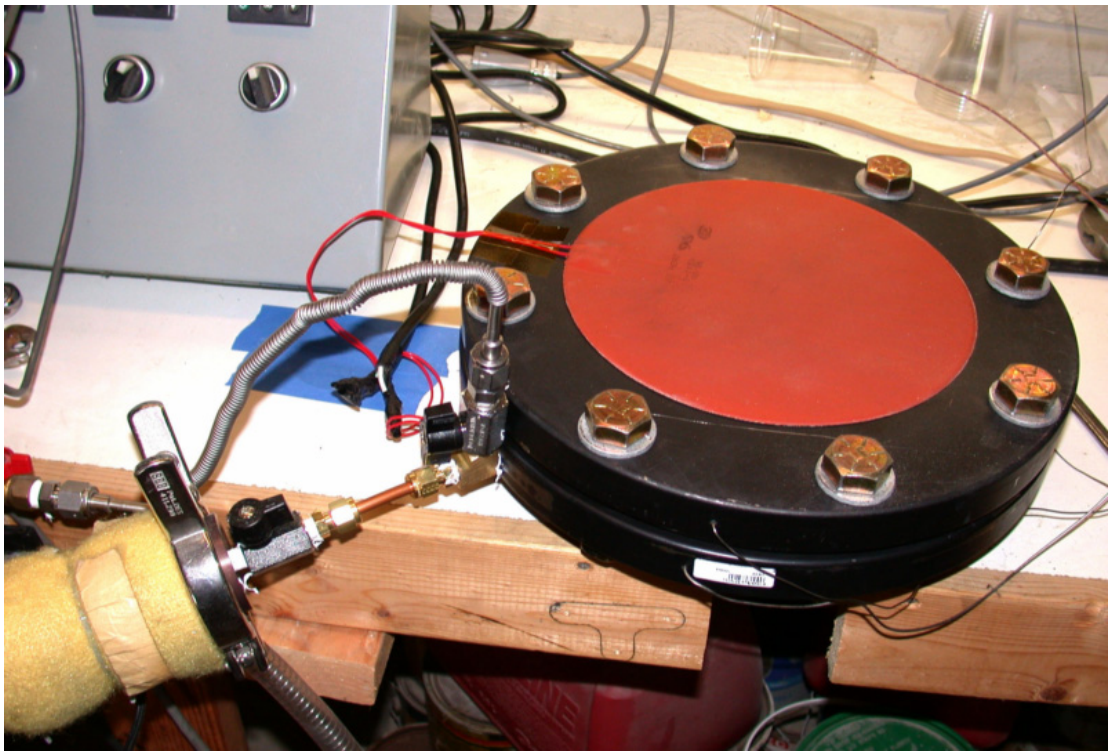

Figure 72. Panel mold connected to resin injector and vacuum line

Testing

For experimentation, the panel mold was cleaned and released. The preform was hand cut from 204 gsm plain weave fiber glass cloth. Ten plies were used in the 1.96 mm (0.077 in) thick panel resulting in fiber volume of approximately 42 %. With the exception of Panel 8, the layup used for all panels was $[(0/90)_w[(\pm45)_w]_2/(0/90)_w]_2$ $(0/90)_w/(\pm45)_w$. The layup of Panel 8 was $[(0/90)_w]_{10}$ in order to simplify preform cutting and preparation. After layup, the upper mold plate was installed and bolted in place. The plumbing connecting to the resin injector and vacuum manifold was installed. The injector and mold were then heated to the processing temperature of 121 ºC. During heat up, vacuum was applied to the system at the prescribed level.

The time required to bring the mold to temperature was on the order of 30 minutes. This dwell time assured similarity in absolute pressure between the vacuum manifold and the preform within the mold. A volume of 84 cm^3 of resin was mixed at a ratio of 26.4 parts per hundred resin (phr). Before introducing the resin into the injector, the valve installed in the resin injector end plug was closed isolating the injector from the mold/vacuum manifold. The end plug was then removed and the resin poured into the cylinder while the piston was in the fully retracted position. The resin injector end plug was then reinstalled. The vacuum level in the manifold was adjusted to the prescribed level for resin degassing and the valve at the end plug opened. Panels 1, 2, 3, 5 and 8 were degassed at a vacuum level of 0.075 mtorr for 10 minutes. Panels 4, 6, 7 and 9 were degassed at 380 torr for 3 minutes. In addition to the resin degassing, this allowed time for the resin temperature to reach approximately 121 ºC before injection.

Panels 2 and 3 used a lower degas pressure (i.e., higher vacuum) relative to the residual gas pressure in the mold. For these parts, once the resin degas was completed, the valve at in the injector end plug was closed and the injection piston immediately advanced pressurizing the resin against the valve. The vacuum level was then adjusted in the vacuum manifold allowing the specified residual gas level to develop within the mold and preform. The time duration allowed for pressure equilibration was approximately one minute. Previous testing on preform degassing (Chapter 4,

Section 4) showed the relation between the vacuum manifold pressure level and the preform residual pressure level. Figure 48 (page 79) shows a nominal equilibrium duration of a few seconds between the manifold and the mold in the pressure range of 5 to 30 torr, the range used for panels 2, 3, 6 and 7.

Panels 4, 6, 7 and 9 were fabricated using a resin degas of 380 torr absolute. For these panels, the preform and injector were degassed as described above. The resin was degassed in a similar fashion but at a pressure of 380 torr and for a 3 minute duration. After resin degas, the plumbing line between the injector and the mold was disconnected and the injector was oriented vertically. The injector piston was then slowly advanced to purge out the air within the resin cylinder. Once resin was witnessed at the injector outlet valve, the valve was closed and the injector was actuated pressurizing the resin against the outlet valve. The plumbing to the mold was then reconnected and vacuum was again applied to the mold/preform to the value specified for that panel (see Results Section). To allow for preform/manifold pressure equilibration on Panels 4, 6, 7 and 9, a dwell time was used. Panels 6 and 7 used a preform gas pressure of 21 torr. Consequently, only one minute was used for pressure equilibration. In order to explore the aspect of preform degassing time, Panel 4 and Panel 9 were processed identically with the exception that Panel 4 used a two minute preform degas duration while Panel 9 used a 10 minute degas duration. After

the above vacuum dwell times, the vacuum valve (Figure 71) was closed and the resin injector valve open to allow resin to flow into the mold and preform.

The resin inlet into the mold cavity is on the perimeter of the part. In addition, a resin flow path around the part periphery was provided specifically to assure the capture of the mega-void in the center of the part.

For all panels, the resin injector pressure was adjusted prior to actuation. Consequently, the resin injection was rapid, lasting a few seconds for all panels. Once injected, the temperature of the resin injector was lowered to 110 ºC to ensure that the resin in the cylinder cured at a slower rate than that in the mold. Lowering of the injector temperature increases the resin viscosity from approximately 30 cps to 50 cps. However, the effect of the viscosity increase is negligible due to the fact that the temperature is lowered after the panel is fully injected. The resin curing pressure was maintained at the specified level (see the Results Section) for the four hour cure of the resin.

The preform for fabrication of the first panel is shown in position in the mold in Figure 73. The preform for fabrication of panel 8 is shown in position in Figure 74. The lab setup is shown during panel processing in Figure 75.

Figure 73. Glass preform, 10 plies ready for injection

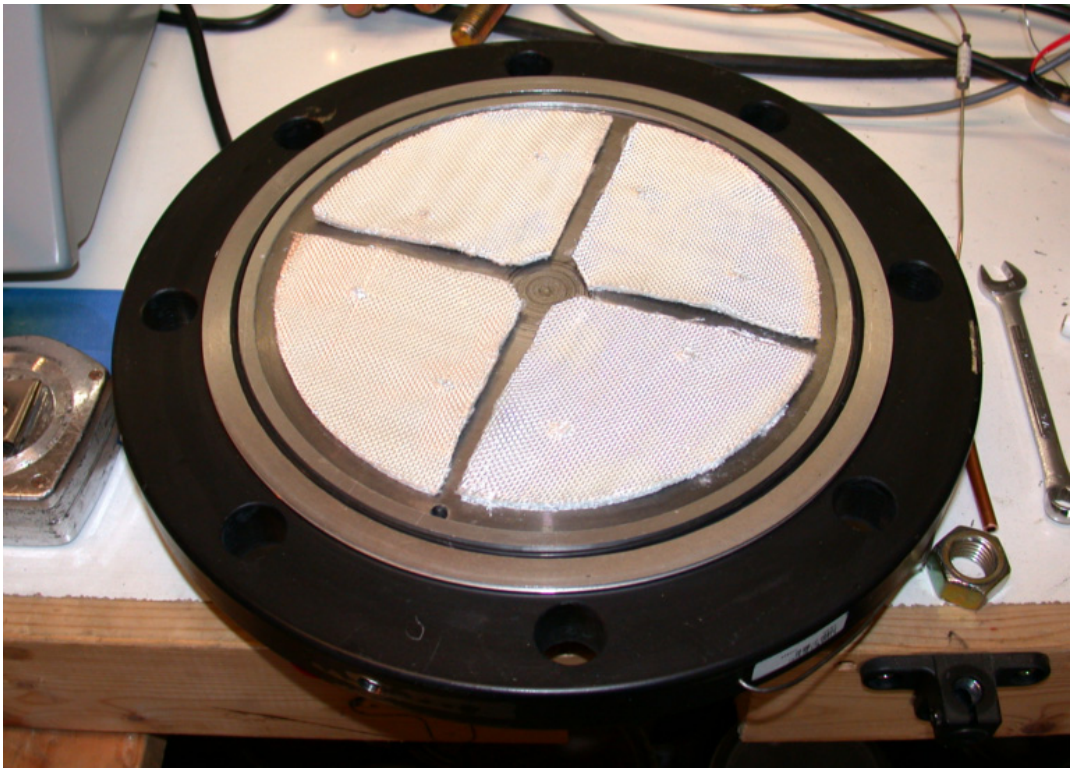

Figure 74. Preform in position for Panel 8

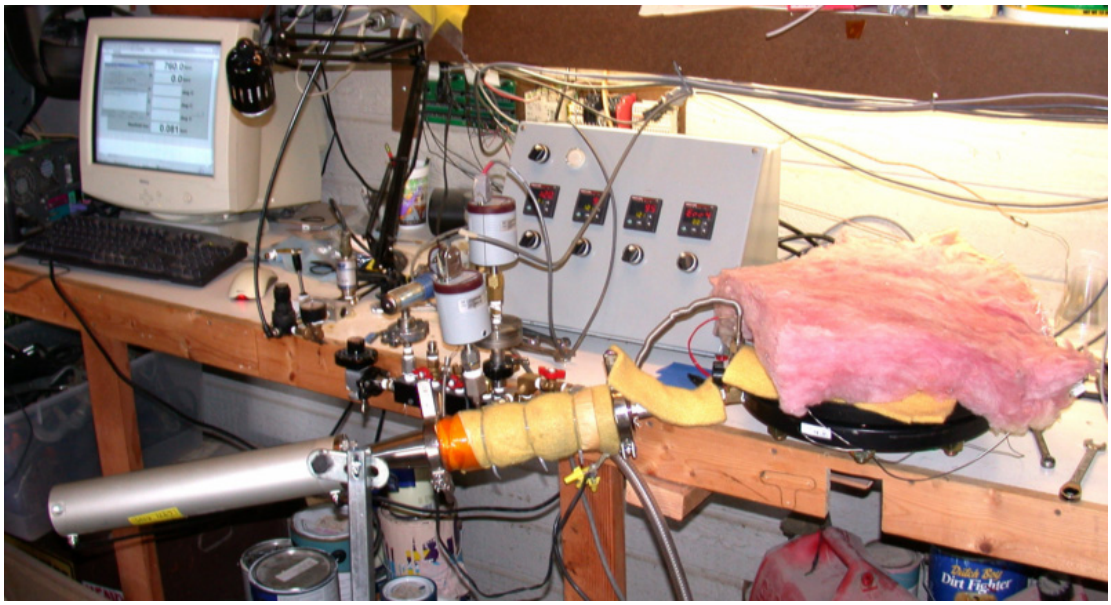

Figure 75. Lab setup during processing of composite panels

Results

Nine panels were fabricated with varying process conditions. The process conditions used for the panels are shown in Table 6. The initial estimated gas mass contained in the mega-void for that panel is also listed in Table 6. The second to the last column has the estimated volume of the persistent mega-void in each panel.

Table 6. Processing parameters for panel fabrication

Panel	Resin Curing Pressure	Resin Degas	Equivalent Preform Residual Gas Pressure	Mass of Gas for Dissolution	Probable Mega-Void Gas	Persistent Mega-Void Size(s)	Compressed Gas Volume
	kPa (psi)	torr	torr	mg		mm^3	mm^3
1	1649 (240)	0.075	0.6	0.023	Resin volatiles	0.0	0.114
2	1374 (200)	0.075	30	1.211	Air	1.3	7.283
3	1649 (240)	0.075	5	0.200	Air	0.3	1.001
4	1649 (240)	380	0.08	0.003	Air	2.0	0.015
5	412 (60)	0.075	0.6	0.023	Resin volatiles	0.1	0.457
6	412 (60)	380	21	1.366	Acetone	0.5	16.994
7	412 (60)	380	21	0.848	Air	3.9	16.994
8	1374 (200)	0.075	37.8	1.521	Air	4 X 1.6	9.146
9	1649 (240)	380	0.07	0.003	Air	0.5	0.014

Panel 1 is shown in Figure 76 after removal of the top mold plate. With the exception of the center of the panel (i.e., the persistent mega-void), Panels 2 to 9 appear similar to panel 1. Panel 8 was unique in that the preform was split into four separate pieces together comprising the same volume as other panels.

Figure 78 to Figure 86 are close up photographs of the center of each panel showing the persistent mega-void or the lack there of. Each photograph is shown at the same level of magnification for comparison purposes.

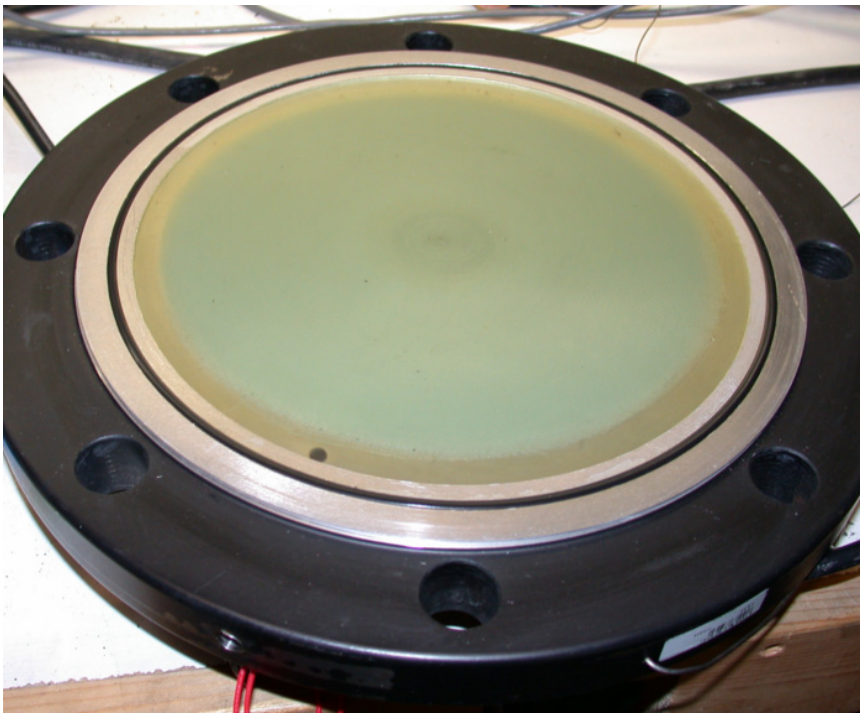

Figure 76. Panel 1 after injection and cure

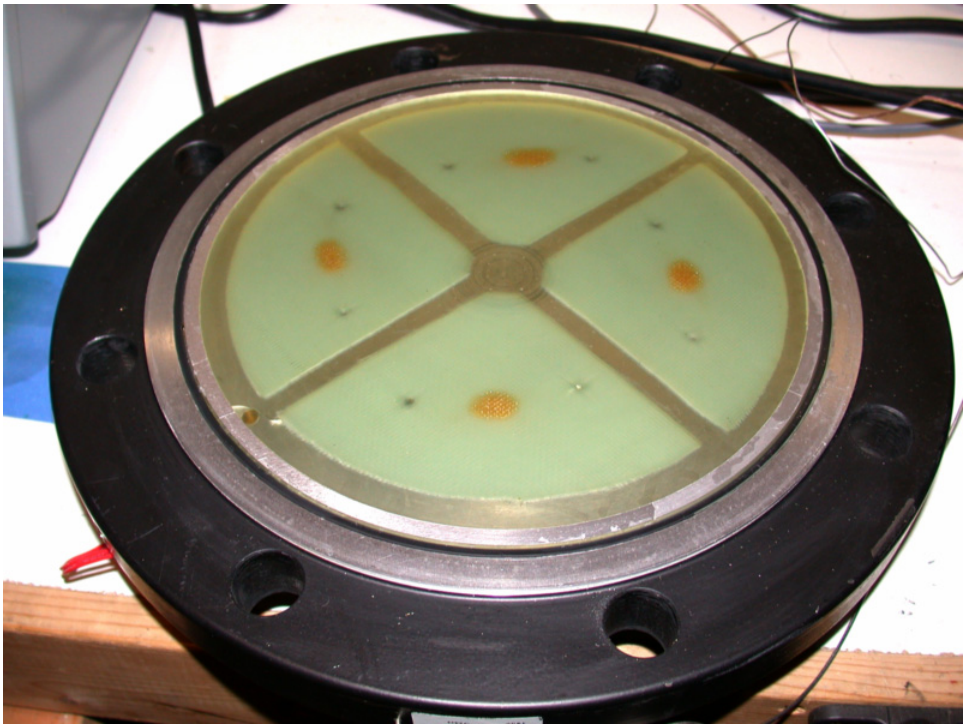

Figure 77. Panel 8 after injection and cure

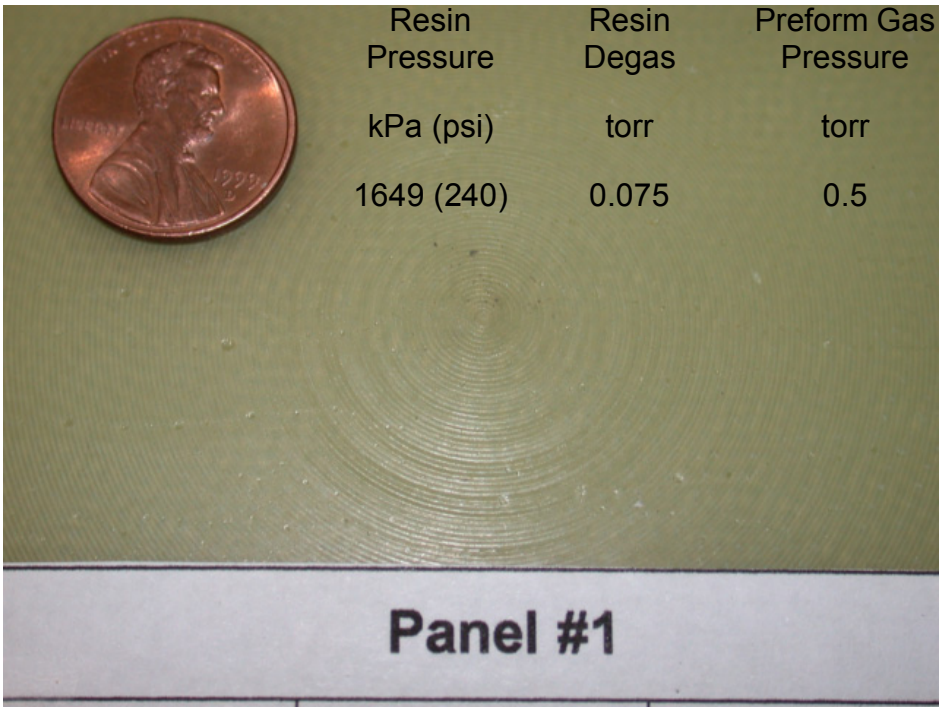

Figure 78. Close-up of center of Panel 1

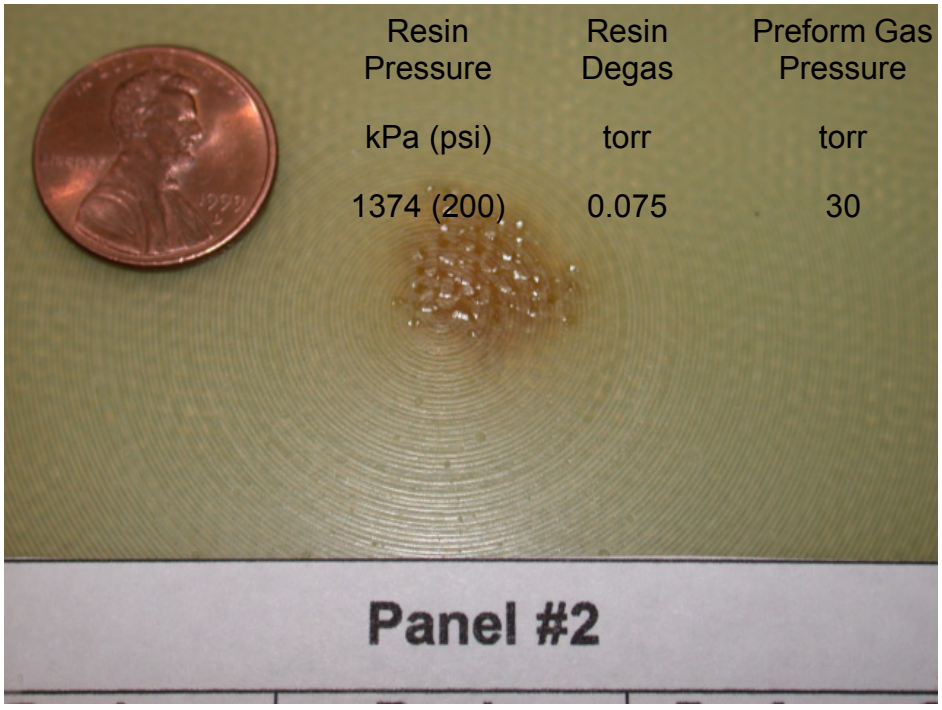

Figure 79. Close-up of center of Panel 2

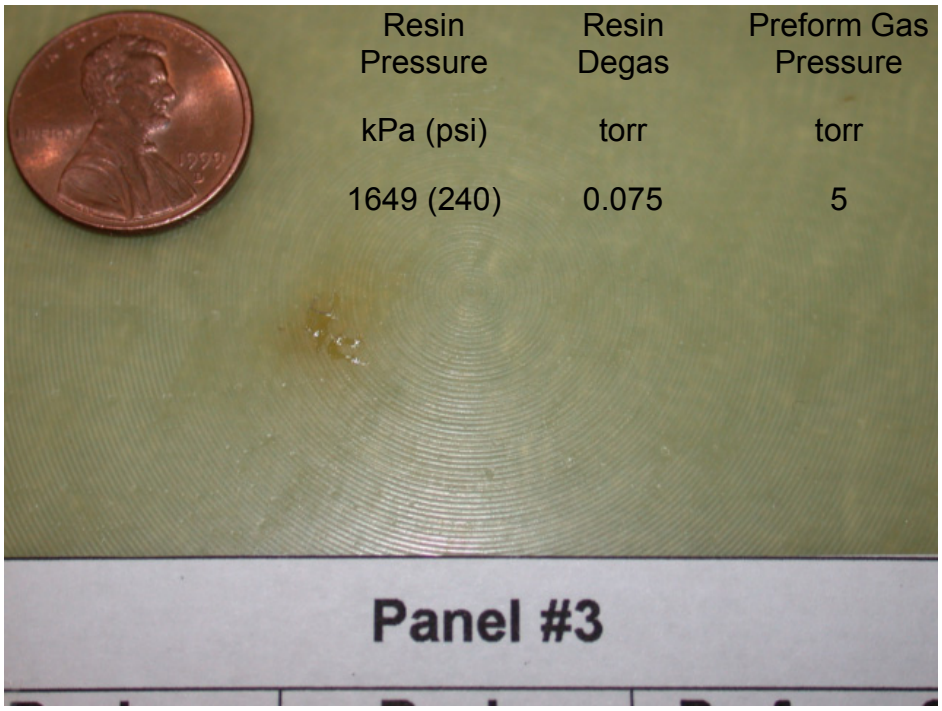

Figure 80. Close-up of center of Panel 3

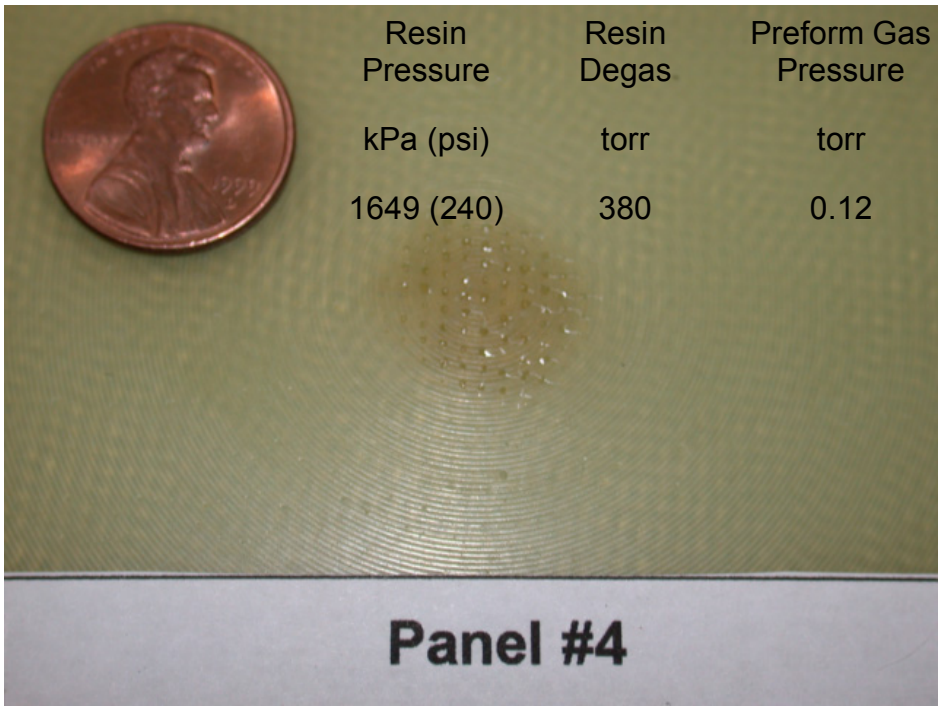

Figure 81. Close-up of center of Panel 4

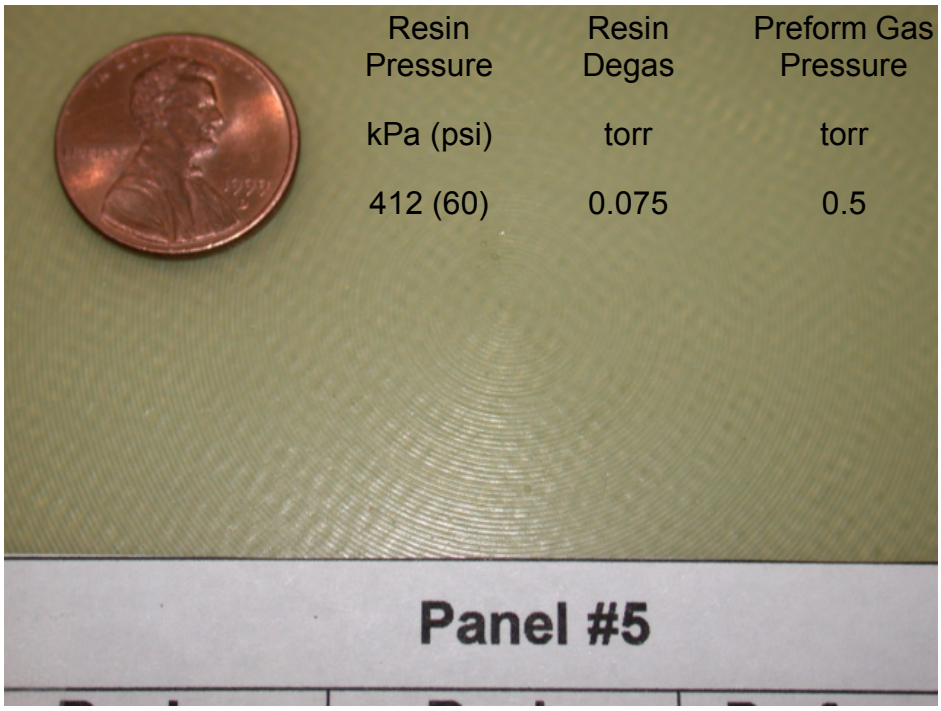

Figure 82. Close-up of center of Panel 5

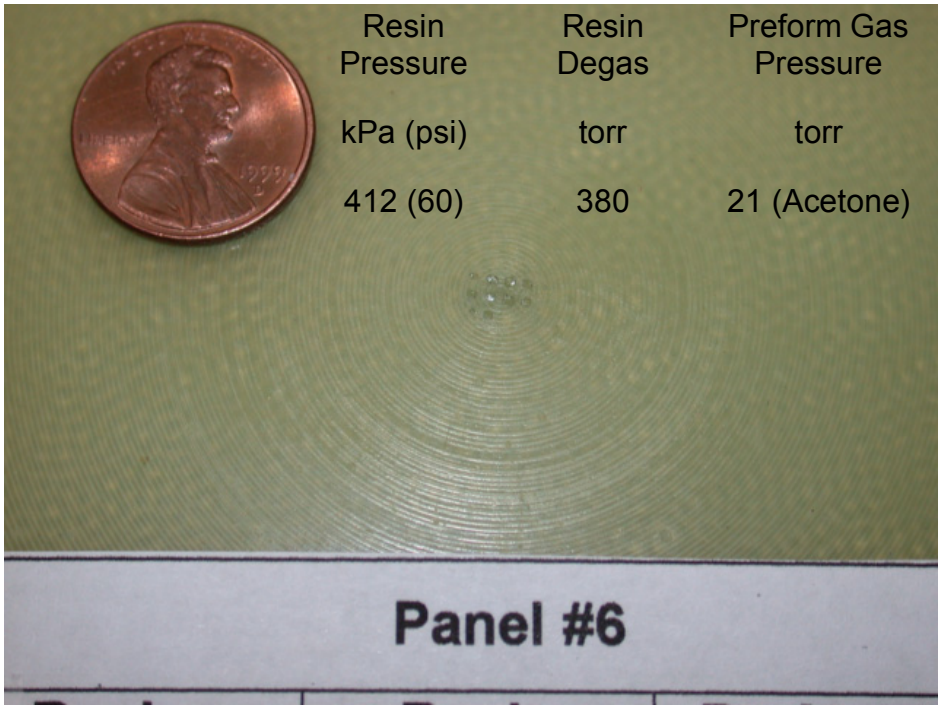

Figure 83. Close-up of center of Panel 6

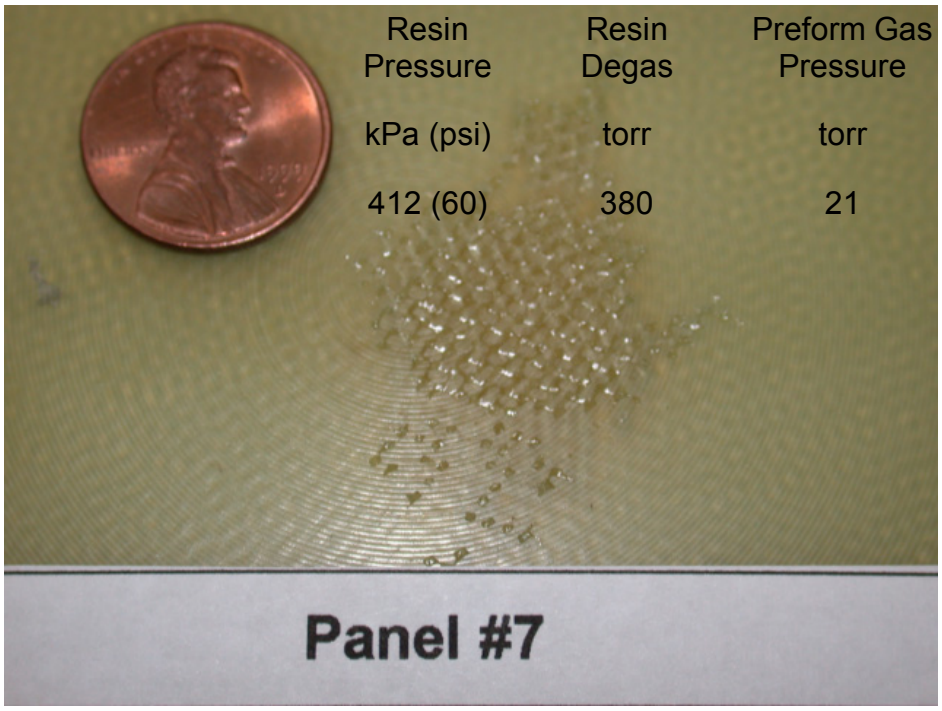

Figure 84. Close-up of center of Panel 7

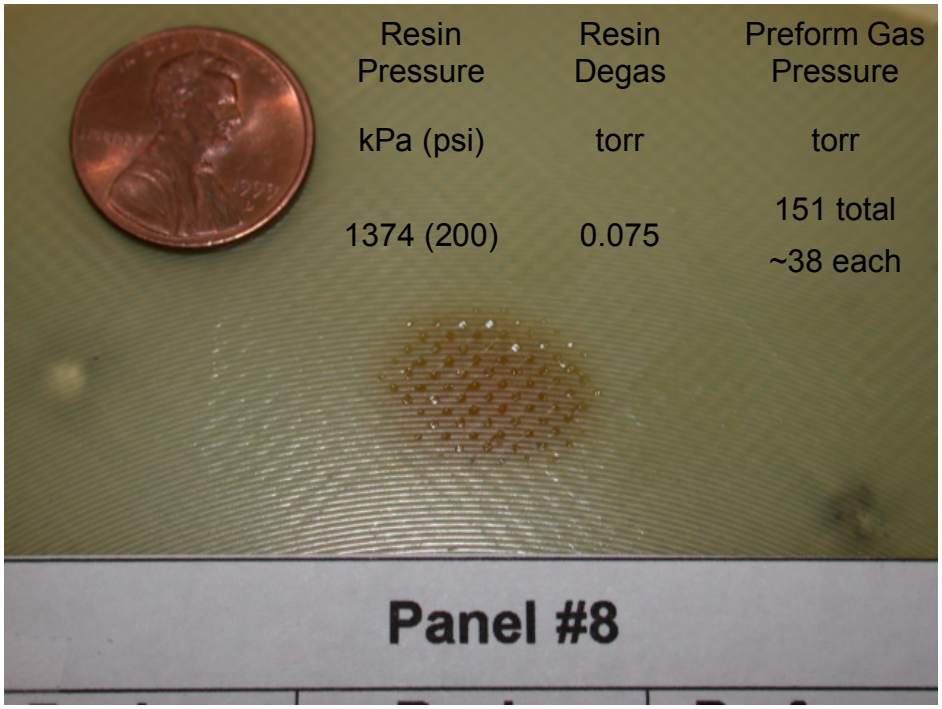

Figure 85. Close-up of center of Panel 8

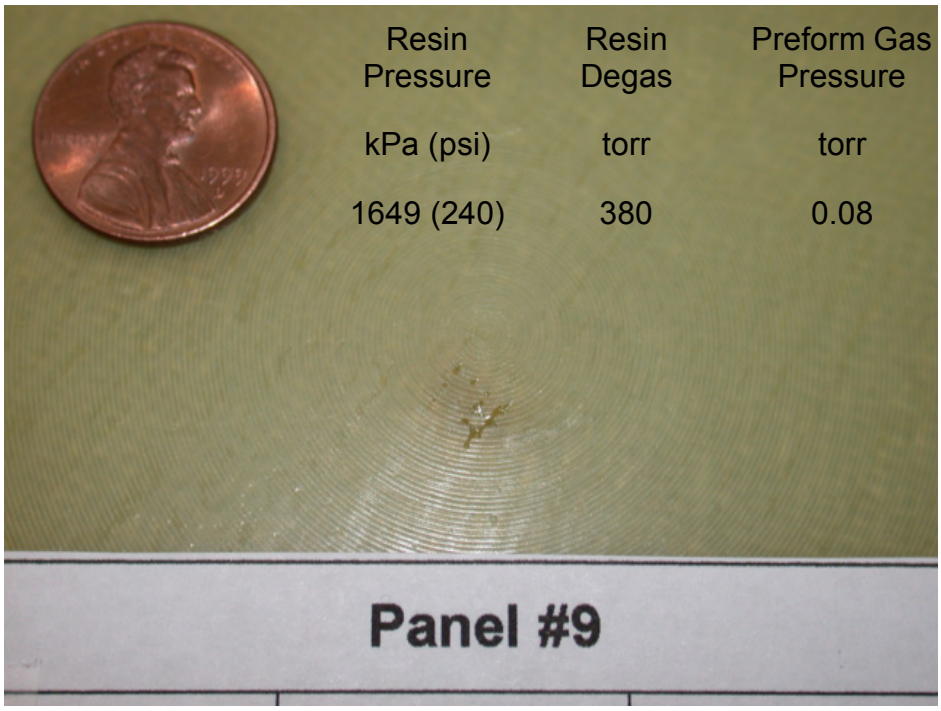

Figure 86. Close-up of center of Panel 9

Conclusions

Panel 1 was fabricated using a 0.075 torr resin degas pressure, 0.6 torr initial residual gas pressure within the mega-void and 1649 kPa (240 psi) resin curing pressure. The resulting panel contained no persistent mega-void. From this panel, it can be concluded that a gas mass of 23 μg was dissolved into the resin.

Panel 2 was fabricated using a 0.075 torr resin degas pressure, 30 torr initial residual gas pressure within the mega-void and 1374 kPa (200 psi) resin curing pressure. These parameters were based upon those developed empirically in Chapter 5. Results of that work (Table 3, on page 95) showed complete gas dissolution for 30 torr residual gas pressure and 1374 kPa

(200 psi) resin pressure. Dissolution occurred essentially irrespective of the resin degas levels used there. The results for Panel 2 show that the resin gas dissolution testing does not correlate with the mega-void dissolution when there is a preform present. This result is not unexpected as the presence of the preform would reduce resin mixing and diffusion. This in turn would limit the amount of resin into which gas could dissolve. Consequently, the resin near to the mega-void becomes saturated with gas and resists additional gas dissolution and the mega-void persists. The persistent mega-void for Panel 2 had a volume of approximately 1.3 mm^3.

Panel 3 was fabricated using a 0.075 torr resin degas pressure, 5 torr initial residual gas pressure within the mega-void and 1649 kPa (240 psi) resin curing pressure. The resulting panel contained a small persistent mega-void with a volume estimated at 0.3 mm^3. This compares to a compressed gas volume of 1 mm^3 indicating that approximately half the gas or 0.1 mg went into solution into the resin. Reduction in the amount of residual gas by 50% to 0.1 mg would have likely resulted in the complete dissolution of the mega-void.

Panels 4 and 9 were fabricated using identical processes with the exception of the preform degassing dwell time. As shown in the preform degassing research in Chapter 4, there is a considerable lag time between the vacuum measured in the vacuum manifold and that present within the preform. The processing of Panels 4 and 9 was designed to highlight this effect. At the end of their respective preform degassing dwell times, the measurement in the

vacuum manifold was 50 mtorr for Panel 4 and 45 mtorr for Panel 9. Panel 4 had a persistent mega-void of approximately 2 mm^3 while Panel 9 and a persistent mega-void of approximately 0.5 mm^3. Based upon the difference in size of the persistent mega-voids, clearly the vacuum level measurement in the vacuum manifold is not representative of the level within the mold. Estimating from the data used to generate Figure 48, the mold internal pressure after 2 minutes of degas is approximately 0.5 torr. After 10 minutes, the mold internal pressure is approximately 0.13 torr. The ratio of these figures compares well with the volume ratios of the persistent mega-voids in Panels 4 and 9.

In addition, resin degassing was also shown in Chapter 4 to have little or no effect on gas dissolution. The process for Panel 4 and 9 was designed to investigate this aspect as well.

Panel 4 and 9 were fabricated using resin degassing of 380 torr. With the exception of resin degassing, the process conditions for Panel 9 was similar to Panel 1. Panel 1 contained no persistent mega-void while Panel 9 had a persistent mega-void with a volume of approximately 0.5 mm^3. The conclusion is that resin degassing does have a beneficial effect for mega-void dissolution. Table 6 shows the estimated gas initially present in the mega-void. The volume of the compressed gas under the resin curing conditions (i.e., temperature and pressure) is also shown in the last column of Table 6. Panel 1 contained no persistent mega-void and was able to absorb 23 μg of

gas. Panel 9 contained 3 μg which was not absorbed by the resin. Comparing the volume of the persistent mega-void in Panel 9 to the compressed gas volume (both in Table 6) shows that the volume of the void is larger than the volume of the mega-void gas under curing conditions. The conclusion is therefore that the resin has out gassed during injection increasing the gas pressure within the mega-void. This amount of gas, once coalesced at the center of the panel is not able to be dissolved back into the resin. This result highlights the fact that even though the majority of the gas resident in the mega-void came out of the resin, the re-dissolution of the gas was not possible due to the concentrating of gas in the resin near to the mega-void. The results of Panels 4 and 9 show that resin degassing is beneficial for the dissolution of the mega-void.

Panel 5 was fabricated using a 0.075 torr resin degas pressure, 0.6 torr initial residual gas pressure within the mega-void and 412 kPa (60 psi) resin curing pressure. The resulting panel contained a small persistent mega-void with a volume estimated at 0.1 mm^3. This compares to a compressed gas volume of 0.46 mm^3 indicating that approximately 80% of the mega-void gas or 0.36 mg went into solution into the resin.

During processing of the panels in this Chapter, it became apparent that the composition of gas within the mega-void may depend on the process parameters. For example, the source of the residual gas in Panels 1 and 5 was the resin outgassing that occurred in parallel with the mold. For Panel 1,

the mold was under a vacuum of < 1 torr when the valve to the resin cylinder was opened to start resin degas. Before opening the valve, there was approximately 1 atm of pressure within the resin cylinder. Consequently, the initial flux of gas out of the resin cylinder backfilled the mold. The composition of the resulting gas in the mold was a mixture of air, resin volatiles and water. Whatever the gas composition that ultimately was trapped in the mega-void, the possibility exists that it was only partially air and that the mixture may very well have had a higher solubility in the resin during mega-void dissolution. In light of this possibility, two panels were fabricated (6 and 7) using identical parameters except that the backfill gas for panel 7 was air and the backfill gas for panel 6 was acetone vapor. Acetone was selected as it was readily available, is highly volatile and is a known solvent for epoxy. Another consideration for the acetone vapor is that it is a 'condensable gas' as opposed to the permanent gases of nitrogen and oxygen in air.

The results of the two panels (Figure 83 and Figure 84) show that the composition of the gas within the mega-void substantially affects the mega-void dissolution. Consequently, the expected (i.e., estimated) residual gas within the mega-void for all panels was added to Table 6 as a consideration of the results.

Another consideration that resulted from the panel fabrication was the size of the mega-void. The initial figure of merit considered for the mega-void was its volume combined with its starting gas pressure. Taken together, these

correspond to a mass of gas. However, it is expected that the mass of the gas within the mega-void is the sole figure of merit. Consequently, the mass of the gas within the mega-void was added to Table 5. To research this aspect, Panel 8 was processed in which the panel preform was split into four pie-shaped pieces as shown in Figure 74. The pieces were then positioned in the mold with resin pathways around each piece. As expected, the resin encapsulated a gas pocket within each of the four preform pieces and four mega-voids were formed. The total mass of gas within the mega-voids of Panel 8 is estimated to be 6 mg. However, because there were four mega-voids formed, each contained approximately one fourth of this amount (i.e., 1.5 mg). The gas mass within the mega-void for Panel 2 is estimated to be 1.2 mg. The resulting size of the persistent mega-void in Panel 8 is very similar in size to the persistent mega-void in Panel 2. This supports the belief that the mass of gas trapped within the mega-void is a key consideration for its dissolution. It is noteworthy that by simply dividing gas volumes trapped within the mold to form multiple mega-voids, there is a better chance for complete dissolution of each mega-void.

With the data generated from the panel molding, a RTM processing continuum figure was developed based upon Figure 6 and shown in Figure 87. The left hand region represents the resin curing pressure. The right hand region represents the mass of residual gas contained in the mega-void. As

previously discussed, the gas mass correlates with the preform residual gas pressure and is considered a better metric for mega-void dissolution.

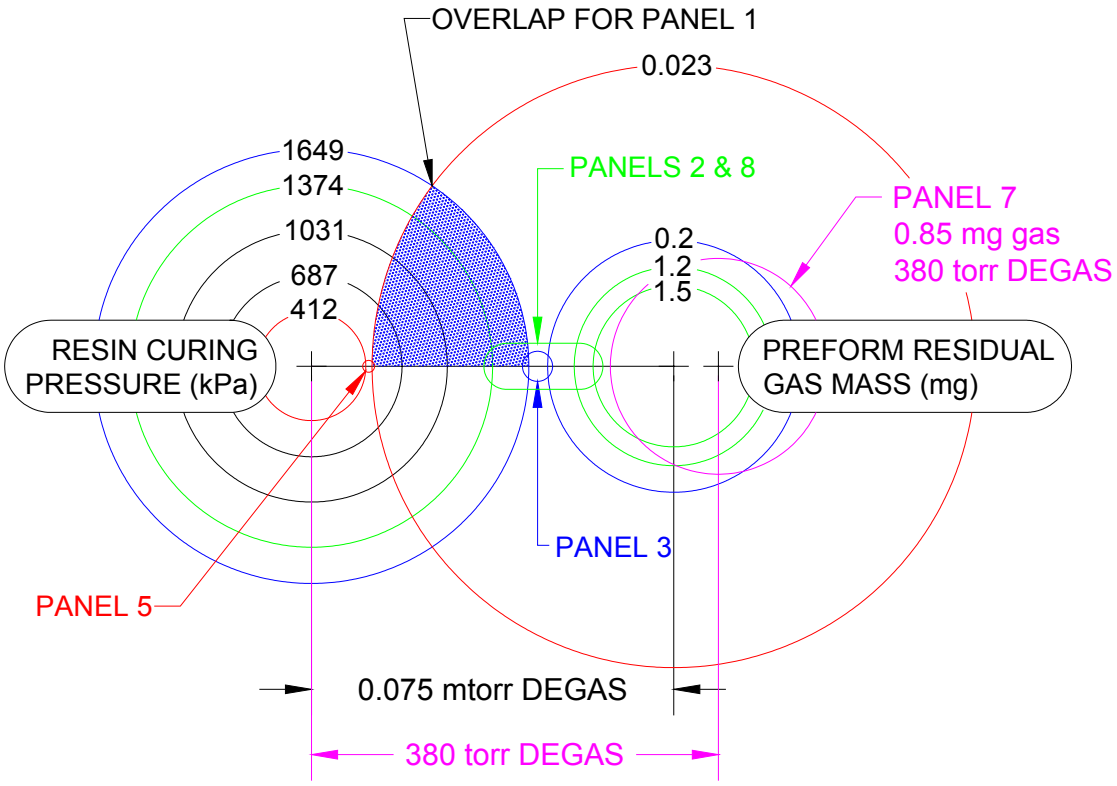

Figure 87. RTM processing continuum using panel fabrication data

The blue overlap region in Figure 87 is shown for Panel 1 indicating dissolution of its mega-void. Other panels are shown with corresponding colors used for their resin curing pressure and preform residual gas mass. The proximity of these two parameters are identified and the distance between the two circles has been scaled to represent the area of the persistent mega-void. For example, Panel 5 contained a persistent mega-void with a volume of approximately 0.1 mm^3. Figure 87 shows process conditions for Panel 5 in

red and no overlap region exists between its circles indicating that dissolution did not occur. The distance between the two circles has been scale relative to the distance for other panels, to indicate the size of the persistent mega-void. As another example, Panel 3 (shown in blue) contained a persistent mega-void with a 0.3 mm^3 volume. Consequently, the distance between the two circles for Panel 3 is a factor of three greater than Panel 5 (i.e., 0.1 versus 0.3).

The distance between the two regions represents resin degassing. Data for Panel 7 is included (magenta) to show how this distance is increased when the resin is degassed at 380 torr. The resin curing pressure data for Panel 7 is 412 kPa, shown in red and the same as Panel 5. The distance between the two circles again represents the size of the persistent mega-void for Panel 7.

Data for Panels 4 and 9 were not included as these panels were designed to explore the duration of preform degassing and how it affects the pressure within the preform. Panel 6 was fabricated using acetone vapor and its data in not relevant to Figure 87.

7. SUMMARY AND CONCLUSIONS

The concept of the mega-void was introduced and it was hypothesized that given the right set of conditions, the gas within the mega-void could be completed consumed with resin such that no void would persist. Four main factors were hypothesized to effect mega-void dissolution; 1) The initial volume of the mega-void, 2) The initial residual gas pressure in the mega-void, 3) The hydrostatic pressure applied to the resin during cure, and 4) The solubility of the mega-void gas in the resin. When considered together, Factors 1 and 2 result in a mass of gas that is contained in the mega-void.

In order to understand the initial residual gas pressure within the mega-void, it is important to understand the residual gas pressure within the mold. Water is a common contributor to residual gases in vacuum systems. Consequently, analytical estimations were made that showed that fiber preforms have the potential to take up a significant amount of water. Subsequently, experiments were performed to measure the mass gain of fabric samples due to aging in a variety of humidity conditions. Glass and carbon fiber preform samples had a measurable weight gain of 0.22% and 0.18% respectively when aged under high humidity conditions. For preform samples aged in moderate humidity conditions, such as those typical for manufacturing environments, very minor mass gains were measured.

The nature of gas flow within a fiber preform was studied in order to better understand the relation between the preform residual gas pressure

within the mold to measurements made external to the mold. The analytical research showed that gas flow within the preform is generally molecular in nature. Consequently, large pressure differentials are expected between the mold internal pressures and measurements made externally. This expectation was confirmed through empirical research conducted to measure pressure differentials between the internal mold pressure and the pressure measured external to the mold during evacuation. A significant pressure difference was measured consistent with the molecular flow of gas within the mold.

Additional experiments using fabric samples that were aged in high humidity conditions required longer durations for pump down than those that were dry. Results using fabric samples aged in practical humidity conditions showed no appreciable difference compared to dried fabric samples.

Chapter 5 presented research conducted to study gas dissolution as a function of resin degas pressure, residual gas pressure and resin curing pressure. The results showed a high sensitivity of resin curing pressure and residual gas pressure on the resin's ability to absorb gas. The results indicate that degassing was not substantially beneficial for the dissolution of gas into the resin. The results of the panel molding in Chapter 6, however, show moderate benefit to resin degassing. Resin degassing reduced the size of persistent mega-voids in the composite panels.

There are obvious differences between the Chapter 5 research and that of Chapter 6. Firstly, the presence of the fabric preform impairs the circulation

of resin and consequently limits the amount of resin that is exposed to the gas and available for gas dissolution. In addition, even if the preform were not present, there is a substantial difference in the aspect ratio of the Chapter 6 panels compared to the Chapter 5 work. The geometry of the flat panels limits the exposure of fresh resin to the mega-void gas for dissolution. Additionally, as with all mega-voids, as the resin infuses the preform, the area of resin at the gas/liquid interface shrinks. Consequently, the gas concentration in the resin near the mega-void is expected to be saturated. Review of the persistent mega-void pictures in Chapter 6 show discoloration of the resin near the persistent mega-void. This may be due to gas saturation of the resin.

The overarching goal of this research is to provide knowledge to help the resin transfer molder make high quality components. The use of process parameters that are favorable to the dissolution of mega-voids will result in a more robust process with a greater chance of producing a high quality, void free component. The three main parameters researched were resin degas, preform residual gas pressure and resin curing pressure. With these three parameters, the best possible process will maximize resin degassing, the preform vacuum level and duration and will utilize the highest possible resin curing pressure. However, limitations will undoubtedly exist. For example, experience shows that the primary limitation is typically resin curing pressure due to mold, press and/or injection equipment limits.

Of the three process parameter researched, it is clear that preform/mold vacuum is paramount for mega-void dissolution. Furthermore, not only is the level of vacuum important, but the duration of its application to the mold as it takes considerable time for gas to migrate out of the preform. The resin curing pressure was found to be the second most effective parameter for mega-void dissolution. Resin degassing was found to be tertiary to preform degassing and resin curing pressure. The use of resin degassing is considered to have a secondary role by allowing the minimization (or maintenance) of low preform residual gas pressures within the mold which is primary.

The results of this research are beneficial to RTM process design. Understanding the hierarchy of the three processing parameters will aid the molder in designing the best process for a given amount of money. Preform vacuum level in most cases is the simplest and least expensive portion of the process to enhance. The ancillary hardware required to achieve high levels of preform degas are a vacuum pump and vacuum transducer. By comparison, resin degassing adds more complexity in the resin preparation and adds more cost in the required equipment to degas resin. Increasing the resin curing pressure is relatively simple but is generally costly. It requires structural considerations for the mold and/or press and requires a resin injection system capable of the higher pressures.

The blind injection setup used for this research is valuable for developing an understanding of the process conditions that effect mega-void

dissolution. However, the blind injection setup is not recommended for producing RTM components as a primary goal is the minimization of trapped gas within the mold. Consequently, it is recommended that vacuum be drawn continuously on the mold during resin injection to minimize the starting size of potential mega-voids. As previously discussed, in RTM components with complex geometries, mega-voids are unavoidable and their dissolution is necessary to result in a high quality part. This fact makes the knowledge on mega-voids resulting from the blind injection setup useful.

Chapter 3 presented some commonly held myths related to the RTM process. This research has addressed all of these myths to some degree. Table 7 summarizes knowledge gained from this research related to each myth.

Table 7. Resin transfer molding myths and related knowledge garnered from this research

Myth	Present State of the Art, Research Findings ,Implication
Resin degassing	**Present State of the Art** Resin degassing is common in RTM processes but there is no consensus as to the procedure or level of degas. **This Research** Resin degassing was found to provide only a small improvement in mega-void dissolution. The research shows that it is tertiary to preform degassing and resin curing pressure. The use of resin degassing is considered to have

Table 7. Resin transfer molding myths and related knowledge garnered from this research, continued

Myth	Present State of the Art, Research Findings ,Implication
	a secondary role by allowing the minimization (or maintenance) of low preform residual gas pressures within the mold which is primary. The lack of consensus in the practice of resin degas is believed to reflect the fact that it only has a small effect on part quality and that of the many degassing variations that exists, they likely all provided approximately the same benefit to the part quality. **Implication** Resin degassing is recommended for use with RTM. However, the degassing procedure used is not critical as there is a low process sensitivity to resin degassing.
Mold vacuum	**Present State of the Art** There is general ambiguity in the literature related to mold vacuum. **This Research** The research shows that mold vacuum is critical for dissolution of mega-voids. The most important aspect to this is the length of time required to achieve low pressures within the mold.

Table 7. Resin transfer molding myths and related knowledge garnered from this research, continued

Myth	Present State of the Art, Research Findings ,Implication
	Related to the ambiguity in the literature, it is possible that for RTM processes that do not utilize curing pressure, the use of mold vacuum during injection on undegassed resin might nucleate bubbles within the resin that would persist after mold filling and cure. This would lead to the conclusion that mold vacuum has a detrimental effect. **Implication** Mold vacuum should be used to maximize the quality of RTM components. Long dwell times are necessary to achieve low pressure within the mold. Consequently, mold evacuation needs to commence well ahead of resin preparation and continue for as long as possible during the process.
Water sorption by the preform prior to placement in the mold	**Present State of the Art** The preform sorbs water during preparation and layup. **This Research** The research shows that water sorption by the preform during handling and storage is in all cases quite small. Even in the extreme case of preform aging in 95 % relative humidity, only a 0.2 % mass gain was measured.

Table 7. Resin transfer molding myths and related knowledge garnered from this research, continued

Myth	Present State of the Art, Research Findings ,Implication
	The belief that the preform sorbs atmospheric water is unfounded. **Implication** Preform water sorption is unlikely to affect any RTM process. The implication of this is that if special provisions are currently practiced to preclude preform water sorption, these can be discontinued as they address a non existent problem.
The use of vacuum on the mold prior to injection in order to remove preform water	**Present State of the Art** Mold vacuum is commonly cited as removing water from within the preform. **This Research** The research shows that the impact of preform water on mold vacuum levels is minor in all but the extreme cases. If water were present in the preform, mold vacuum would remove it. However, the presence of water in the preform in any significant amounts is unlikely. The research has shown that mold vacuum is primary for the dissolution of mega-voids. The processing benefits of high vacuum levels that

Table 7. Resin transfer molding myths and related knowledge garnered from this research, continued

Myth	Present State of the Art, Research Findings ,Implication
	might be credited with removing preform water are in fact simply removing the residual air from the preform. **Implication** As stated above, mold vacuum should be used to maximize the quality of RTM components. However, the purpose of the mold vacuum is to simply remove air. Preform water is minimal.
The treatment of vacuum as discrete	**Present State of the Art** Vacuum is either on or off irrespective of its actual level. **This Research** The research shows that vacuum can be treated as discrete in some cases. For example, resin degassing was shown to have a low sensitivity to vacuum level and so considering the vacuum as either on or off is acceptable. However, discrete vacuum is wholly inadequate for preform degassing/mold vacuum. In this case, the level of vacuum and the duration over which it is applied are both critical for the dissolution of mega-voids.

Table 7. Resin transfer molding myths and related knowledge garnered from this research, continued

Myth	Present State of the Art, Research Findings ,Implication
	Implication Vacuum can be treated as discrete for resin degassing but not for mold evacuation.
The measurement of vacuum levels outside the mold as representative of the actual vacuum levels within the mold	**Present State of the Art** Vacuum is measured outside the mold and consider representative of the internal pressure. **This Research** The research shows that vacuum measurements made outside the mold are only indicative of internal pressures over a very narrow range near atmospheric pressure. As the pressure is reduced, the difference becomes considerable at times differing by a factor of 1000. Even more poignant is the considerable lag time between the external pressure and internal pressure. For the small panels made in this research, 10 minutes was the smallest lag time between the external pressure reaching 0.1 torr and the internal pressure reaching 0.1 torr. **Implication** Vacuum level measurements made external to the mold are not indicative to internal pressures. Ideally,

Table 7. Resin transfer molding myths and related knowledge garnered from this research, continued

Myth	Present State of the Art, Research Findings ,Implication
	preprocessing measurements should be made directly on the mold to provide a basis for comparison for subsequent use during component fabrication.

8. IMPLICATIONS AND FUTURE RESEARCH

This research has developed an understanding of the processing continuum shown conceptually in Figure 6 and quantitatively in Figure 87. For RTM components processed within the overlap, dissolution window, the resin can absorb the gas present inside the mega-void and no voids will persist. In this case, it is noteworthy that flow artifacts such as capillary action, flow rate, micro/macro/mega-void, and race-tracking are relevant only to processing outside the window. These mechanisms may occur transiently during processing inside the window but their individual magnitudes are not relevant. For example, consider 'Part X,' molded having significant race-tracking and using a flow rate favorable to minimizing macro and micro voids. This processing will result in a situation near the end of injection where there would be a large mega-void if processing occurred outside the window. 'Part Y' could be made using processing conditions such that no race-tracking occurred and using a high flow rate conducive to the formation of micro-voids. For processing outside the window, the resulting part would contain a fine distribution of micro-voids. For both Part X and Part Y, processing changes might be made which would bring about a low void, acceptable quality part while still processing outside the proposed window. For example, in Part X, a vent port could be machined into the mold at location of the mega-void resulting in the elimination of the mega-void. In Part Y, the flow rate could be reduced to a level favorable for a balance between micro flow and macro flow

so as to eliminate micro and macro voids. Having made the processing changes, both Part X and Part Y would be of acceptable quality having been processed outside the window. This demonstrates the utility of the significant research performed on resin flow fronts, flow rates, formation of micro voids, macro voids etc. These are issues that required understanding when processing outside the continuum window in order to bring about an acceptable part. Now consider processing inside the window. Part X results in a mega-void which would be absorbed in the latter stages of the injection, during the application of resin curing resin pressure. Processing Part Y inside the window would result in the distribution of voids being absorbed again during the latter stages of the injection. For processing inside the window, significantly different processing parameters (i.e., Part X verses Part Y) both result in an acceptable quality part. This shows the benefit of this processing science. All flow patterns, gate design etc. have a better chance of producing an acceptable part. The formation of micro-voids, macro-voids and mega-voids during injection does not affect the final part quality. This is the value of this research.

This research has demonstrated the dissolution of mega-voids in RTM. This work lays the foundation from which models and subsequently analytical tools may be developed. Resin degassing, preform degassing/mold vacuum and resin cure pressure were all shown to affect mega-void dissolution. The size (i.e., the gas mass within) of the mega-void was also shown to be a

critical factor for its dissolution in addition to the composition of the residual gas in the mega-void.

Analytical models are needed to quantitatively frame mega-void dissolution. The models would at a minimum consider the five items above. Implementation of the models into analytical tools such as flow modeling would significantly enhance their fidelity and validity. The initial starting pressure would be defined and the software, in addition to estimating the resin infiltration, would track and estimate the residual gas position and pressures, When an area of gas is calculated to be trapped, (i.e., a mega-void), the software would evaluate criteria for its dissolution. For example, based upon the panels fabrication in this research, the criteria would be for resin degassed at torr levels and resin curing pressures of 1649 kPa (240 psi), mega-voids that contain less than 23 μg of gas would be completely dissolved.

The makeup of the gas within the mega-void effects its dissolution. Models could be developed to estimate the gas composition. Addition experimental work is required to understand the gas composition. At higher residual gas pressures, the gas composition is expected to be air. At lower pressures, it may be largely water. However, during resin infiltration dependant upon the process parameters, the gas composition may change significantly. For example, in a scenario where the residual gas is largely air, if resin/volatiles displace or dilute the air and end up being trapped in the mega-void, there will be enhanced gas dissolution. This bodes well for RTM

injection setups where resin degas occurs through the mold (in series) as shown in Figure 1. Alternatively, the use of a pressure pot for injection would likely have mold evacuation occurring in parallel with the pressure pot. Comparing these two setups, all else being equal, the composition of gas within the mold for the series resin degas would likely contain more resin volatiles compared to the parallel degas.

In this research, in addition to air, only acetone vapor was evaluated for gas dissolution within the mold. Future research that would investigate alternate vapors and other permanent gases such as helium may produce very interesting results (e.g., what mass of helium can be absorbed by the resin). With alternate gases, condensable gases are expected to more easily lead to elimination of the mega-void. However, the liquid phase of the starting vapor may or may not be miscible in the resin. If the preform were backfill with water vapor for example, under the appropriate pressure and temperature conditions, the water would condense and the mega-void would collapse. However, the liquid water solubility in the resin is limited and undoubtedly has structural considerations that are outside of the scope of this research. In addition to the preform gas composition, resin additives (e.g., wetting, air release) can be evaluated to discern their ability to aid gas dissolution.

For the composite panels fabricated in this research, the resin injection rate used was always high. Future research may evaluate how a high flow rate compares to the low flow rate. In addition, the type of flow (i.e., flow

controlled versus pressure controlled) may provide further insight into mega-void formation and dissolution. For the blind injection setup, at the beginning of resin injection, there is a finite amount of gas within the mold. Process techniques that can effect the final location of the gas will likely dictate techniques that will increase the quality of the final part. As resin flows into mold, a slow resin flow rate allows capillary action to do its work and minimize microvoids. An optimal injection rate per Chen (Ref. 2) would result in the coalescence of residual air into one large mega-void. This might be optimal for a situation where the displaced air is pushed out through a vent. However, for the case where a mega-void will form, it is expected to impair the dissolution of the gas into the resin. With the mega-void, the encroaching resin might become saturated locally near the resin flow front and not be able to absorb any additional gas. Dissolution of the mega-void could occur over time but after initial flow front saturation, a saturation gradient exists and the dissolution of the gas would become diffusion limited (i.e., the gas would have to diffuse through the resin). Consequently, gas saturated resin diffusion through the preform may not be possible on a timescale compatible with the curing resin. In contrast, a high resin injection rate would maximize the distribution of micro voids and thereby reduce the size of the mega-void. For the blind injection setup, both injection scenarios are assumed to have equal amounts of gas present in the mold/preform at the start of injection. A more uniform distribution of gas is expected within the mold resulting from a higher

injection flow rate. With more uniformly distributed gas in the mold, void dissolution is expected to occur more rapidly and with a better chance of complete dissolution.

APPENDIX 1: EXPERIMENTAL HARDWARE INFORMATION

Item: Vacuum Pump

Manufacturer: Varian

Model: P1111-307

S/N: 317357

Description: Two stage rotary vane vacuum pump

Used in: Preform drying, preform pump down studies, resin dissolution study, resin dissolution scaling study, panel molding study

Picture:

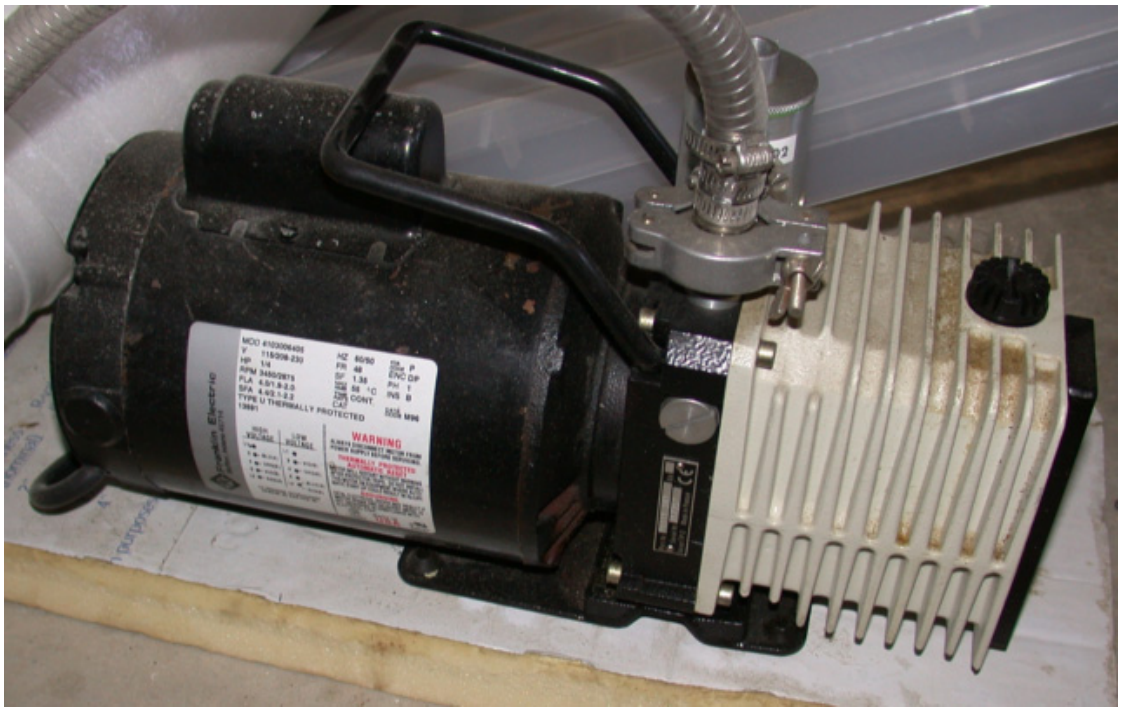

Figure 88. Varian vacuum pump used for all experiments

Item: Resin Injector

Manufacturer: Designed by Author

Model: NA

S/N: NA

Description: Fabrication drawings provided in Appendix 3,

Used in: Resin dissolution scaling study, panel molding study

Picture: Pictures, cross section in Figure 59, on page 99.

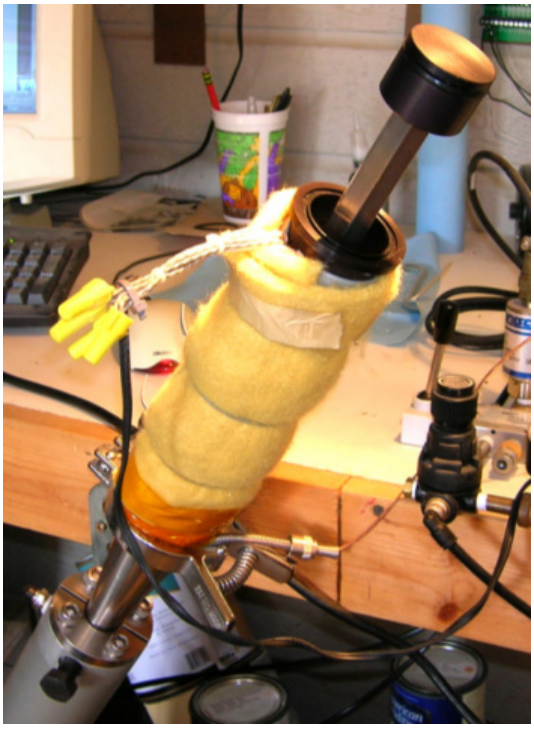

Figure 89. Resin injector with piston extended for cleaning

Figure 90. Injector with end plug installed and clamped. Outlet valve and VCO fitting are also visible.

Figure 91. Pressure regulator, 3-way 5-port control valve and pressure transducer for resin injector control

Item: Vacuum transducer – capacitance manometer

Manufacturer: MKS

Models:

626A13TAE, Qty 2, 0.1 – 1000 torr range

626A11TAE, Qty 2, 0.001 – 10 torr range

S/N: 001822626, 001827086, 001827087, 001822625

Description: Capacitance manometer vacuum transducers

Used in: Preform degassing studies, resin gas dissolution study, resin gas dissolution scaling study, panel molding study

Picture:

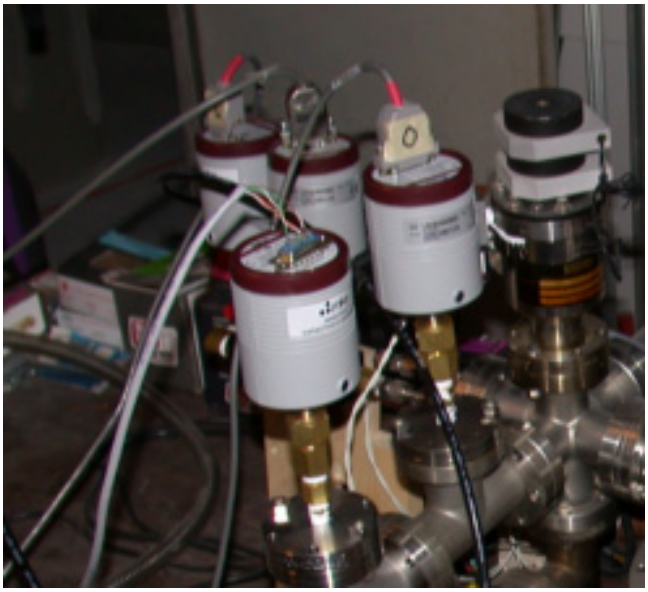

Figure 92. Four capacitance manometer vacuum transducer used for research

Item: Vacuum transducer – convector

Manufacturer: Granville Phillips

Model: NA

S/N: NA

Description: Fabrication drawings provided in Appendix X,

Used in: Resin dissolution scaling study, panel molding study

Picture:

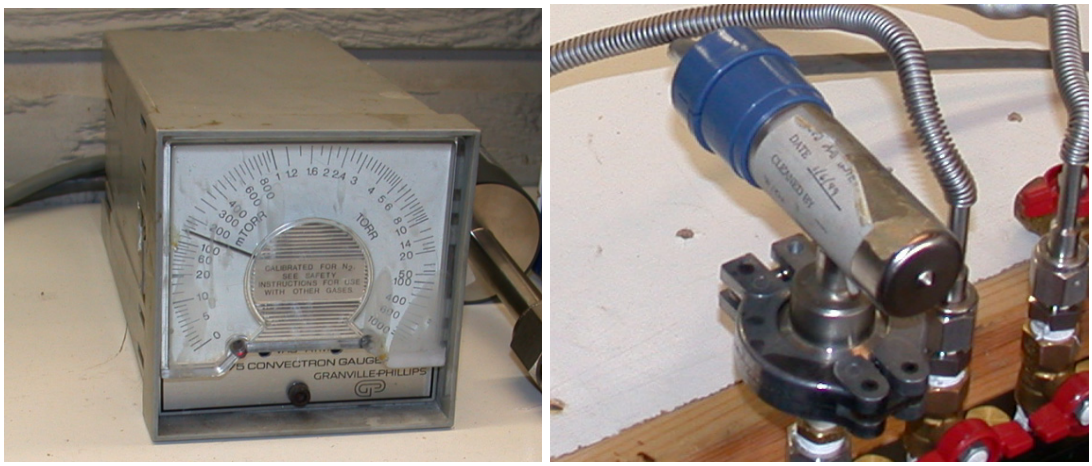

(a) (b)

Figure 93. Convector vacuum transducer, (a) display, (b) transducer

Item: Hygrometer

Manufacturer: Extech Instruments

Model: Microzelle, MN2400

S/N: 1103

Description: Fabrication drawings provided in Appendix X,

Used in: Resin dissolution scaling study, panel molding study

Picture:

Figure 94. Hygrometer

Item: Vacuum chamber

Manufacturer: Unknown

Model: NA

S/N: NA

Description: Stainless steel high vacuum chamber

Used in: Preform degassing studies, clamped plate setup

Picture:

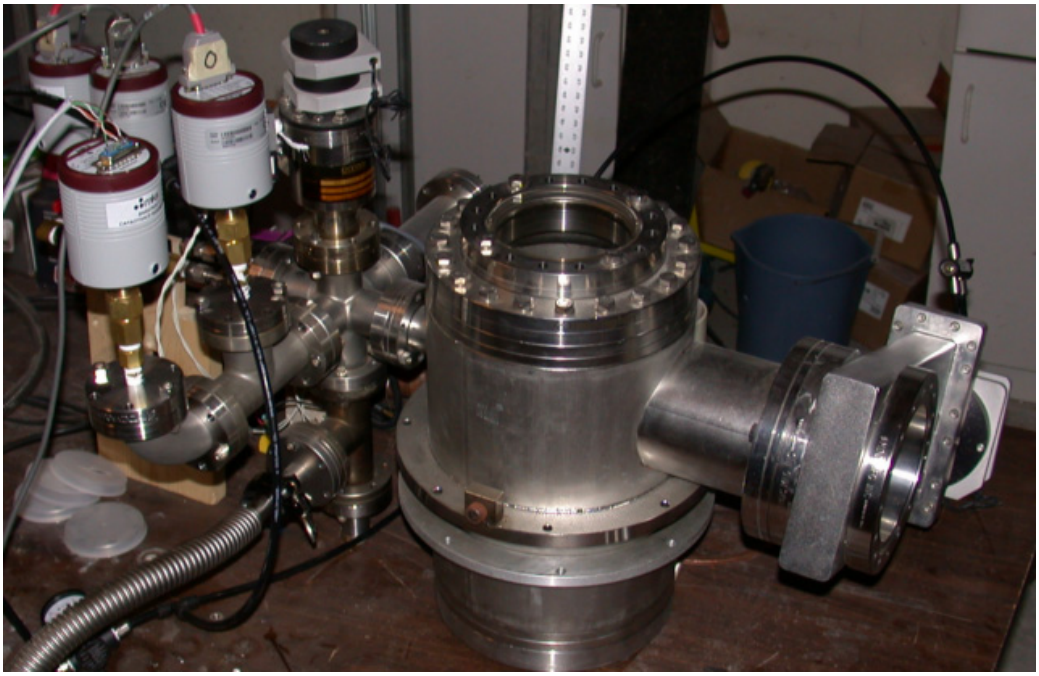

Figure 95. Vacuum chamber used for preform pump down experiments

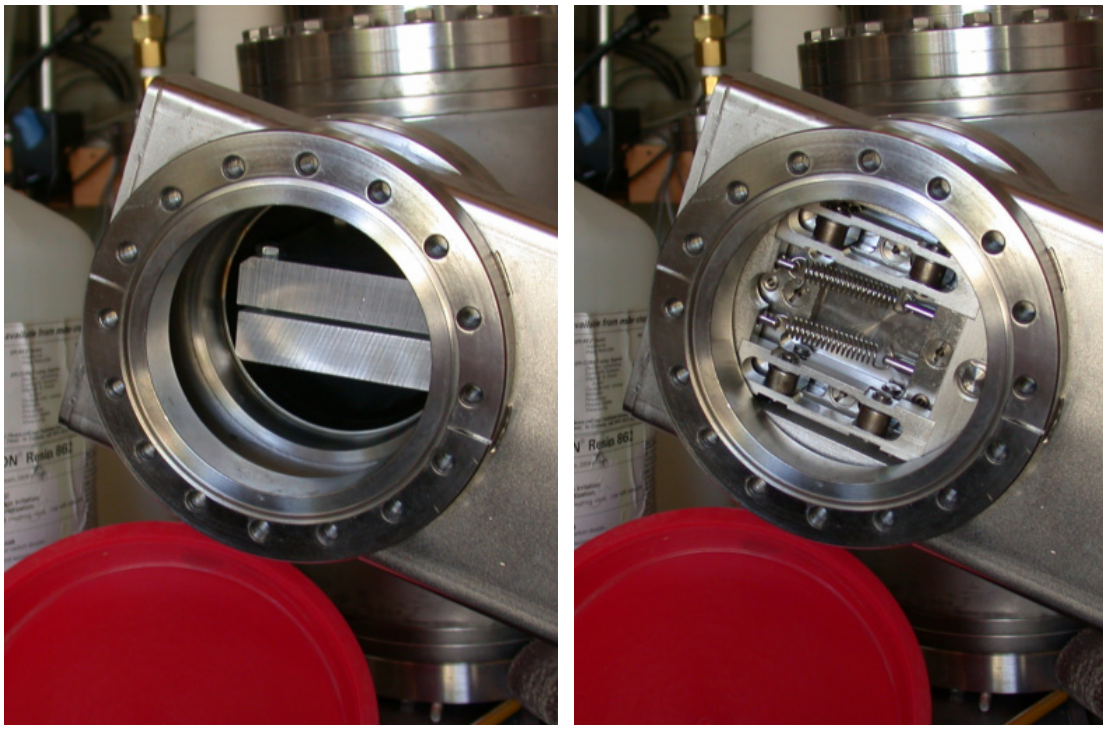

(a) (b)

Figure 96. Gate valve open (a) and closed (b)

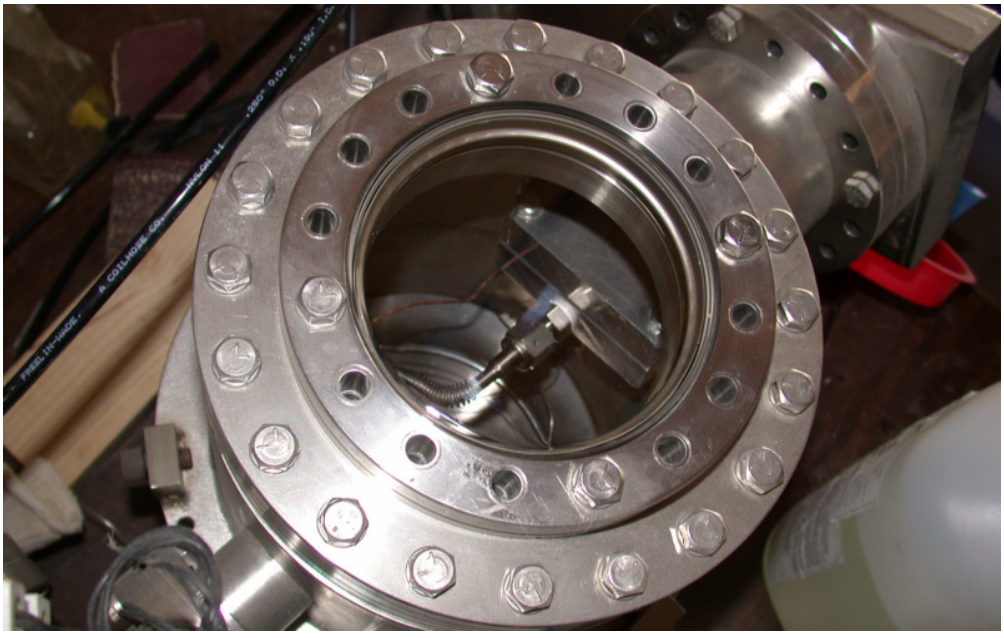

Figure 97. Looking through window at preform clamp fixture inside vacuum chamber

Item: Mass Scale

Manufacturer: Ohaus

Model: Explorer

S/N: A365002454

Description: 62 g max, reads to 0.1 mg

Used in: Preform moisture sorption studies

Pictures:

Figure 98. Microgram scale used to weight mass changes in preform samples

Item: Preform drying chamber

Manufacturer: NA

Model: NA

S/N: NA

Description: Drying chamber was a 12-inch conflate nipple closed at one end and configured with an NW25 (ISO-KF) vacuum fitting at the other end. Nipple was wrapped with a band heater and a thermocouple was secured to the nipple OD with a stainless steel hose clamp. Heating was accomplished using the four zone temperature controller.

Used in: Preform drying

Picture:

Figure 99. Preform drying chamber shown picture center

Item: Four zone temperature control system

Manufacturer: Built for this research

Model: NA

S/N: NA

Description: Four zone temperature control system uses four Watlow Series 96 PID temperature controllers

Used in: Resin dissolution & scaling study, panel molding

Picture:

Figure 100. Temperature control system used for research

Item: Panel Mold

Manufacturer: Designed and built by Author

Model: 8 inch blind flanges, McMaster Carr PN 68095K263

S/N: NA

Description: Refer to Chapter 6 for description

Used in: Resin dissolution scaling study, panel molding study

Picture:

Figure 101. Panel mold bottom with aluminum rings and O-ring in position

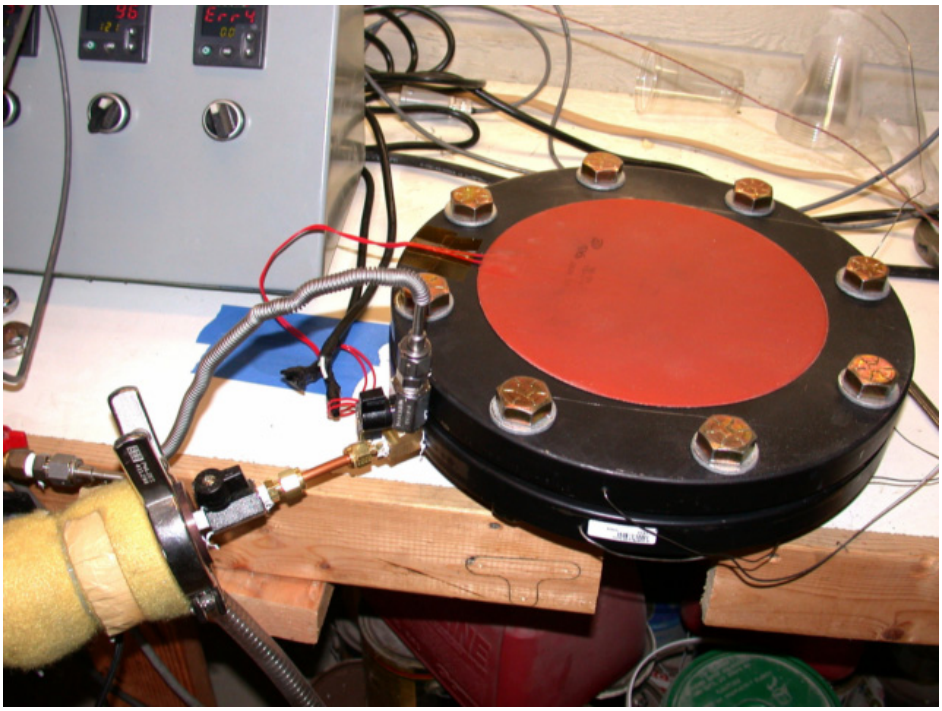

Figure 102. Panel mold closed and connected to injector. Note control TC inserted into flanges (foreground). Note red pad heater.

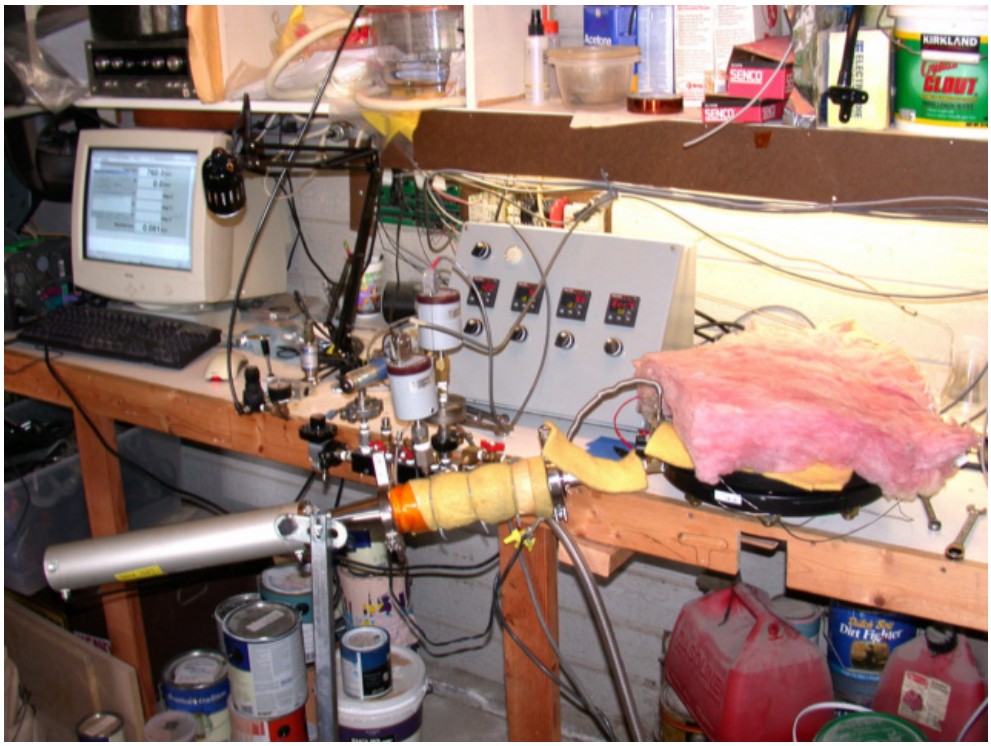

Figure 103. Overall setup for injection of panels

Item: Data acquisition software

Manufacturer: Code written by Author using Visual Basic Version 6

Model: NA

S/N: NA

Description: Control and data acquisition software written to support this reserach.

Used in: Preform degassing, resin study, resin scaling study, continuum study

Picture: (next page)

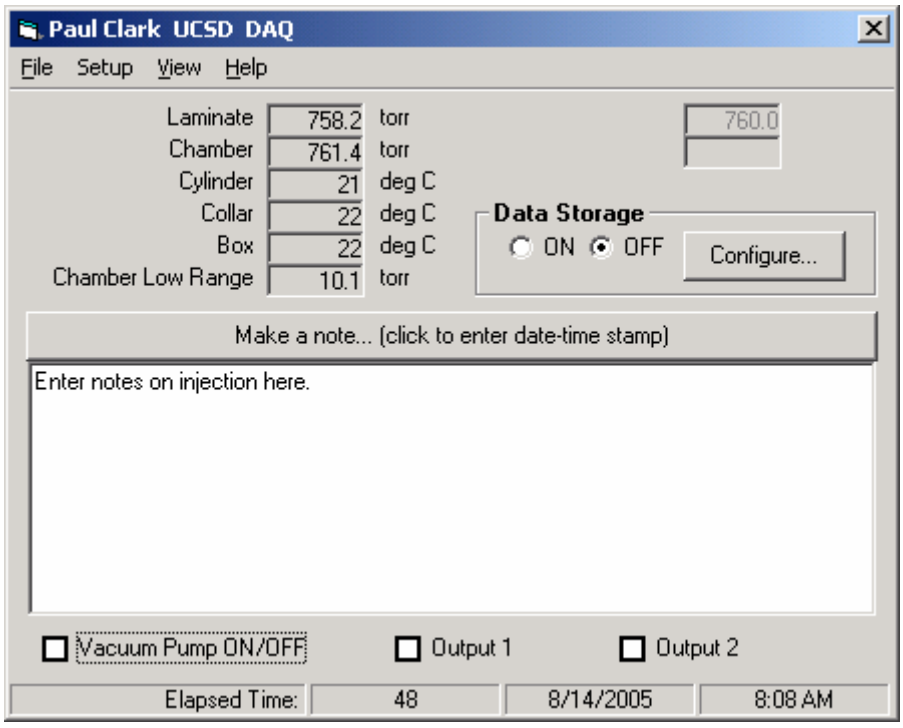

(a)

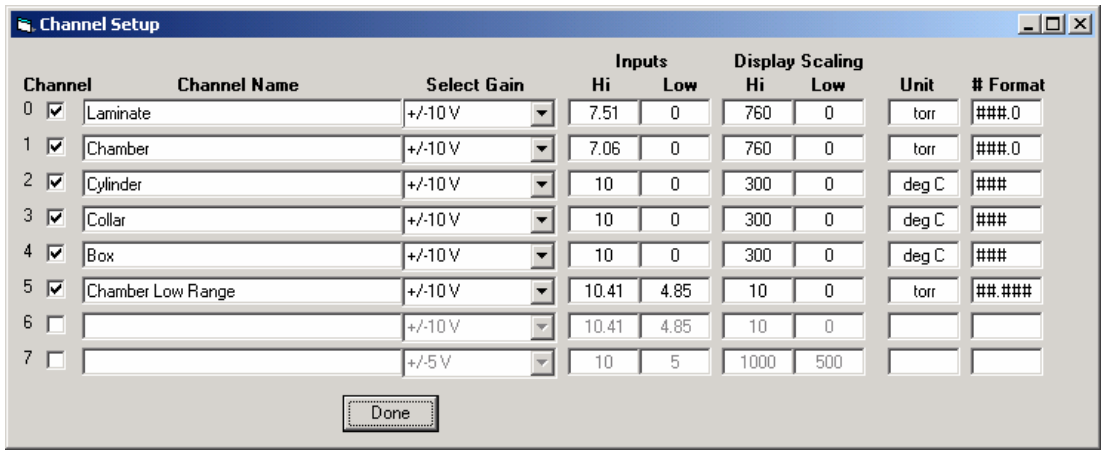

(b)

Figure 104. Data acquisition screen shots, (a) main screen, (b) channel setup

Item: Data acquisition hardware

Manufacturer: Measurement Computing

Model: PCI-DAS1000

S/N: NA

Description: Computer card, PCI-DAS1000, 250 kHz PCI-bus compatible, 16-channel analog input board with 24 digital I/O bits

Used in: All testing

Picture:

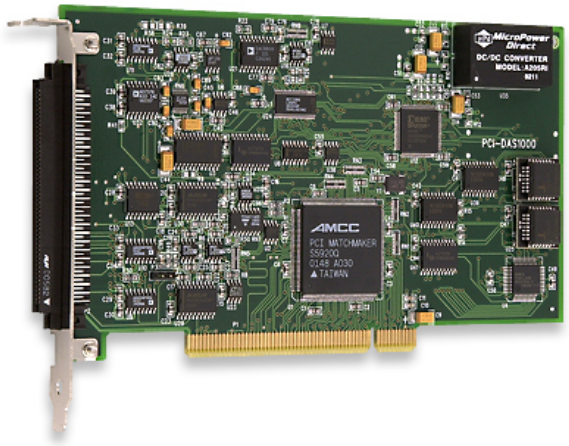

Figure 105. Data acquisition card used for research

Item: Pneumatic pressure transducer

Manufacturer: Dynisco

Model: PT160-1C

S/N: 11-17-986521

Description: Pressure transducer, 16-32 VDC input, 0-10 VDC output, shunt at 80% full scale

Used in: Resin gas dissolution study, resin gas dissolution scaling study, panel molding

Picture:

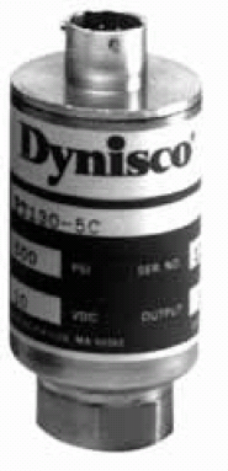

Figure 106. 0-687 kPa (0-100 psi) range pressure transducer

Item: Precision leak valve for vacuum level control

Manufacturer: Edwards

Model: NA

S/N: NA

Description: Computer card, power supplies

Used in: Resin dissolution scaling study, panel molding study

Picture:

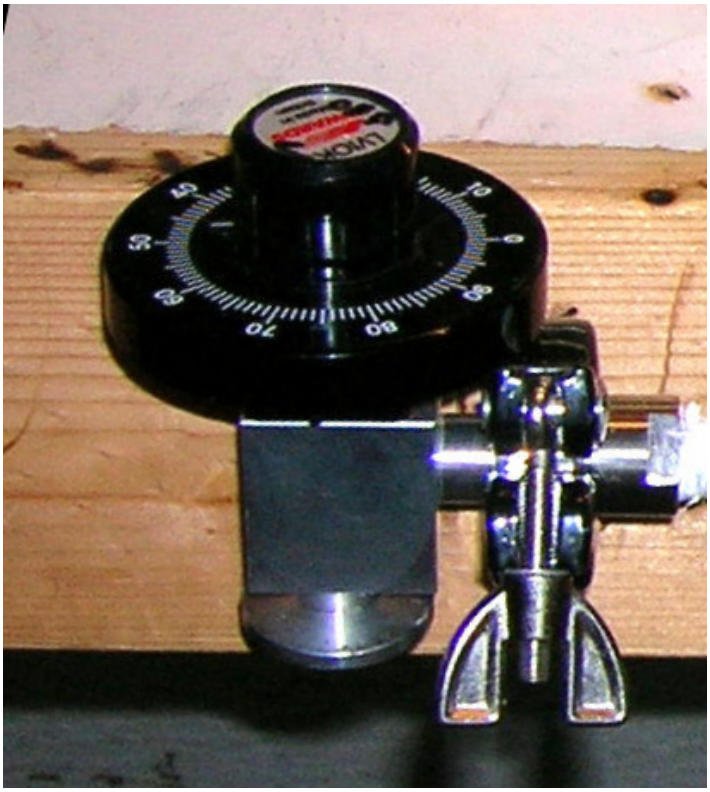

Figure 107. Precision vacuum leak valve

Item: Microscope

Manufacturer: Wild

Model: M5A

S/N: 187239

Description: Stereo microscope

Used in: Resin scaling study, continuum experiments

Picture:

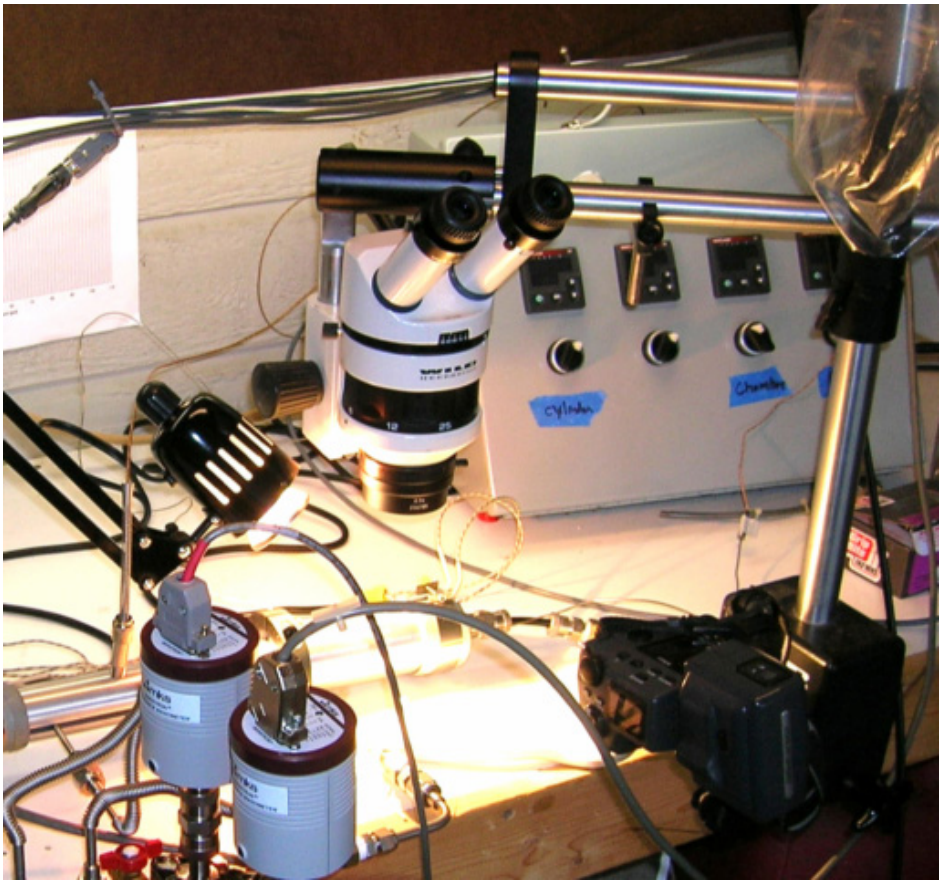

Figure 108. Stereo microscope used during research

Item: Resin dissolution test apparatus

Manufacturer: Design and built by Author

Model: NA

S/N: NA

Description: Refer to Chapter 5 for description

Used in: Resin gas dissolution study

Picture:

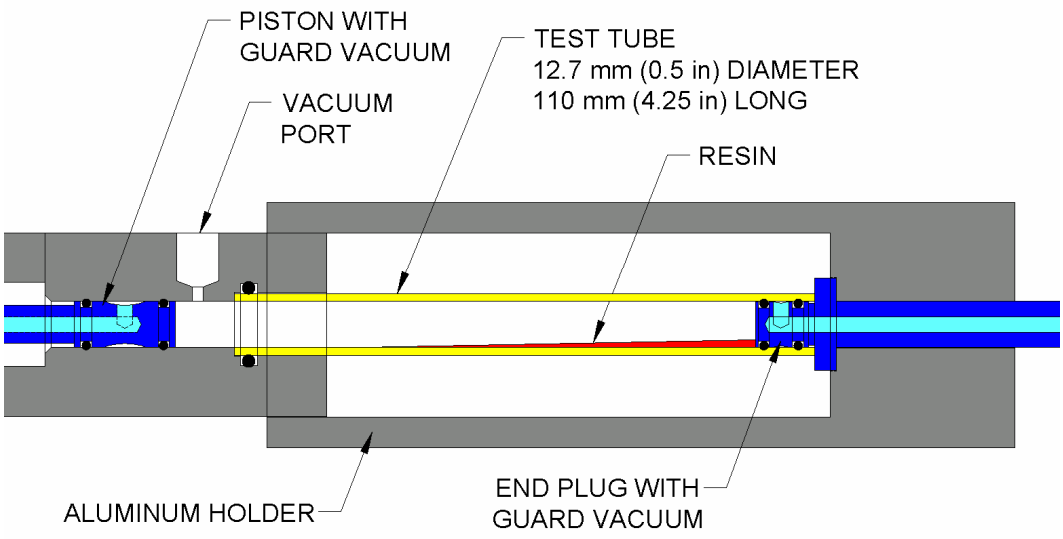

Figure 109. Cross section of resin gas solubility testing apparatus

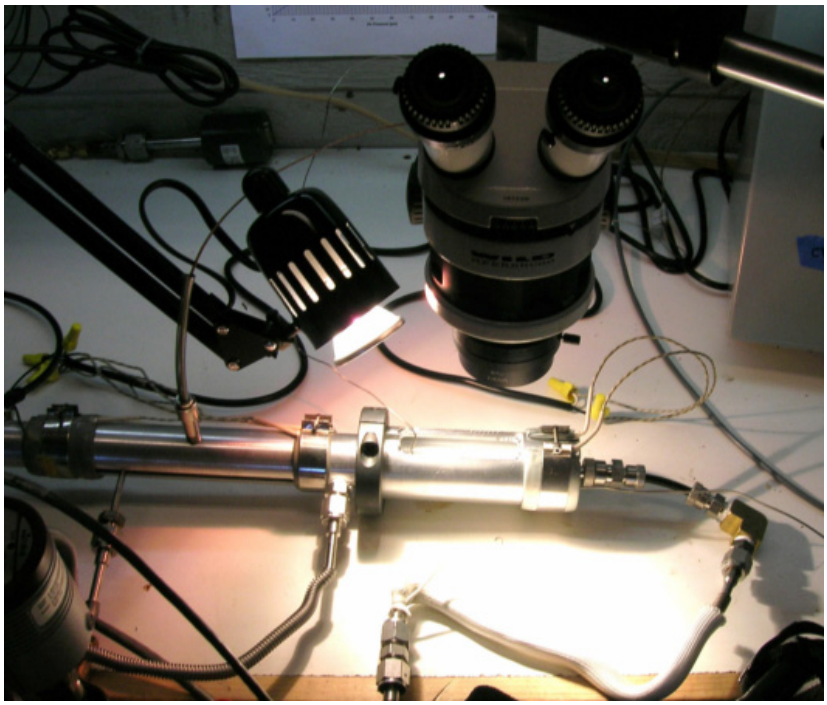

Figure 110. Setup for resin gas dissolution studies, thermal insulation not installed, microscope in position

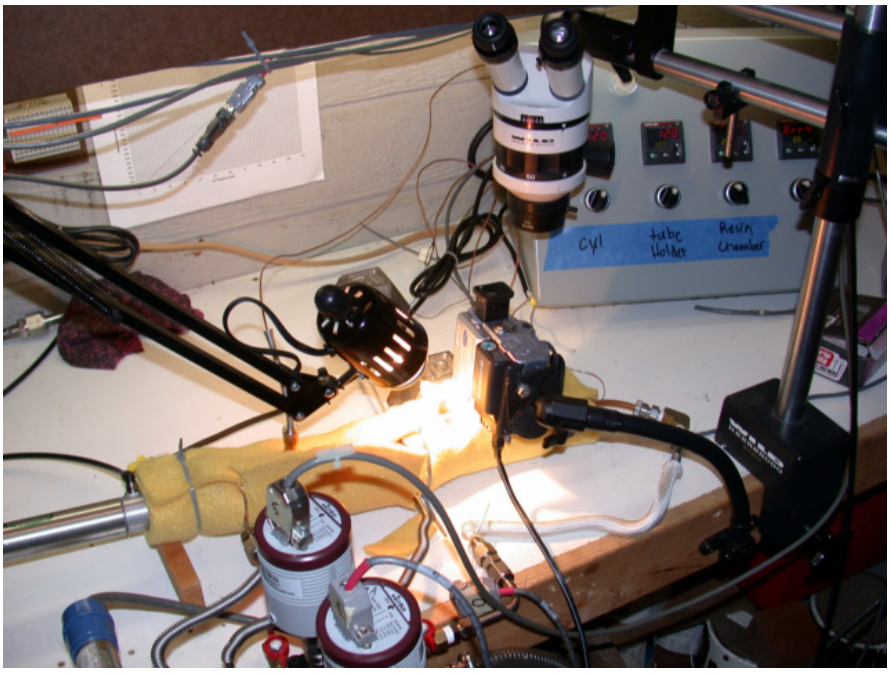

Figure 111. Setup for resin gas dissolution studies, digital camera in position

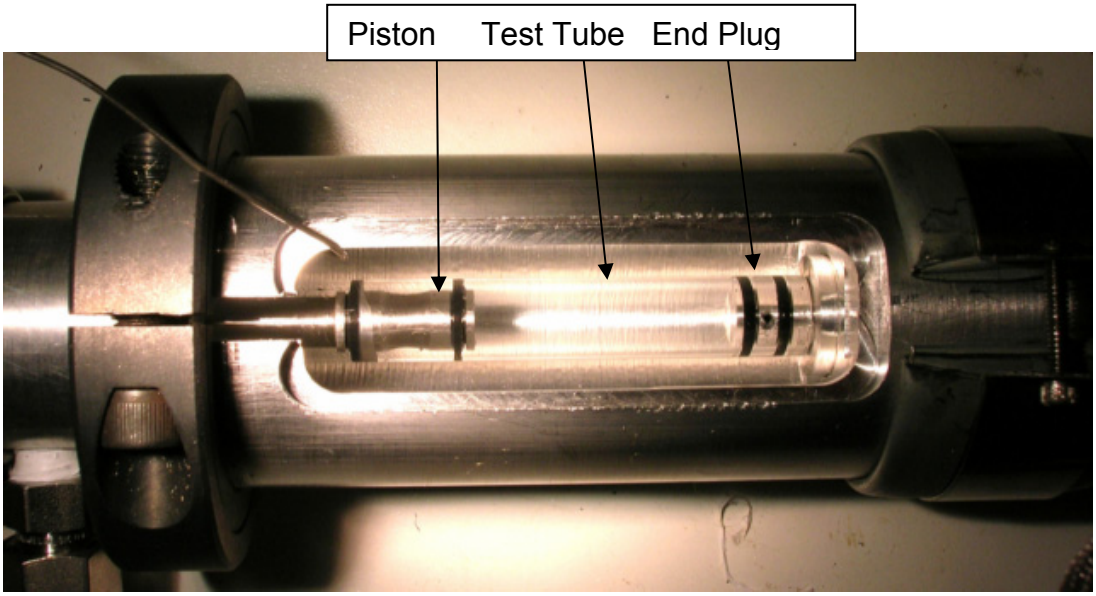

Figure 112. Resin gas solubility testing apparatus

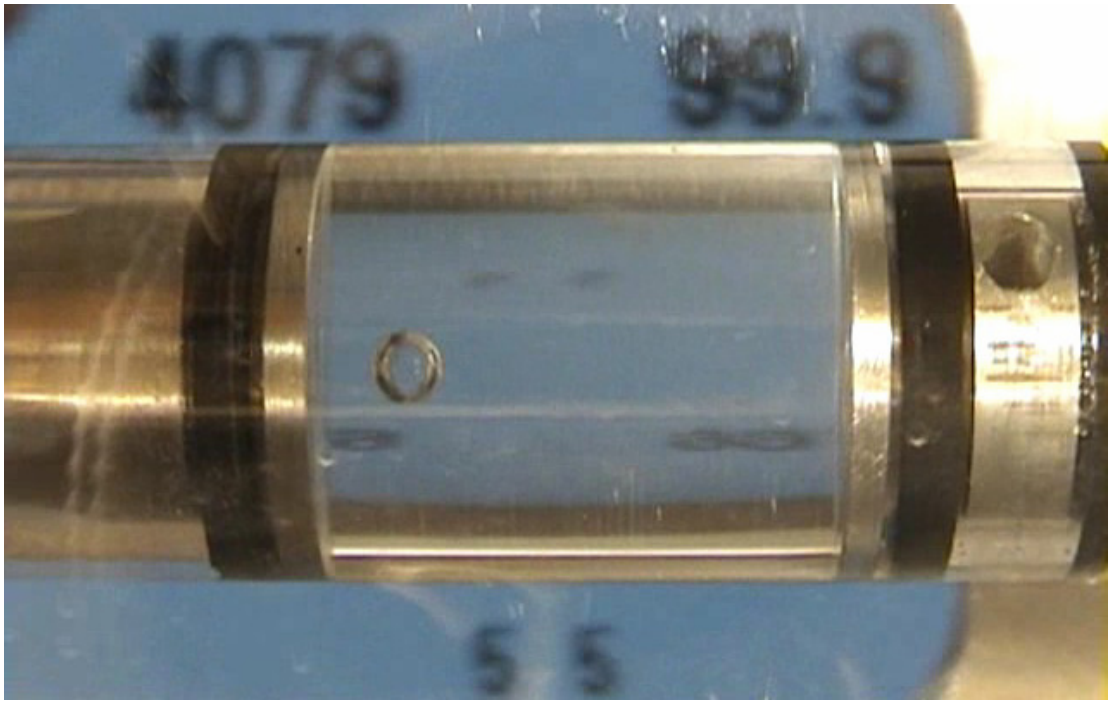

Figure 113. Frame captured from video documentation. Note LCD computer display in background showing relevant information

APPENDIX 2: EXPERIMENTAL MATERIALS

Item: Fiber Glass Cloth Preform Material

Manufacturer: Hexcel, 6 oz. glass cloth, Style 3733, 50-F16, 76035-002-02, #SPL PO 17782, Packed by 56 on 3-1-05

Description: Plain weave fiber glass cloth

Used in: Preform pump down studies, panel molding

Picture:

Figure 114. Glass fiber cloth positioned in panel mold

Item: Carbon Fiber Cloth Preform Material

Manufacturer: Hexcel, 370 gsm, SGP370-4, 8HS, 6k, IM7 GP

Description: Eight harness satin cloth

Used in: Preform water sorption and preform pump down studies

Picture:

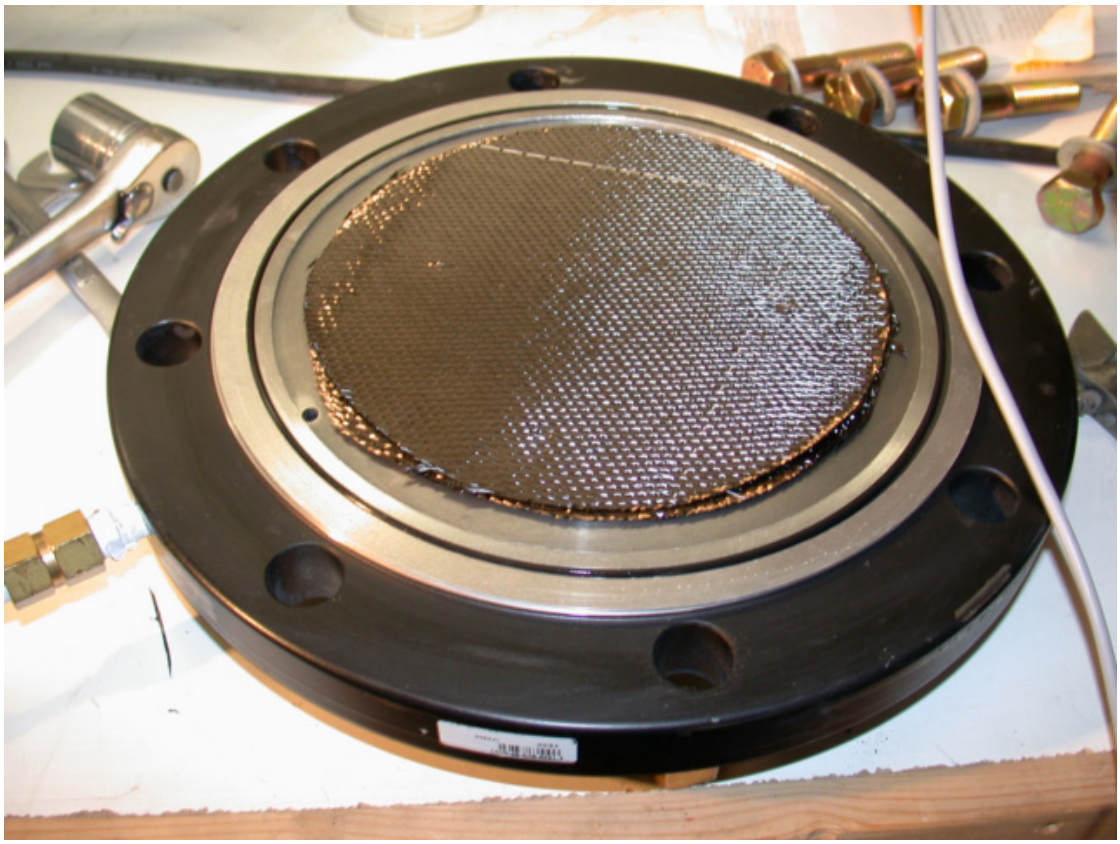

Figure 115. Stack of carbon fiber fabric positioned in panel mold

Item: Epoxy resin and hardener

Manufacturer: Resolution Performance Products, procured from Miller Stephenson Chemicals

Description:

Resin: 862, 1 gal, Lot EJAL0088/0965GG

Hardener (curing agent): W, 1 quart, Lot ECXC4701/0965GG

Used in: All resin experiments and panel molding

Picture:

Figure 116. EPON 862 resin and EPI Cure Curing Agent W hardener

Item: Mold Release

Manufacturer: Zyvax

Description: Mold surface cleaner, sealer and release agents

Used in: Resin scaling studies, panel molding

Picture:

Figure 117. Mold release and preparation products

APPENDIX 3: EQUIPMENT DRAWINGS

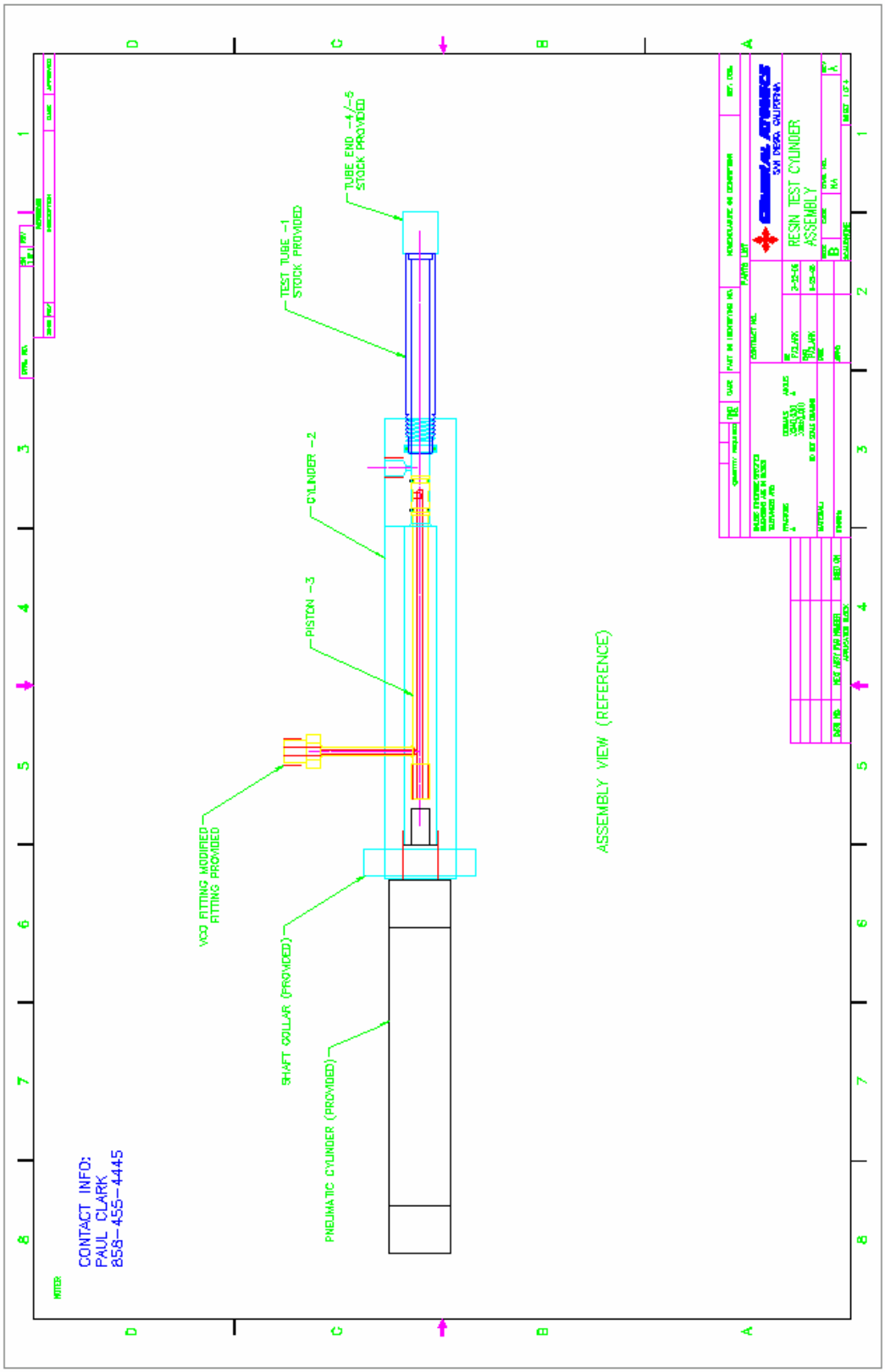
TUBE END -4/-5
STOCK PROVIDED
TEST TUBE -1
STOCK PROVIDED
CYLINDER -2
PISTON -3
VCO FITTING MODIFIED
FITTING PROVIDED
SHAFT COLLAR (PROVIDED)
PNEUMATIC CYLINDER (PROVIDED)
ASSEMBLY VIEW (REFERENCE)
RESIN TEST CYLINDER
ASSEMBLY
CONTACT INFO:
PAUL CLARK
858-455-4445

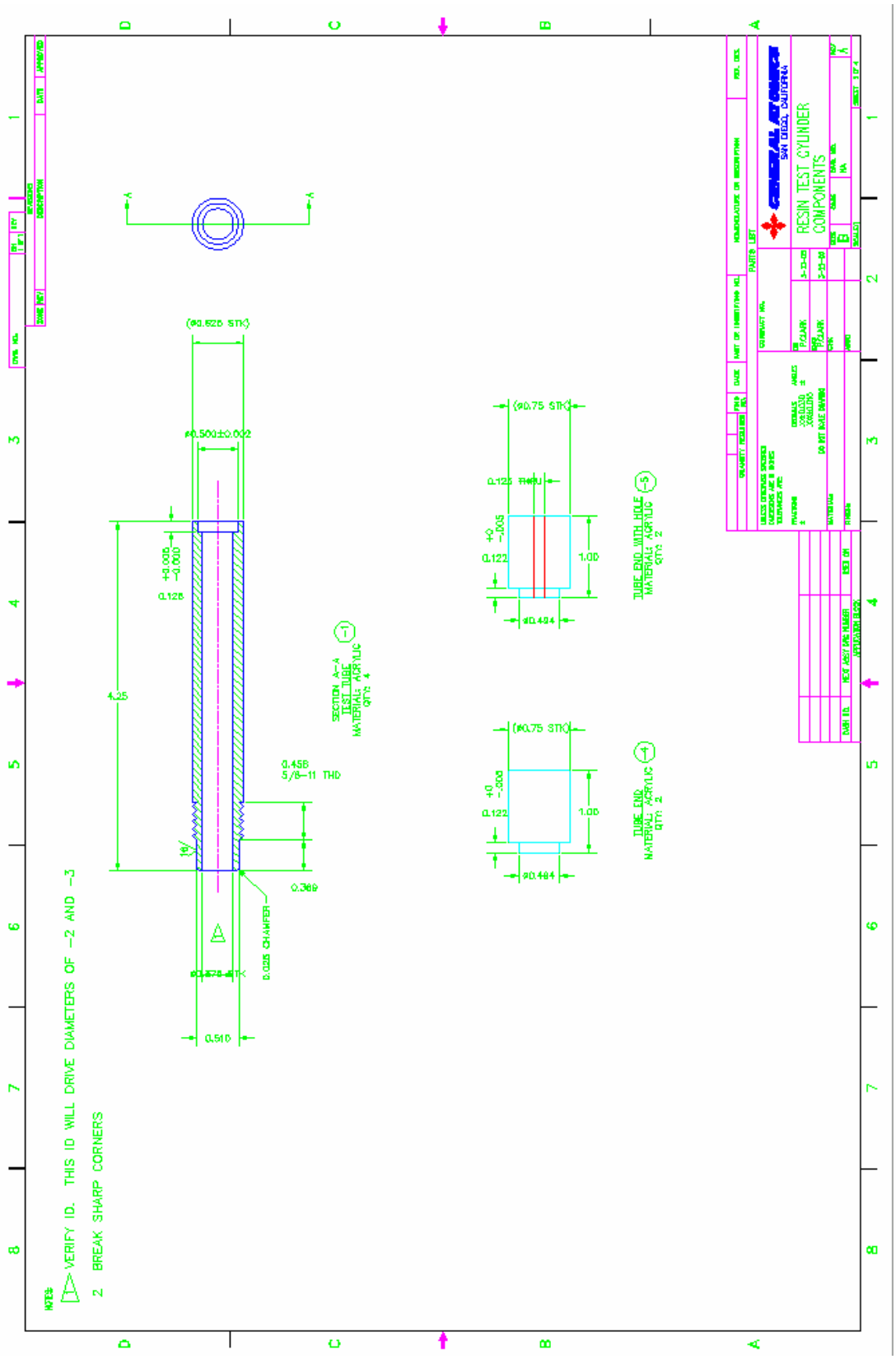
RESIN TEST CYLINDER COMPONENTS
CATERPILLAR
SAN DIEGO, CALIFORNIA
NOTES:
1. VERIFY ID. THIS ID WILL DRIVE DIAMETERS OF -2 AND -3
2. BREAK SHARP CORNERS
(Ø0.625 STK)
Ø0.500±0.002
4.25
0.128
0.456
5/8-11 THD
0.369
0.035 CHAMFER
0.510
SECTION A-A
TEST TUBE
MATERIAL: ACRYLIC
QTY: 4
(Ø0.75 STK)
0.125 RADIUS
0.122
1.00
Ø0.484
TUBE END WITH HOLE
MATERIAL: ACRYLIC
QTY: 2
TUBE END
MATERIAL: ACRYLIC
QTY: 2

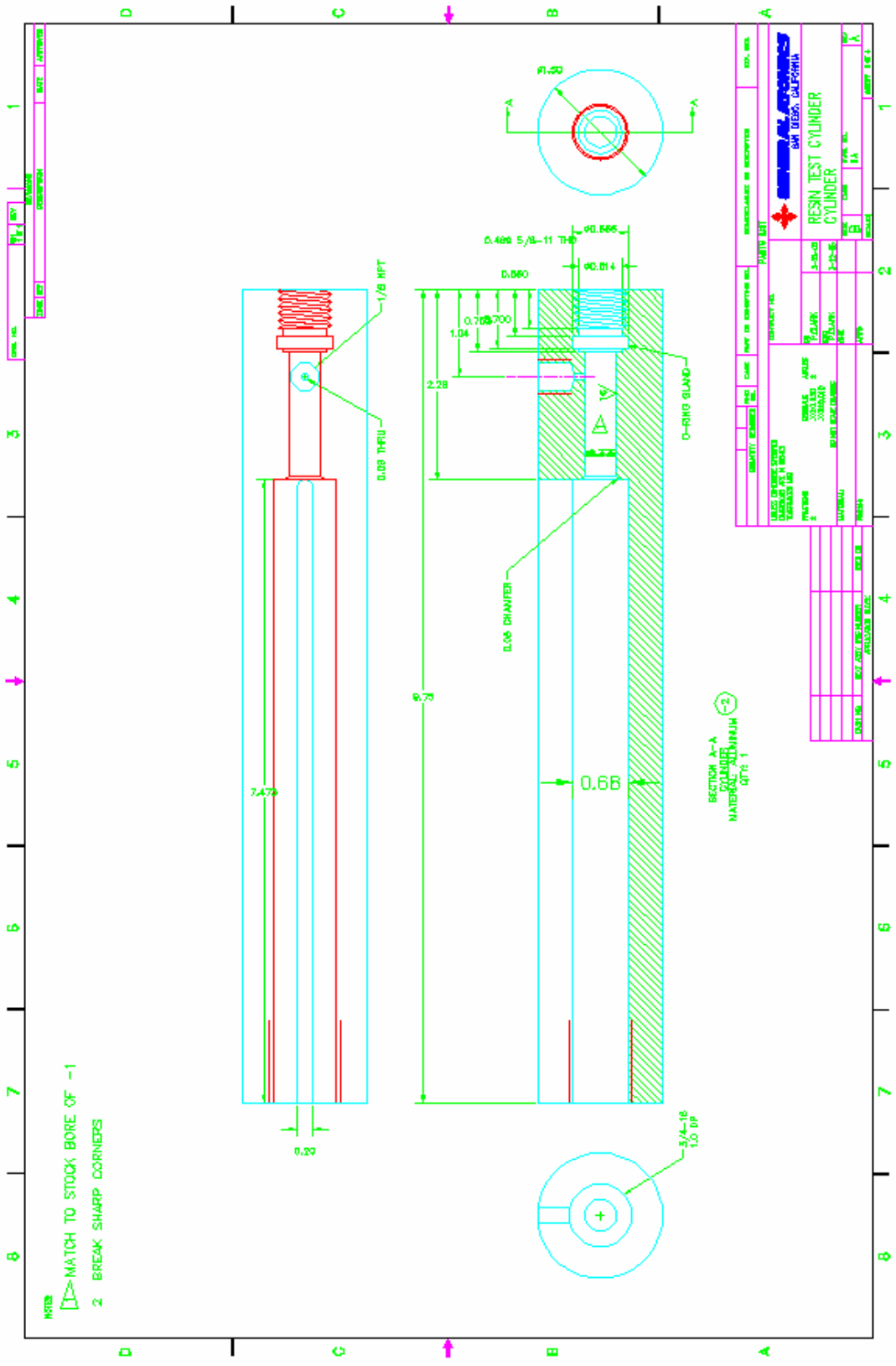
RESIN TEST CYLINDER
CYLINDER
NOTES:
1 MATCH TO STOCK BORE OF -1
2 BREAK SHARP CORNERS
0.68
2.28
1.04
0.56 CHAMFER
O-RING GLAND
1/8 NPT
0.09 THRU
3/4-16
1.0 DP

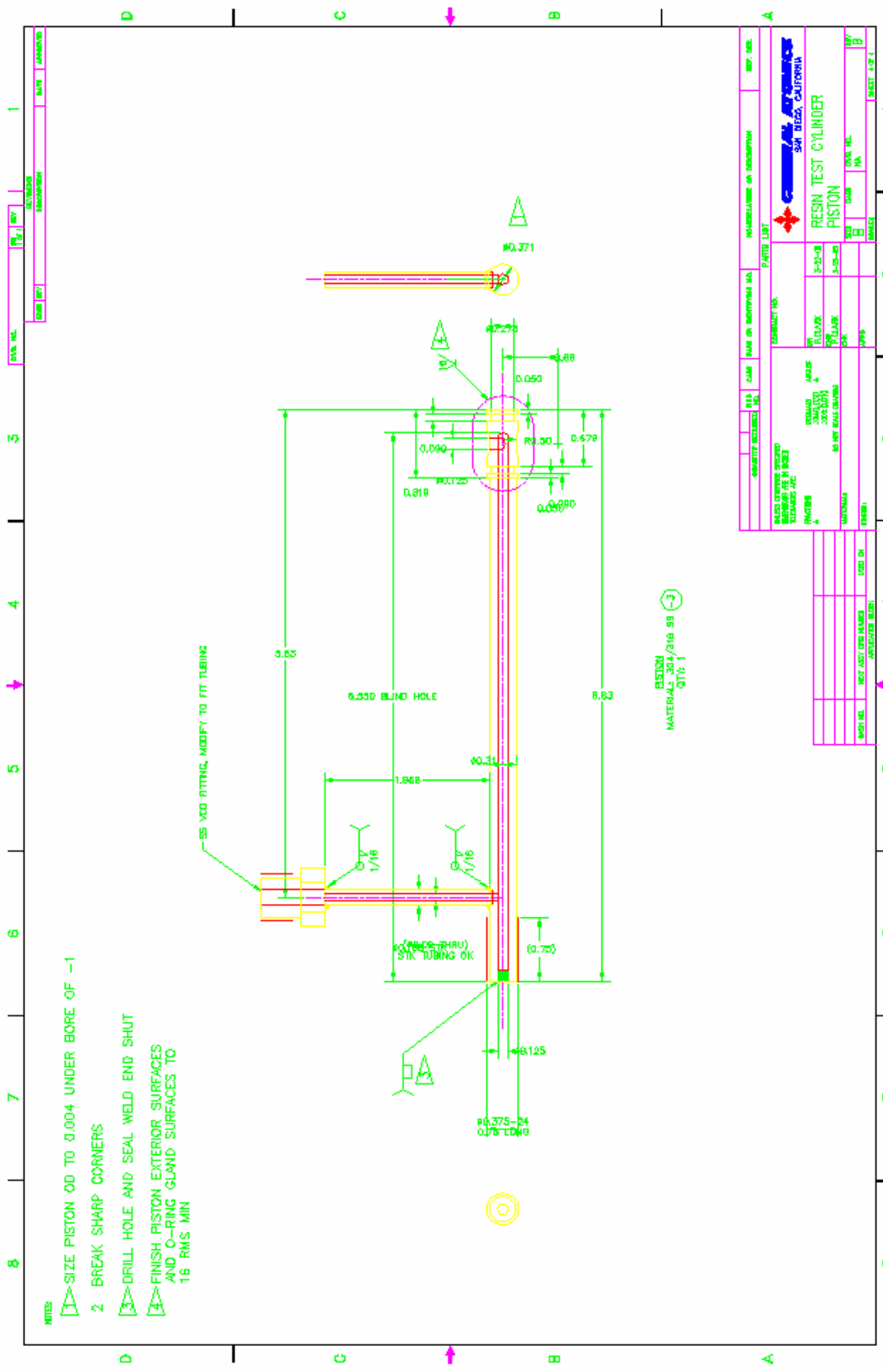
RESIN TEST CYLINDER
PISTON
SAN DIEGO, CALIFORNIA
NOTES
1 SIZE PISTON OD TO 0.004 UNDER BORE OF -1
2 BREAK SHARP CORNERS
3 DRILL HOLE AND SEAL WELD END SHUT
4 FINISH PISTON EXTERIOR SURFACES AND O-RING GLAND SURFACES TO 16 RMS MIN
5.530 BLIND HOLE
SS VCO FITTING, MODIFY TO FIT TUBING
STK TUBING OK
PISTON
MATERIAL: 304/316 SS
QTY: 1

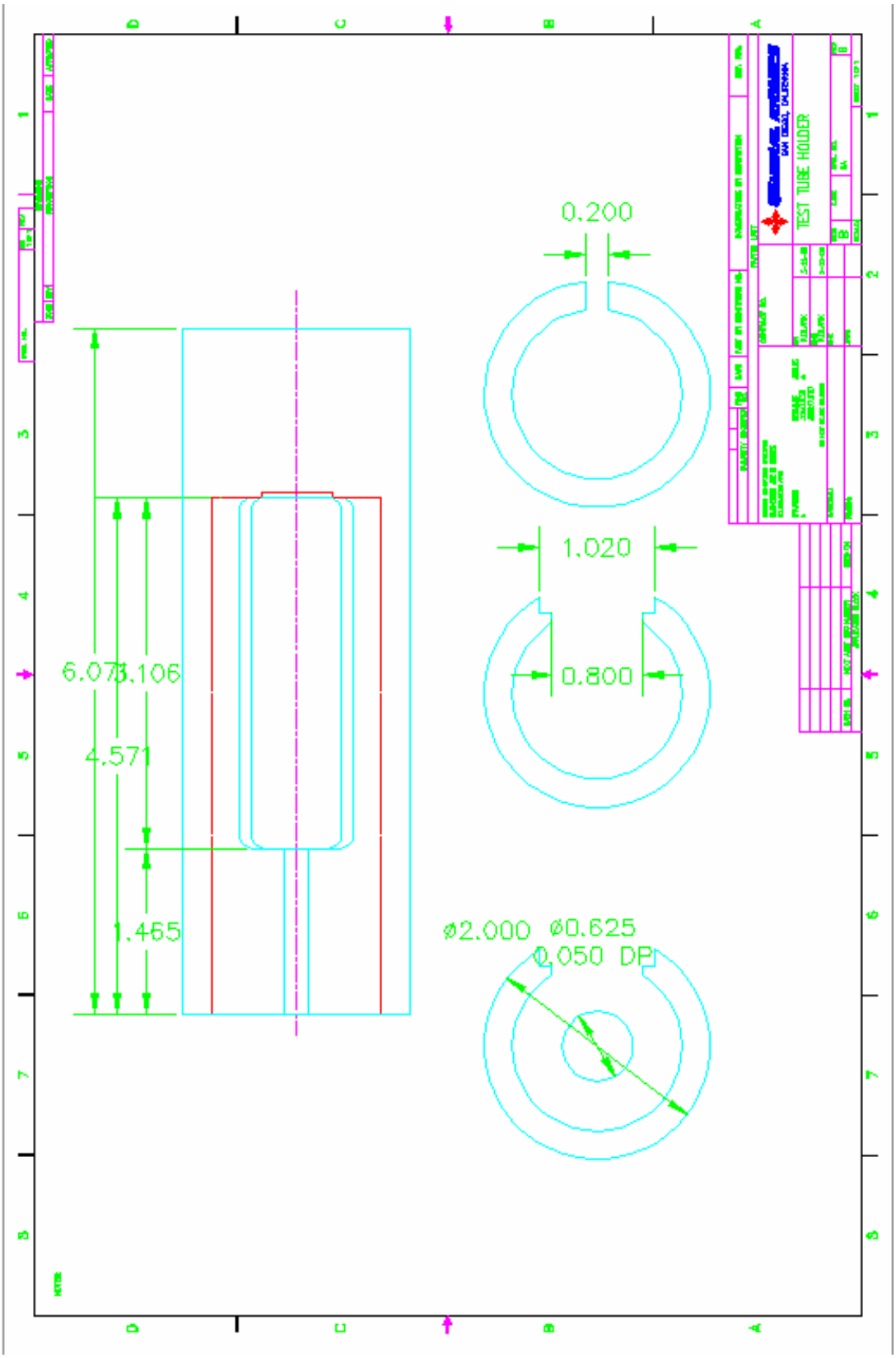
TEST TUBE HOLDER
0.200
1.020
0.800
6.073.106
4.571
1.465
ø2.000 ø0.625
0.050 DP

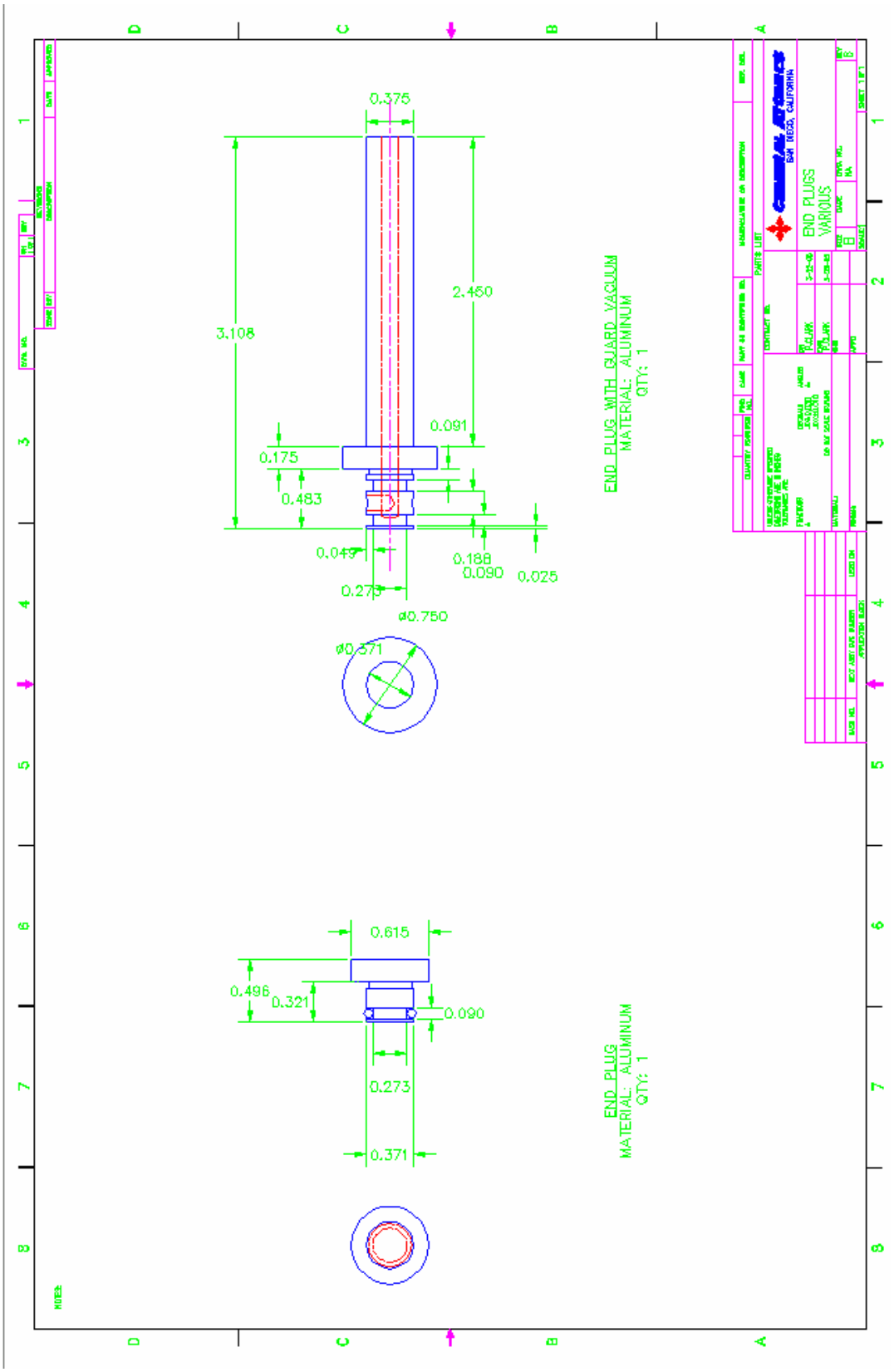
0.375
3.108
2.450
0.091
0.175
0.483
0.049
0.188
0.090
0.025
0.273
ø0.750
ø0.371
END PLUG WITH GUARD VACUUM
MATERIAL: ALUMINUM
QTY: 1
END PLUGS
VARIOUS
0.615
0.496
0.321
0.090
0.273
0.371
END PLUG
MATERIAL: ALUMINUM
QTY: 1

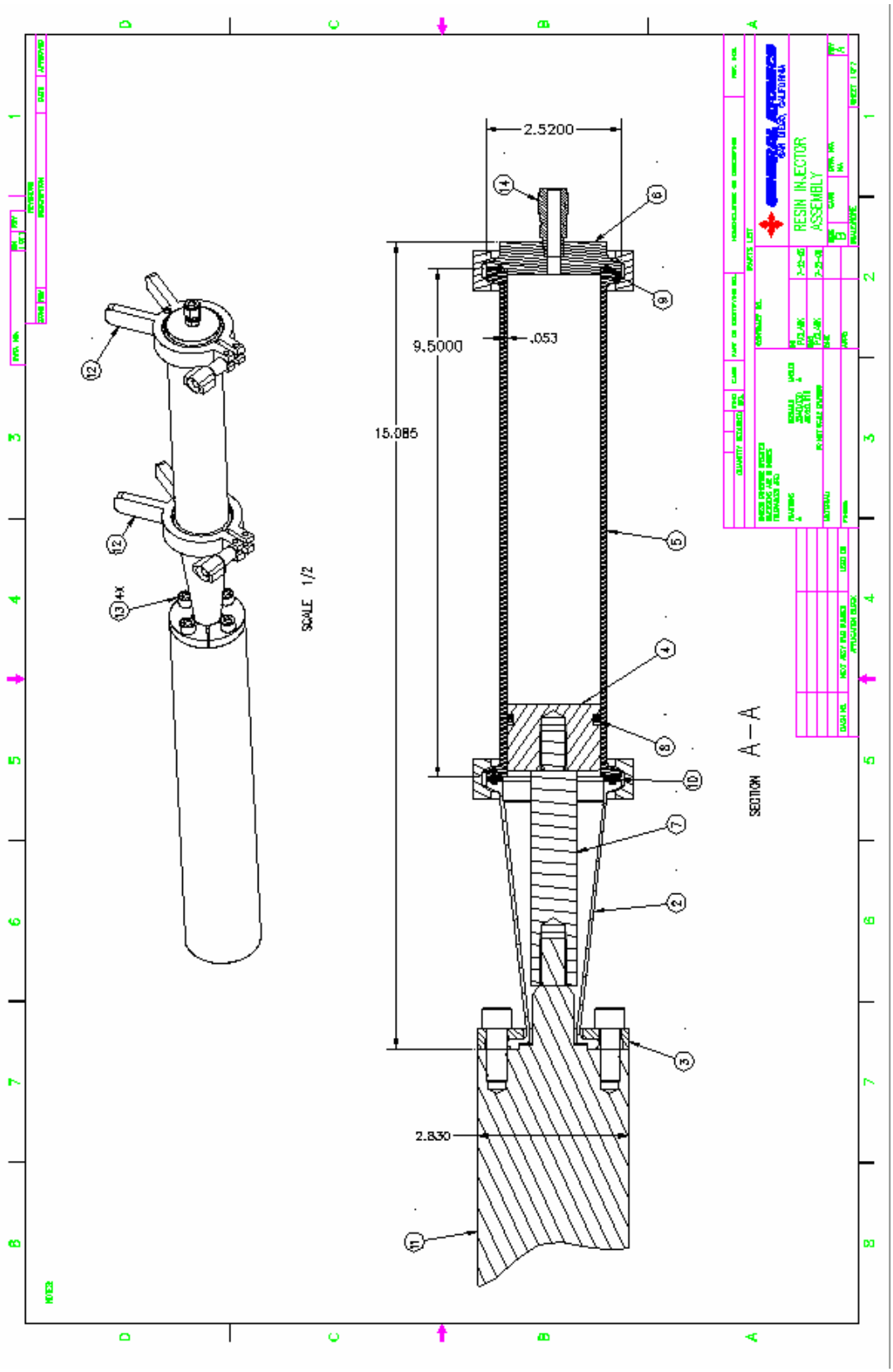
2.5200
9.5000
.053
15.085
2.830
SCALE 1/2
SECTION A-A
RESIN INJECTOR ASSEMBLY

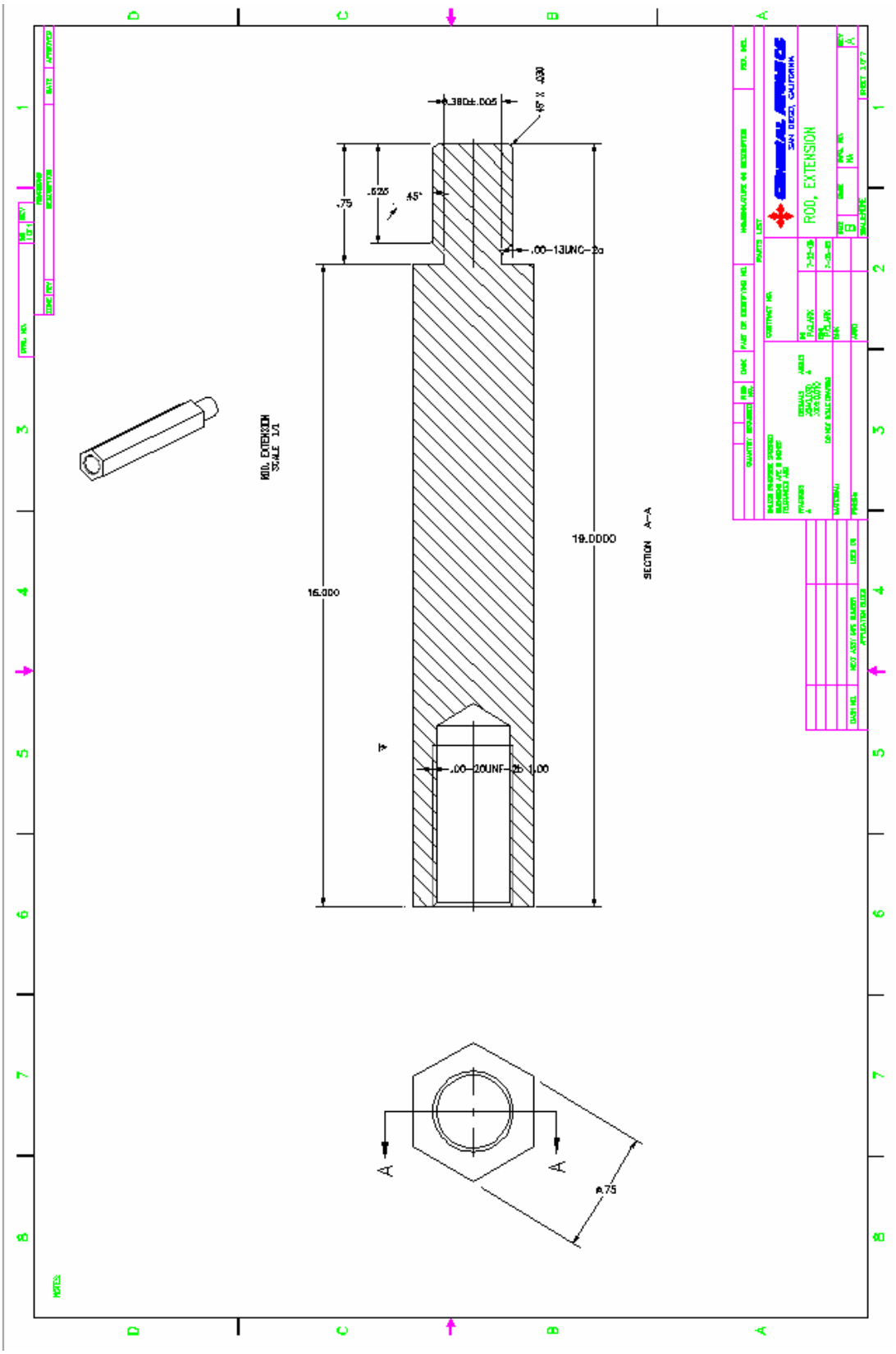
ROD, EXTENSION
SAN DIEGO, CALIFORNIA
.380±.005
45° X .030
.75
.625
45°
.00-13UNC-2a
16.000
19.0000
.00-20UNF-2b
1.00
SECTION A-A
ROD, EXTENSION
SCALE 1/1
A
A
.75
NOTES:

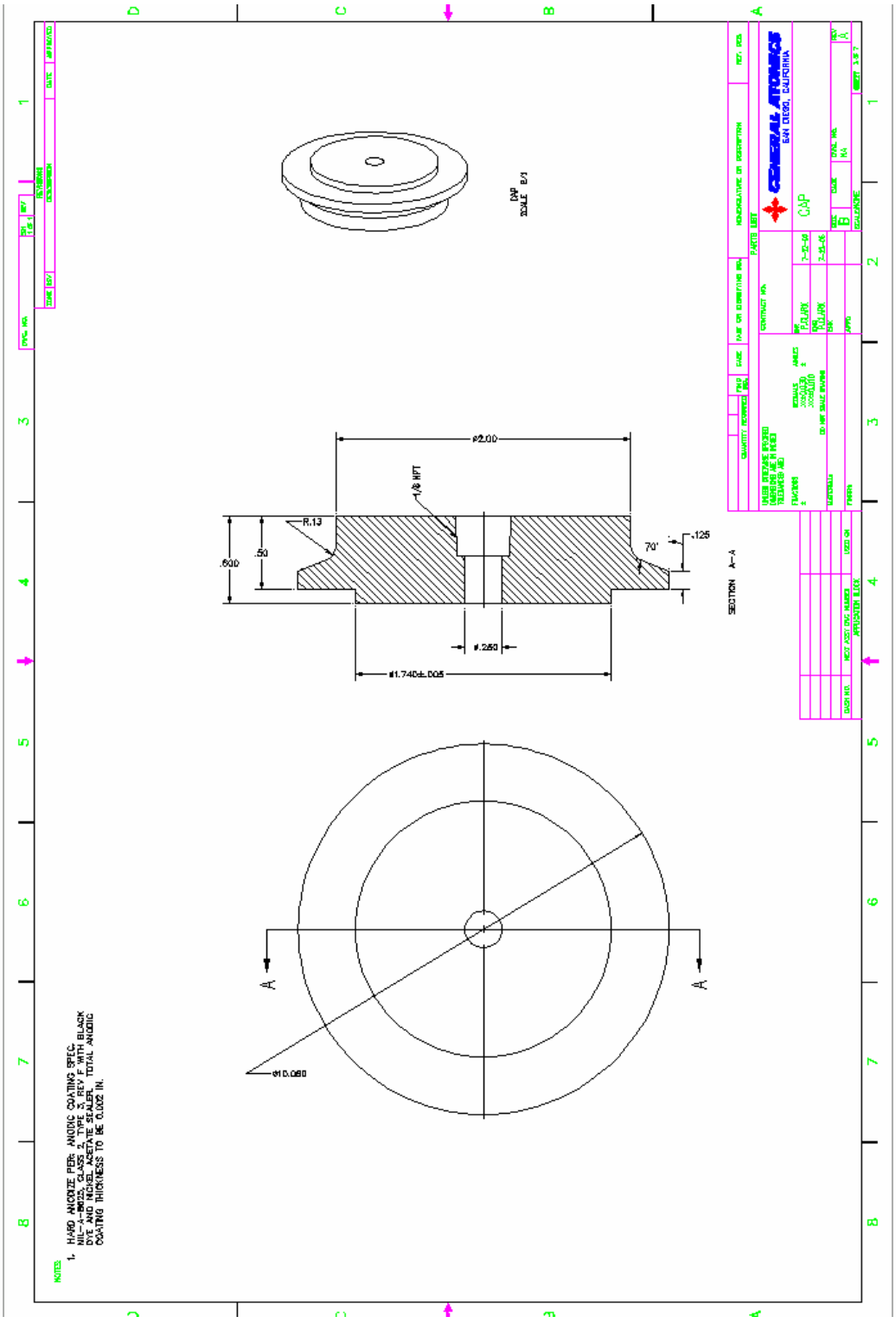
CAP
SCALE 3/1
ø2.00
1/8 NPT
R.13
.600
.50
70°
.125
ø.250
ø1.740±.005
SECTION A–A
A
A
ø10.060
NOTES:
1. HARD ANODIZE PER: ANODIC COATING SPEC.
MIL-A-8625, CLASS 2, TYPE 3, REV F WITH BLACK
DYE AND NICKEL ACETATE SEALER. TOTAL ANODIC
COATING THICKNESS TO BE 0.002 IN.
CANOGA AVIONICS
SAN DIEGO, CALIFORNIA
CAP

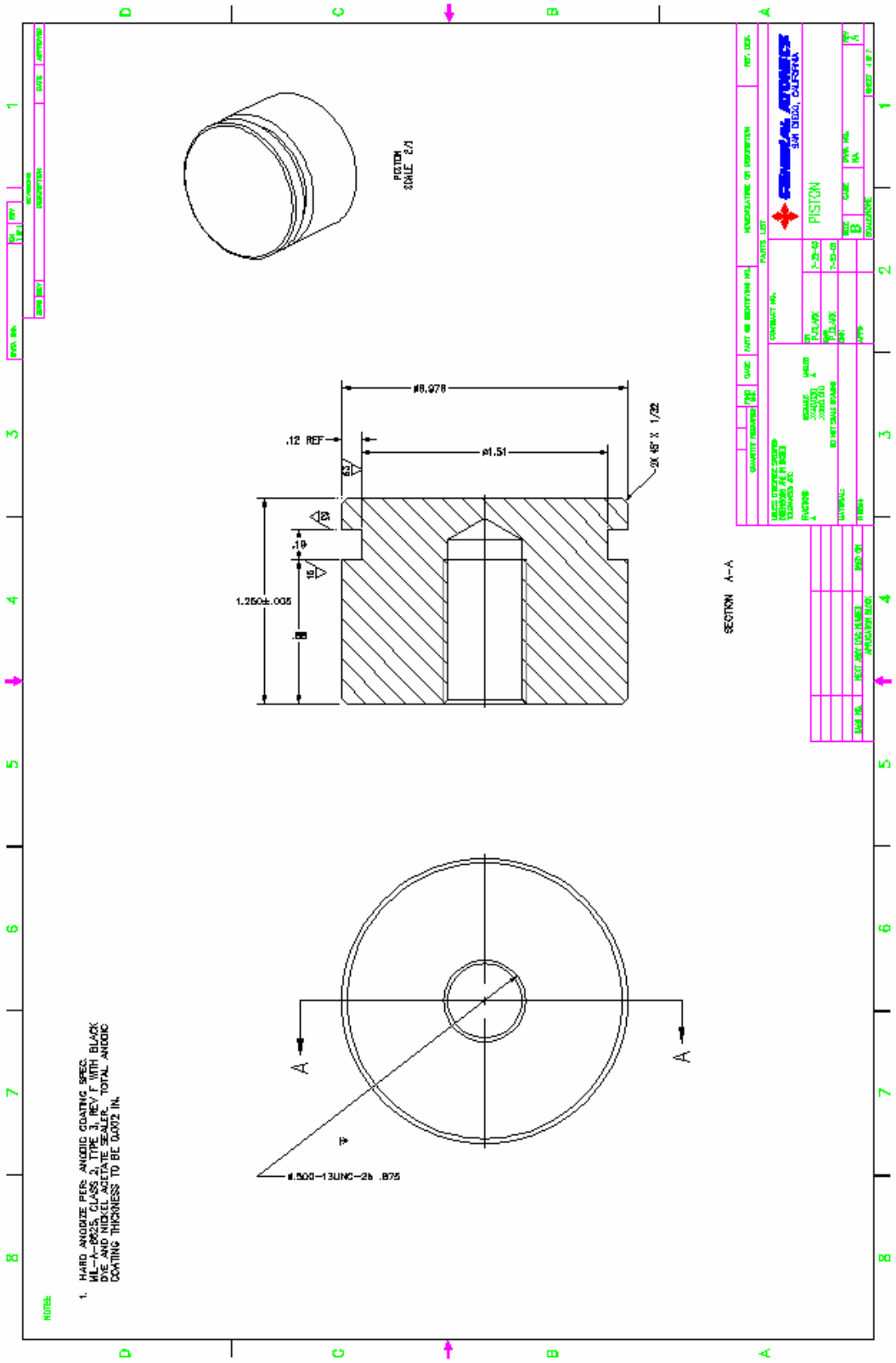
PISTON
SCALE 2/1
ø0.978
.12 REF
ø1.51
20X 45° X 1/32
1.250±.005
SECTION A-A
A
A
ø.500-13UNC-2b .875
NOTES:
1. HARD ANODIZE PER ANODIC COATING SPEC. MIL-A-8625, CLASS 2, TYPE 3, REV F WITH BLACK DYE AND NICKEL ACETATE SEALER. TOTAL ANODIC COATING THICKNESS TO BE 0.0002 IN.
PISTON

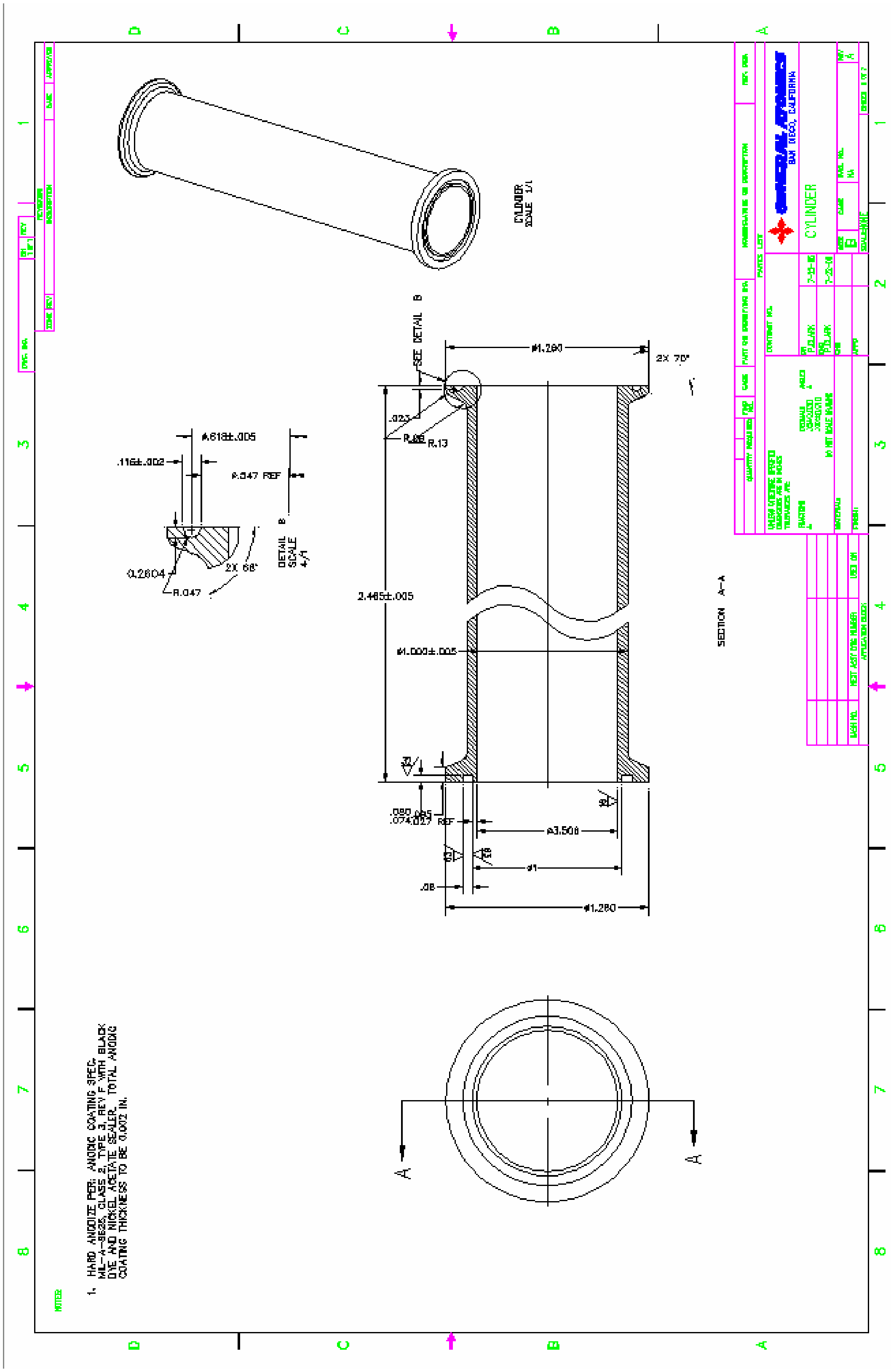
CYLINDER
SCALE 1/1
SEE DETAIL B
DETAIL B
SCALE 4/1
SECTION A-A
2X 70°
2X 68°
A
A
CYLINDER
SAN DIEGO, CALIFORNIA
NOTES:
1. HARD ANODIZE PER: ANODIC COATING SPEC. MIL-A-8625, CLASS 2, TYPE 3, REV F WITH BLACK DYE AND NICKEL ACETATE SEALER. TOTAL ANODIC COATING THICKNESS TO BE 0.002 IN.

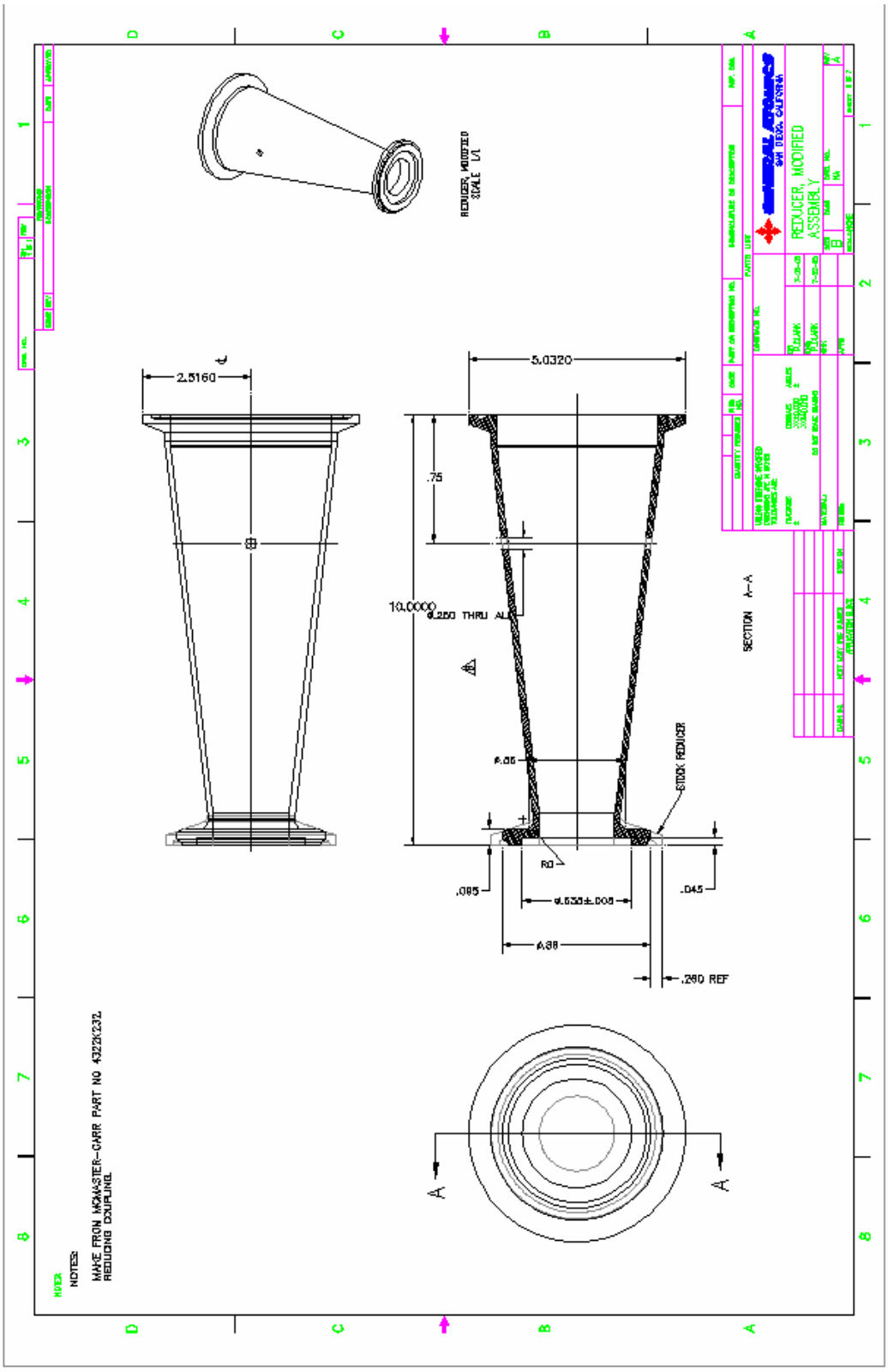
REDUCER, MODIFIED
SCALE 1/1
2.5160
5.0320
.75
10.0000
Ø.250 THRU ALL
Ø.55
STOCK REDUCER
R.0
.085
Ø.650±.005
.045
A.38
.280 REF
SECTION A-A
REDUCER, MODIFIED
ASSEMBLY
NOTES:
MAKE FROM MCMASTER-CARR PART NO 4323K232
REDUCING COUPLING

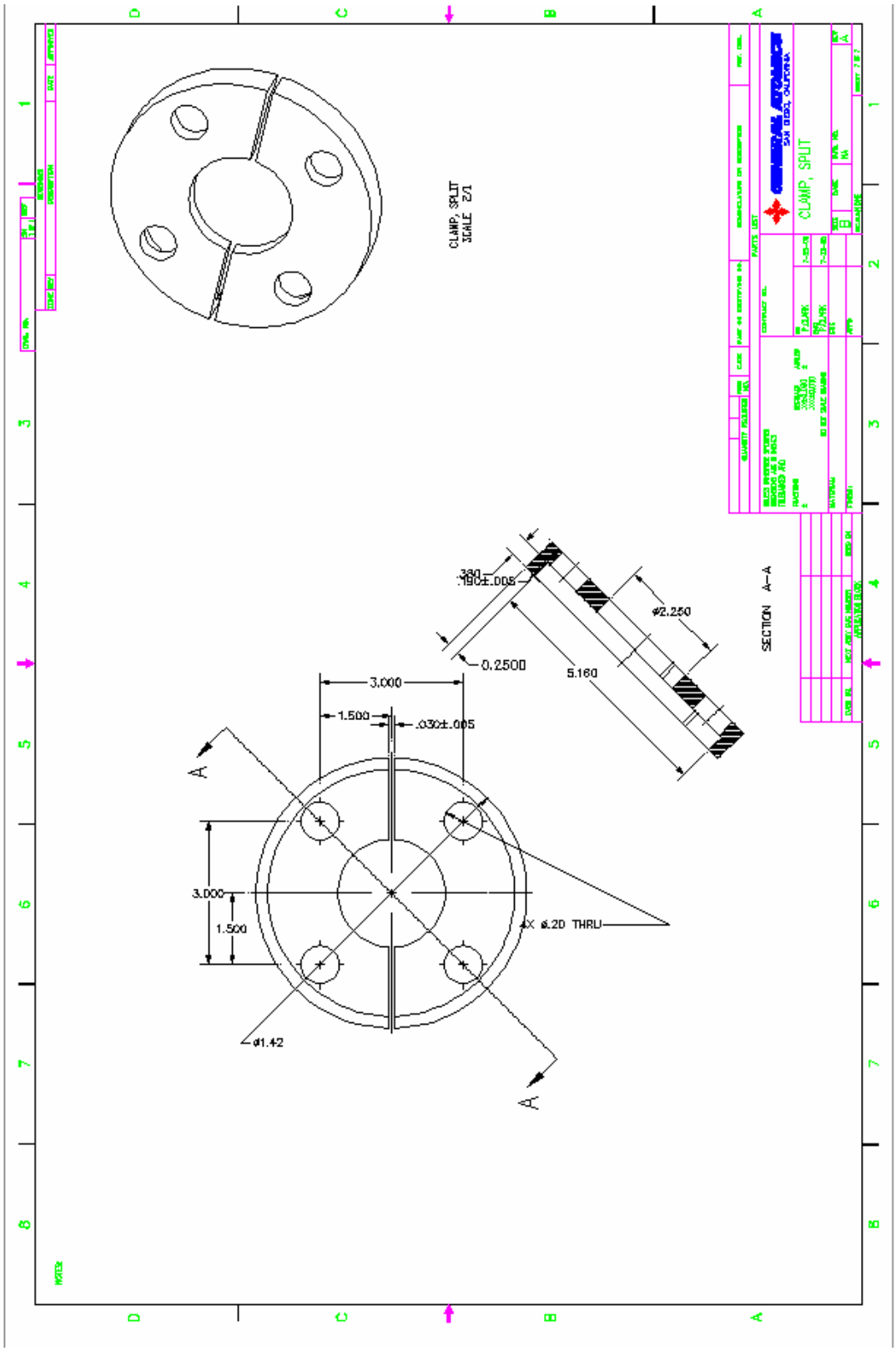
CLAMP, SPLIT
SCALE 2/1
CLAMP, SPLIT
SECTION A–A
.380
.190±.005
ø2.250
0.2500
5.160
3.000
1.500
.030±.005
3.000
1.500
X ø.20 THRU
ø1.42
A
A

REFERENCES

1. Chui, W.K., Glimm, J., Tangerman, F.M., Jardine, A.P., Madsen, J.S., Donnellan, T.M., Leek, R., Process modeling in Resin Transfer Molding as a Method to Enhance Product Quality, Society of Industrial and Applied Mathematics, V39, N4, pp 714-727, Dec-97.
2. Chen,Y.T., Davis, H.T., Macosko, W., Wetting of Fiber Mats for Composites Manufacturing: I. Visualization Experiments, A.I.Ch.E. Journal, Vol. 41, No. 10, pgs 2261-2281, Oct-95.
3. Bickerton, S., Advani, S.G., Mohan, R.V., Shires, D.R. Experimental Analysis and Numerical Modeling of Flow Channel Effects in Resin Transfer Molding, Polymer Composites, V21, N1, Feb 2000.
4. Varma, R.R., Advani, S.G., Three-Dimensional Simulations of Filling in Resin Transfer Molding, American Society of Mechanical Engineers, Fluids Engineering Division (Publication), V200, 1994.
5. Andersson H.M., Lundstrom, T.S., Gebart, B.R., Numerical Model for Vacuum Infusion Manufacturing of Polymer Composites International Journal of Numerical Methods for Heat and Fluid Flow, V13, N2-3, 2003.
6. Lundstrom, T.S. and Gebhart, B.R., Influence From Process Parameters on Void Formation in RTM, Poly Comp, V15, N1, pgs 25-33, Feb-94.
7. Szekely, J. and Martins, G.P., Non Equilibrium Effects in the Growth of Spherical Gas Bubbles Due to Solute Diffusion, Chem Eng Sci, Vol. 26, pgs 147-159, 1971.
8. Vakilotojjar, M. and Javdani, K., Bubble Growth in a Viscous Newtonian Liquid, Chem Eng Sci, Vol. 35, pgs 2352-2358.
9. Lundstrom, T.S., Measurement of Void Collapse During RTM, Comp. Part A, 28 A, pgs. 201-214, 1997.
10. Labordus, M. and Hoebergen, A., Avoiding Voids by Creating Bubbles: Degassing of Resins Before Vacuum Infusion, www.lightweight-structures.com, Netherlands, Apr 2000.
11. Rohatgi, V. and Patel, N. and Lee, L.J., Experimental Investigation of Flow-Induced Microvoids During Impregnation of Unidirectional Stitched Fiberglass Mat Poly Comp, Vol. 17, No. 2, pgs 161-170.
12. Roychowdhury, S., Gillespie Jr., J.W., Advani, S.G., Volatile-Induced Void Formation in Amorphous Thermoplastic Polymeric Materials: I. Modeling and Parametric Studies, J. of Comp. Mat., Vol. 35, No. 04/2001, pgs 340-366, 2001.

13. Chang, C.Y., Hourng, L.W., Study on Void Formation in RTM, Poly Eng and Sci, Vol. 38, No. 5, pgs 809-818, May-98.

14. Barraza, H.J., Hamidib, Y.K., Aktasb, L., O'Rear, E.A., Altan, M.C., Porosity Reduction in the High-Speed Processing of Glass-Fiber Composites by RTM, J of Comp Mat, Vol. 38, No. 3/2004, pgs. 195-226, 2004.

15. Jinlian, H., Yi, L., Xueming, S., Study on Void Formation in Multi-Layer Woven Fabrics, Comp. Part A, Vol. 35, pgs. 595-603, 2004.

16. EOM, Y. and Boogh, L., Michaud, V., Manson, J., A Structure and Property Based Process Window for Void Free Thermoset Composites, Poly Comp Vol. 22, No. 1, pgs 22-31, 2001.

17. Tang, J.M., Lee, W.I., Springer, G.S., Effects of Cure Pressure on Resin Flow, Voids, and Mechanical Properties, J of Comp Mat Vol. 21, No. 6/1987, pgs. 421-440, 1987.

18. Chui, W.K., Glimm, J., Tangerman, F.M., Jardine, A.P., Madsen, J.S., Donnellan, T.M., Leek, R., Porosity Migration in RTM, Proc. 9th International Conference on Numerical Methods in Thermal Problems, Atlanta, GA, 1995.

19. J.R. Wood and M. G. Bader, Modeling the Behaviour of Gas Bubbles in an Epoxy Resin: Evaluating the Input Parameters for a Diffusion Model Using a Free-Volume Approach, Journal of Materials Science, V30, N4, pgs 916-922, Feb 15 1995.

20. J.R. Wood and M. G. Bader, Modeling the Behavior of Gas Bubbles in an Epoxy Resin: Evaluating the Input Parameters for a Diffusion Model Using a Solubility Parameter Approach, Journal of Materials Science, V29 N3 pgs 844-850, Feb 1, 1994.

21. J.R. Wood and M. G. Bader, Void Control for Polymer-Matrix Composites (2): Theoretical and Experimental Evaluation of a Diffusion Model for the Growth and Collapse of Gas Bubbles, Composites Manufacturing, 5(3), 148-158, 1994.

22. J.R. Wood and M. G. Bader, Void Control for Polymer-Matrix Composites (2): Theoretical and Experimental Evaluation of a Diffusion Model for the Growth and Collapse of Gas Bubbles, Composites Manufacturing, 5(3), 148-158, 1994.

23. M. Labordus, M. Pieters, A. Hoebergen, J. Soderlund, The Causes of voids in Laminates Made with Vacuum Injection, Proceedings of the 20th International SAMPE Europe Conference, Paris, April 13th-15th, 1999.

24. Fowler, G., Phifer, S., Resin Transfer Molding for High Fiber/Low Void Content, Advanced Materials: Performance Through Technology Insertion

International SAMPE Symposium and Exhibition (Proceedings), V38, N1, SAMPE, Covina, CA, USA. p 471-476, 1993.

25. Varna, J., Joffe, R., Berglund, L.A., Lundstrom, T.S., Effect of Voids on Failure Mechanisms in RTM Laminates, Composite Science and Technologies, V53, 1995.
26. Ref. Darcy's Law, http://biosystems.okstate.edu/darcy/LaLoi/basics.htm, Darcy's Law Basics and More, Glenn Brown, Oklahoma State University.
27. Ebbing, D., General Chemisty, Houghton Mifflin Co., Boston, 1984.
28. Patel, N., Lee, L.J., Effects of Fiber Mat Architecture on Void Formation and Removal in Liquid Composite Molding, Polymer Composites, V16 N5, 1995.
29. Richardson, M.O.W. and Zhang, Z.Y. Experimental Investigation and Flow Visualisation of the Resin Transfer Mould Filling Process for Non-Woven Hemp Reinforced Phenolic Composites, Comp. Part A, 31 pgs. 201-214, 2000.
30. Kingery, W.D., Introduction of Ceramics, John Wiley & Sons, Inc., New York, 1960.
31. EOM, Y. and Boogh, L., Michaud V., Sunderland, P., Manson, J.A., Stress-Initiated Void Formation During Cure of a Three-Dimensionally Constrained Thermoset Resin, Poly Eng and Sci, V41, N3, pgs 492-503, Mar 2001.
32. Lee, H. and Neville, K., Handbook of Epxoy Resins, McGraw-Hill, New York, 1967.
33. Hayward J.S., Harris B., Effect of Process Variables on the Qualtiy of RTM Moulding, Sampe, J26, pgs 39-46, 1990.
34. Hayward, J.S., Harris, B., Processing Factors Affecting the Quality of Resin Transfer Moulded Composities, Plastics & Rubber Processing & Applications, V11, N4, pgs 191-198, 1989.
35. Hayward, J.S., Harris, B., The Effect of Vacuum Assistance in Resin Transfer Moulding, Composites Manufacturing, 1(3), pgs 161-166, 1990.
36. Clark, P. and R. P. Reed, (2000). Resin Transfer Molding of ITER US CS Model Coil. Society for the Advancement of Material and Process Engineering (SAMPE) Symposium and Exhibition, Long Beach, CA.
37. WWW.newportad.com/nbv800.html, 5/13/04, Newport Adhesives and Composites, Inc.NBV-800, Product Technical Data Sheet, VaRTM Epoxy.
38. Cycom 5555 RTM Epoxy Technical Datasheet, pg 5, dated 5/16/02, Cytec Engineered Materials, Tempe, AZ.
39. Colton, J.S., Suh, N.P., Nucleation of Microcellular Foam: Theory and Practice, Poly Eng and Sci, V27, N7, pgs 500-503, Apr-87

40. Hablanian, Marsbed H., High-Vacuum Technology, A Practical Guide, Marcel Dekker, Inc., New York 1990.

41. Sagara, H., Arai, Y., Saito, S., Calculation of Henry's Constant of Gas in Hydrocarbon Solvent by Regular Solution Theory, J. of Chem Eng of JP, V8, N2, pgs 93-114, 1975.

42. Hildebrand, J.H., Lamoreaux, R.H., Solubility of Gases in Liquids: Fact and Theory, Ind. Eng. Chem. Fund., V13, N2, 1974.

43. Stark, E.B., Breitigam, W.V., Farris, R.D., Davis, D.G., Stenzenberger, H.D., Resin Transfer Molding (RTM) of High Performance Resins, Technical Paper SC:1207-01, Resolution Performance Products, 2001.

44. Battino, R., Clever, H.L., The Solubility of Gas in Liquids, Chem. Rev., 66, 395-463, 1966.

45. Banks, A.M., Kirkwood, W.M., Bubble Free Resin for Infusion Process, Composites Part A, V36, N6, pgs 739–746, 2005.

46. Prausnitz, J.M. and Shair, F.H., A Thermodynamic Correlation of Gas Solubilities A.I.Ch.E. Journal V7, N4, pgs 682-687, Dec-61

47. Weast, R.C. Editor, Handbook of Chemistry and Physics, 61st Ed., CRC Press, Tables for Vapor Pressures of Organic Compounds, D-199, 1980.

48. Epstein, P.S., Plesset, M.S., On the Stability of Gas Bubbles in Liquid-Gas Solutions, J. Chemistry Physics, V18 pg 1505, 1950.

49. Abraham, D., McIlhagger, R., Experimental Investigation of Design Rules for Resin Gating and Venting Using the Vacuum Injection Technique, Polymers & Polymer Composites, V6, N7, pgs 455-464, 1998.

50. Young, Wen-Bin and Tseng, Chaw-Wu, Study on the Preheated Temperatures and Injection Pressures of RTM Process, J. Reinforced Plastics & Comp, V13, May-94.

51. Palmese, G.R. and Karbhari, V.M., Effects of Sizing on Microscopic Flow In Resin, Poly Comp, V16, N4, pgs 313-318 Aug-95.

52. Restagno, F., Bocquet, L., Biben, T. Metastability and Nucleation in Capillary Condensation Physical Review Letters, V84, N11, March 2000.

53. Jacob N. Israelachvili, Intermolecular and surface forces, London , San Diego, Academic Press, 1991.

54. ASM Handbook, Vol. 13, Corrosion, ASM International, pg 82, 1987.

55. O'Hanlon, John F., A Users Guide to Vacuum Technology, 3rd Ed. John Wiley & Sons, Inc., Hoboken, NJ, 2003.

56. Astrom, B.T., Manufacturing of Polymer Composites, Chapman & Hall, 2-6 Boundary Row, London, 1997.